

**Molecular Structures
and
Bio-redox Reaction Mechanisms
of
Vitamin E Models**

A Quantum Chemical Study

David Hadrian Setiadi

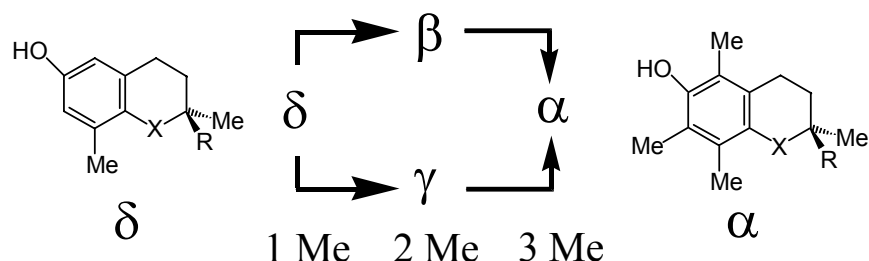
A dissertation submitted in conformity with the requirements of the Ph.D. degree



Department of Medical Chemistry
University of Szeged
Szeged, Hungary
2004

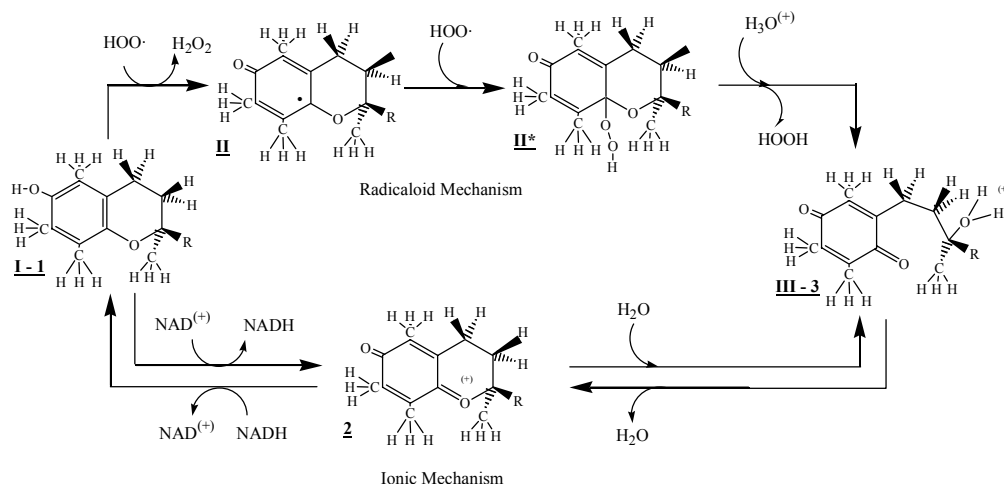
ABSTRACT

“Mother Nature” provided 4 homologues (α , β , γ , δ) of tocopherol, all of which are components of the naturally produced Vitamin E. They have the same ring structures and sidechains, but they differ from each other in the extent of methylation in their aromatic ring.



The various homologues have different activities, with the most methylated, α -tocopherol, being the most active yet being the least stable due to the congestion caused by the six substituents attached to the benzene ring.

The free radical scavenging mechanism which leads to a quinoidal structure via a radical oxidative ring opening is exothermic. However, the ionic oxidative ring opening is endothermic. Consequently, the ionic reductive ring closing is exothermic.



This leads to the suggestion that Vitamin E may be recovered unchanged, thus it effectively it becomes a catalyst for the following reaction.



Vitamin E is “recycled” biologically and as a single α -tocopherol molecule may convert numerous $\text{HOO}\cdot$ radicals to H_2O_2 . These peroxide molecules will accumulate if not removed enzymatically at the formation rate through the participation of Catalase(Fe) or Glutathione Peroxidase, $\text{GP}_x(\text{Se})$. This accumulation of peroxide, which may be referred to as a “peroxide traffic jam”, may be the reason for the pro-oxidant effect of Vitamin E. This may be regarded as the molecular explanation of the poetic expression that Vitamin E is considered as a “Janus” molecule with anti-oxidant and pro-oxidant activity.

DISCLAIMER

Vitamin E was discovered in 1922 taking a considerable length of time to be recognized for its anti-oxidant activity. The medical importance of tocopherols and tocotrienols, all of which have Vitamin E activity, became apparent in the 1990's and its role in cardiovascular medicine is now eminently obvious. In general, it helps remedy all degenerative diseases either directly, indirectly or in combination with good diet.

In spite of all these developments, Vitamin E's mechanism of scavenging reactive oxygen species (ROS) is not fully understood. The term ROS includes everything from singlet oxygen *via* superoxide anion and hydrogen peroxide, all the way to hydroxyl radical. Yet, it remains to be seen what the role of Vitamin E is in the multifaceted reactions of ROS.

The present dissertation will concentrate on the various congeners of tocopherol and tocotrienol models. Since the electron density distribution of all the various congeners containing O, S and Se are different. Therefore, they will have different chemical reactivity. It is not unreasonable to expect that these different chemical reactivities may well predetermine the anti-oxidant activities of Tocopherol congeners, isomers and conformers. A combined putative mechanism of action of the redox activity of tocopherols and tocotrienols is reported here in detail.

Not all aspects of Vitamin E are investigated in this research. The present dissertation represents a 'progress report' on the molecular structure of Vitamin E model compounds. Thus, this dissertation may have raised more questions than answers.

TABLE OF CONTENTS

Title page	(i)
Abstract	(ii)
Disclaimer	(iii)
Table of Contents	(iv)
List of Tables	(v)
List of Figures	(vi)
Acknowledgements	(viii)
Published Papers	(viii)
1. Preamble	1
1.1. Predicaments	1
1.2. The Economic Burden of Illness	2
1.3. The Nature of Oxidative Stress	3
1.4. Essential Nutrient Components	3
1.5. Diet and Dietary Supplements	5
1.6. The role of Vitamin E in Cardiovascular Diseases as an Oxidative Protector of LDL	7
2. Choice of Topic	
3. Introduction	9
3.1. The Consequences of Oxidative Stress	12
3.2. Structural Background	12
4. Aim of Study	12
5. Method	14
5.1. Computational Background	15
5.2. Models A and B	15
5.3. Models C and D	16
5.4. Model E	16
5.5. Redox Reaction Mechanisms	17
6. Results and Discussion	18
6.1. Molecular Structures	19
6.1.1. Ring Conformations of Vitamin E models (Models A and B)	19
6.1.1.1. Molecular geometries at transition structures	19
6.1.1.2. Energetics of Ring inversion	19
6.1.2. Ring Substitutions of Vitamin E models (Models C and D)	20
6.1.2.1. Molecular Geometry of Stable Structures	21
6.1.2.2. Molecular Energetics	21
6.1.3. Aromatic Methyl Substitution of Vitamin E models (Models E)	21
6.1.3.1. Molecular Geometries	22
6.1.3.2. Molecular Energetics	23
6.2. Redox Reaction Mechanism	23
6.2.1. The dichotomy of anti-oxidant and pro-oxidant nature of Vitamin E	25
6.2.2. Molecular geometries	30
6.2.3. Free radical oxidativering opening mechanism for α -tocopherol	30
6.2.4. Ionic Oxidative Ring Opening Mechanism for α -tocopherol	33
6.2.5. Ionic Reductive Ring Closing Mechanism for α -tocopherol	34
6.2.6. Mechanistic Comparison of O, S, Se congeners	36
6.3. Further study of Vitamin E models	38
6.3.1. Full conformational space of tocopherol models	45
6.3.2. Preliminary Results	4
7. Conclusions	47
7.1. Model A and Model B	47
7.2. Model C and Model D	47
7.3. Model E	49
7.4. Mechanism	50
8. References	

LIST OF TABLES

- Table 1:** Costs of Degenerative Diseases in Canada during 1993
- Table 2:** Suggested dosage of Vitamin E for various medical conditions
- Table 3:** Recommended (RDA) and Optimum (ODA) Daily Allowance at Minerals and Vitamins
- Table 4:** Typical Vitamin E content of selected foods (based on α -tocopherol activity)
- Table 5:** Characteristics of the Major Classes of Lipoproteins in Human Plasma
- Table 6:** Methyl substituted homologues of Tocopherol and Tocotrienol
- Table 7:** Natural and synthetic compounds of the Vitamin E family
- Table 8:** Energy Components and hydride affinities for hydride abstraction as compute at the B3LYP/6-31G(d) level of theory
- Table 9:** Energy Components, necessary to balance the redox reactions, computed at the B3LYP/6-31G(d) level of theory
- Table 10:** Previously reported and presently optimized dihedral angles of cyclohexene, computed at the B3LYP level of theory
- Table 11:** Computed stabilization energies resulting from sequential substitution
- Table 12:** Total energies (hartrees) computed for the 24 optimized structures computed at the B3LYP/6-31G(d) level of theory
- Table 13:** Energy of stabilization associated with single or multiple methyl group transfers computed at the B3LYP/6-31G(d) level of theory
- Table 14:** Relative biological activity of tocopherols and computed stabilization energy values of model compounds.
- Table 15:** Energies of stabilizations calculated as a sum of components or through direct computations
- Table 16:** Total energy values of α -tocopherol model and its oxidized forms computed at the B3YP/6-31G(d) level of theory
- Table 17:** Total and relative energies for the free radical mechanism
- Table 18:** Total and relative energies for the ionic mechanism
- Table 19:** Total energy values of α -tocopherol and its congeners and its oxidized forms computed at the B3YP/6-31G(d) level of theory
- Table 20:** Total and relative energies for the ionic mechanism of α -tocopherol and its congeners.
- Table 21:** Total energies for free radical mechanism of α -tocopherol and its congeners
- Table 22:** Total and relative energies for the free radical mechanism of α -tocopherol and its congeners.
- Table 23:** Full mechanistic relative energies for O, S, Se congeners
- Table 24:** Presently optimized dihedral angles of the α -tocopherol sidechain and its congeners.
- Table 25:** Presently optimized ring dihedral angles for O, S, Se compounds.

LIST OF FIGURES

Figure 1: Biochemical pathway of glutathione peroxidase (E-Se⁻)

Figure 2: Diagram of LDL, the major cholesterol carrier of the bloodstream. This spheroidal particle consists of some 1500 cholesteryl ester molecules surrounded by an amphiphilic coat of ~800 phospholipid molecules, ~500 cholesterol molecules and a single 550-kD molecule of apolipoprotein B-100.

Figure 3: The Structure of Tocopherol

Figure 4: The Structure of Tocotrienol

Figure 5: Stereoisomers of tocopherols

Figure 6: The Structure of Seleno-tocopherol

Figure 7: Ring flip in dihydropyran

Figure 8: Conformation and dihedral angles of cyclohexene previously obtained on the basis of molecular modelling

Figure 9: Tetralin as well as chroman and its congeners, with their respective Groups in the periodic table.

Figure 10: Models of tocopherols

Figure 11: Definition of key dihedral angles.

Figure 12: Optimized minimum energy and transition structures for chroman (X=O). The sulphur and selenium congeners have analogous geometries.

Figure 13: Variation of ring inversion energy of activation with the size of the heteroatom

Figure 14: Variation of total stabilization energy with C-X bond length (X=O, S, Se)

Figure 15: Isodesmic Reactions for the incorporation of aromatic methyl substituents.

Figure 16: Three optimized structures of the shortened sidechain model of the α -tocopherol computed at the B3LYP/6-31G(d)

Figure 17: Computed stabilization energies

Figure 18: Aromatic methyl substitution of α , β , γ and δ tocopherol

Figure 19: Modified relative activity of tocopherol vs relative stabilization energies of tocopherol model

Figure 20: A schematic mechanistic representation of non-destructive and destructive free radical oxidation of α -tocopherol by HOO \cdot .

Figure 21: A schematic mechanistic representation of non-destructive and destructive ionic oxidation of α -tocopherol.

Figure 22: Radical and ionic mechanism of α -tocopherol oxidation.

Figure 23: Structures of α -tocopherol (top) and α -tocopherolquinone corresponding to reduced [Red] and oxidized [Ox] forms respectively in equation (2). All aromatic CC bond lengths in the top structure are in the vicinity of 1.40Å. The single and double bond lengths in the ring of the bottom structures are in the vicinity of 1.49Å and 1.35Å respectively

Figure 24: Reaction profile of non-destructive free radical oxidation of α -tocopherol model by $\text{HOO}\cdot$.

Figure 25: Reaction profile for ionic oxidation mechanism using $\text{Li}^{(+)}$, a hydride abstractor modeling $\text{NAD}^{(+)}$

Figure 26: The connection of a combined non-destructive free-radical and reversible ionic mechanism of oxidation of α -tocopherol quinone. Note the reversible nature of the ionic process.

Figure 27: Full cycle of reaction mechanism involving free radical open shell oxidation and closed shell recovery of α -tocopherol. The energy difference between initial and final states is related to the process: $2\text{HOO}\cdot + \text{Li-H} \rightarrow \text{HOOH} + \text{HOOLi}$

Figure 28: The role of various enzymes and antioxidants in the reduction of concentration of Reactive Oxygen Species (ROS)

Figure 29: Overall representation of the catalytic effect of α -tocopherol

Figure 30: Variation of total stabilization energy with C-X bond length (X=O, S, Se)

Figure 31: Ionic reaction profile for X=O, S, and Se oxidative ring opening and reductive ring closing mechanism using LiH, a hydride donor modeling NADH

Figure 32: Models of tocopherols.

Figure 33: B3LYP/6-31G(d) optimized minimum energy structure for fully extended tail of Selenium congener.

Figure 34: RHF/6-31G(d) optimized minimum energy structure for gauche- trend of α -tocopherol.

ACKNOWLEDGEMENTS

The author wishes to acknowledge the moral support of Professor Botond Penke, Professor Julius Gy. Papp, as well as the encouragement and helpful discussions of Dr. Bela Viskolz. The author is also grateful to Dr. Gregory A. Chass and Professor I.G. Csizmadia for their inspiration and guidance during this research as well as during the preparation of this dissertation. Special thanks to the members of GIOCOMMS for their support and resources provided. Support from Uniseti Inc., PDS and Aristosystems Inc. is also acknowledged.

PUBLISHED PAPERS

1. **David H. Setiadi**, Gregory A. Chass, Ladislaus L. Torday, Andras Varro and Julius Gy. Papp, Vitamin E Models. Conformational Analysis and Stereochemistry of Tetralin, Chroman, Thiochroman and Selenochroman, THEOCHEM **2002**, **594**, **161-172**.
IF: **1.014**
2. **David H. Setiadi**, Gregory A. Chass, Ladislaus L. Torday, Andras Varro and Julius Gy. Papp, Imre G. Csizmadia, Vitamin E Models. The effect of heteroatom substitution in 2-ethyl-2-methyl chroman and 2-ethyl-2-methyl-6-hydroxychroman, Eur. Phys. J. D **2002**, **20**, **609-618**.
IF: **1.300**
3. **David H. Setiadi**, Gregory A. Chass, Ladislaus L. Torday, Andras Varro and Julius Gy. Papp, Vitamin E Models. Shortened Sidechain Models of α , β , γ and δ Tocopherol and Tocotrienol. A Density Functional Study, J. Mol. Struct. THEOCHEM **2003**, **637**, **11-26**.
IF: **1.014**
4. **David H. Setiadi**, Gregory A. Chass, Ladislaus L. Torday, Andras Varro and Julius Gy. Papp, Vitamin E Models. Can the anti-oxidant and pro-oxidant dichotomy of α -tocopherol be related to an ionic ring closing and ring opening redox reaction. THEOCHEM **2003**, **620**, **93-106**.
IF: **1.014**
5. **David H. Setiadi**, Gregory A. Chass, Joseph C. P. Koo, Botond Penke and Imre G. Csizmadia, Exploratory study on the full conformation space of α -tocopherol and its selected congeners. THEOCHEM **2003**, **666-667**, **439-443**.
IF: **1.014**

PUBLISHED AND ACCEPTED PAPERS :

Cumulative IF : 5.356

First Author in : 5

1. PREAMBLE

1.1 Predicaments

The following quote¹ summarizes the future predicaments in the USA. Clearly, the situation is expected to be analogous to the entire Western World or perhaps to the entire Human Race.

"It is rare to see a day pass in which we are not told through some popular medium that the population is becoming older. Along with this information comes the 'new' revelation that as we enter the next millennium there will be increases in age-associated diseases (e.g., cancer, cardiovascular disease) including the most devastating of these, which involve the nervous system (e.g., Alzheimer's disease [AD] and Parkinson's Disease[PD]). It is estimated that within the next 50 years approximately 30% of the population will be aged 65 years or older. Of those between 75 and 84 years of age, 6 million will exhibit some form of AD symptoms, and of those older than 85 years, over 12 million will have some form of dementia associated with AD. What appears more ominous is that many cognitive changes occur even in the absence of specific age-related neurodegenerative diseases. Common components thought to contribute to the manifestation of these disorders and normal age-related declines in brain performance are increased susceptibility to long-term effects of oxidative stress (OS) and inflammatory insults. Unless some means is found to reduce these age-related decrements in neuronal function, health care costs will continue to rise exponentially. Thus, it is extremely important to explore methods to retard or reverse age-related neuronal deficits as well as their subsequent, behavioural manifestations. Fortunately, the growth of knowledge in the biochemistry of cell viability has opened new avenues of research focused at identifying new therapeutic agents that could potentially disrupt the perpetual cycle of events involved in the decrements associated with these detrimental processes. In this regard, a new role in which certain dietary components may play important roles in alleviating certain disorders are beginning to receive increased attention, in particular those involving phytochemicals found in fruits and vegetables."

Undoubtedly, the situation that is now at hand will intensify in the future.

1.2 The Economic Burden of Illness

Besides creating human suffering, illness is also a source of an economic burden. This is true, irrespectively of whether one has a national healthcare system or the cost of medical care falls on the shoulders of individuals.

Sometime, where the economic burden becomes unbearably drastic, measures are taken. In an individual case, it may mean not seeking the help of medical doctors, as the family may be unable finance it. In the case of a national healthcare system, extra tax is levied either universally or in the form of “user fees”.

Table 1 shows the Canadian Scenario as it was in 1993. About 40% of the national budget was spent on degenerative diseases (**Table 1**) of which more than 20% was related to cardiovascular cases. An educated guess suggested that a possible cut of these expenses to about a half may be possible with the tools of “Preventive Medicine” utilizing dietary supplements in which Vitamin E plays a significant role.

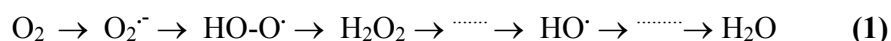
Table 1 - Costs of Degenerative Diseases in Canada during 1993

	Billion \$	Percentage
Cardiovascular		
Coronary	30.294	23.447%
Stroke		
Cancer	14.341	11.100%
Alzheimer's		
Parkinson's (approximately)	7.045	5.453%
Degenerative Diseases	51.680	40.000%
All other Medical Expenses	77.520	60.000%
Total for 1993	129.200	100.000%
Possible to cut in half		
Degenerative Diseases	25.840	20.000%
All other Medical Expenses	77.520	60.000%
Total Predicted	103.360	80.000%

In closing, it might be mentioned that the cost of a heart transplant in the 1990's was about US\$250,000 and in 1999, the USA performed 2184 heart transplants (US \$546 million). In contrast, to that dietary supplements could reduce the severe cardiovascular cases dramatically for approximately US\$1.00 per day/person.

1.3 The Nature of Oxidative Stress

Since chemical reactions are usually not quantitative, up to 5% of the oxygen we are inhaling is converted to "reactive oxygen species" (or ROS for short). During the normal metabolism while the food is oxidized in the living cells, oxygen is also being reduced to water. The reduction is a multi-step process, and the intermediate stages are these ROS.



When any of these ROS escapes from this sequence of reductive reactions, they damage the structure of the cell, including the DNA, the RNA, proteins, as well as cell membranes. Such damages also lead to degenerative diseases, as well as a weaker immune system.

Considering that in every human being these ROS strike and fracture every single one of the DNA molecules 10,000 times a day. About 9,900 of these breaks in the DNA strands are restored by DNA repair enzymes. About 100, or 1%, escape the enzymes' activity. These unrepaired damages, accumulated over time, set the stage for atherosclerosis, cancer and other degenerative diseases. It is clear that slowing the damage – by increasing antioxidant protection – translates directly into a healthier and longer life span.

The body has two types of mechanisms to eliminate these ROS before they can make significant damage. These include the following:

- i) Enzymatic reductions, beyond the regular process
- ii) Scavenging these ROS by antioxidant compounds naturally supplied by a healthy diet

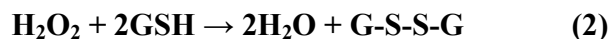
Both of these mechanisms fight a losing battle against ROS with advanced age. However even at a younger age the ammunition for these mechanisms must come from a healthy diet, which is not always available. In such a case, the 'healthy diet' does include dietary supplement. Needless to say, for long term benefits it is important that young people acquire, as early as possible, an attitude which is pro 'healthy diet'.

1.4 Essential Nutrient Components

Both of the above two mechanisms to fight ROS require certain special nutrients.

For *Mechanism (i)*, it may be some trace element such as Magnesium, Vanadium, Chromium, Manganese, Iron, Copper, Zinc or Selenium (Mg, V, Cr, Mn, Fe, Cu, Zn, or Se), that may be essential at the active site of a particular enzyme. If these trace elements are not available, *Mechanism (i)* will not be operative. For example, the natural selenium (Se) level in the soil is highly variable. In the USA, the Eastern Coastal Plain and the Pacific Northwest have the lowest levels of Se. In these areas, the daily Se intake of the population is in the range of 60 to 90 micrograms (μg). In contrast, in the Se rich areas, the range of daily Se intake is 60 to 200 μg . The average daily US intake is 125 μg . People living where the highest levels of Se exist have the lowest levels of lung, colon, bladder, pancreas, breast and ovarian cancers. Clearly, if the soil is depleted of Se, the vegetation cannot have enough and therefore, the local diet would have insufficient amounts of Se. It is stipulated that the daily intake should be in the vicinity of 300 μg . It may well be that the diet of the whole North American continent is too low in Se. This may be responsible for some of the high levels of degenerative ailments, such as cancer and cardiovascular diseases. Of course, an overdose of Se is dangerous, however this is not expected to happen before the daily intake reaches 1000 μg .

Figure 1 shows the putative mechanism of **Glutathione Peroxidase** in a schematic fashion. E-Se⁽⁻⁾ symbolizes the selenium deprotonated enzyme. This enzyme only catalyzes the overall reaction of hydrogen peroxide decomposition, since it is not consumed during the reaction but is in fact recovered unchanged. The stoichiometry of the reaction involving hydrogen peroxide and reduced glutathione (GSH) is as follows:



Of course, the selenium deprotonated enzyme, E-Se⁽⁻⁾, has a deprotonated selenocysteine (Sec) residue at its active site. This Selenocysteine sometimes is called the 21st amino acid because it can be incorporated in a protein. However, it only has an RNA codon but no DNA codon.

The other important enzyme is superoxide dismutase (**SOD**) which converts the highly dangerous (reactive, oxidizing) superoxide (O₂⁻) to the not so dangerous H₂O₂. The enzyme structure contains Zn and Cu ions.



The H₂O₂ thus formed is further reduced to H₂O with the help of glutathione peroxidase discussed above.

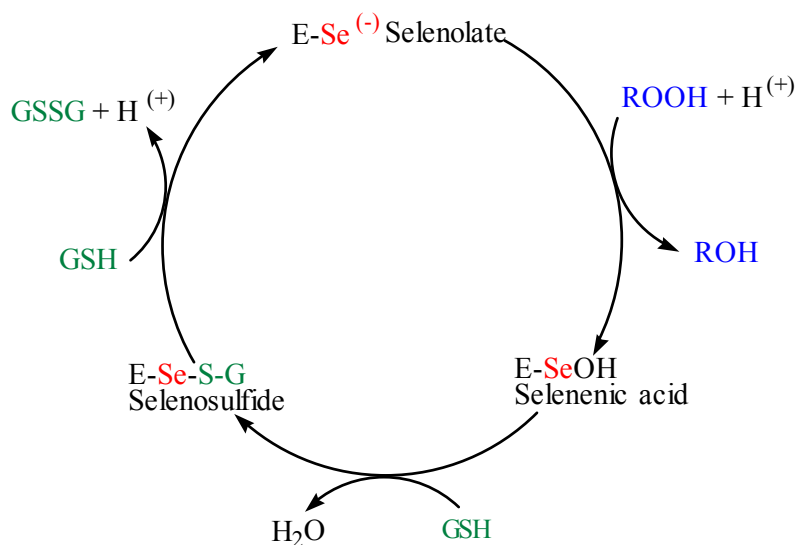


Figure 1 - Biochemical pathway of glutathione peroxidase (E-Se⁻)

For *Mechanism (ii)*, certain vitamins (like C and E) as well as certain antioxidants such as lycopene, β -carotene, flavones, farnesol, allyl-methyl-disulfide, lipoic acid, coenzyme Q₁₀ or ubiquinone, may also be required. Plants produce these antioxidants thus fruits and vegetables are expected to supply them. However, the level of these antioxidants in fruits and vegetables may vary according to the geographical location where they were produced, and could also vary from season to season, or even with distance of transportation. Consequently, for a healthy diet, the antioxidants may have to be added to the food items or must be provided as a supplement. If regular food was sufficiently nutritious, or if dietary supplements were included in meals, degenerative diseases may be reduced substantially, which in turn could considerably reduce health care costs.

1.5 Diet and Dietary Supplements

Ideally, the purpose would be to produce food products at accessible prices that will prevent, or at least forestall, the development of degenerative diseases such as cancer, heart attack, stroke, as well as Alzheimer and Parkinson's diseases. All of these ailments are due, to a great extent, to oxidative stresses. The presence of certain natural products, which may currently be inadequate in our daily diets, that if taken within the right range of concentrations can prevent, or at least forestall the development of such ailments. In addition, to reduce the risk of such degenerative diseases, some of these natural products can strengthen the immune system leading to fewer viral or bacterial infections. The loss of fewer workdays may be expected due to the reduction of illness and infection. In general, with proper diet our entire society could become healthier, stronger, and less vulnerable to degenerative diseases. In the absence of a perfect diet, dietary supplements must be considered.

However, the suggested dosage does change from one medical condition or another as shown in **Table 2**. Also, **Table 3** shows the RDA (recommended daily allowance) and ODA (optimum daily allowance). For a defensive strategy within the field of preventive medicine the ODA is sometimes more than an order of magnitude higher than the RDA. This is the case for Vitamin E; the RDA values range from 8-10mg and the ODA values are within 250-1000mg or 400-1600IU.

Table 2 - Suggested dosage of Vitamin E for various medical conditions

Condition	Suggested Dosage
Aging	400-800 IU
Cancer Prevention	400-800 IU
Cardiovascular disease prevention	400-800 IU
Diabetes	800-1600 IU
Fibrocystic breast disease	800-1600 IU
Menopausal "hot flashes"	800-1600 IU
Poor circulation	800-1600 IU
Premenstrual syndrome	800-1600 IU
Prevention of excessive bleeding with IUDs	100-400 IU
Wound healing	400-800 IU

Table 3 – Recommended (RDA) and Optimum (ODA) Daily Allowance for Minerals and Vitamins

NUTRIENT	RDA (Men)	RDA (Women)	ODA
Minerals			
Boron	none	none	1-3mg
Calcium	800 mg.	800 mg.	1,000-2,000 mg.
Chromium	50-300 mcg.	50-200 mcg.	100-600 mcg.
Copper	1.5-3 mg.	1.5-3 mg.	1-3 mg.
Iodine	150 mcg.	150 mcg.	225 mcg.
Iron	10 mg.	15 mg.	0-40 mg.
Magnesium	350 mg.	280 mg.	500-1,000 mg.
Manganese	2-5 mg.	2-5 mg.	5-15 mg.
Molybdenum	75-250 mcg.	75-250 mcg.	75-250 mcg.
Potassium	none	none	100-500 mg.
Selenium	70 mcg.	55 mcg.	100-300 mg.
Vanadium	none	none	25-100 mcg.
Zinc	15 mg.	12 mg.	15-50 mg.
Vitamins			
A	1,000 mcg. (5,000 IU)	800 mcg. (4,000 IU)	1,000-10,000 IU
Thiamin (B1)	1.5 mg.	1.1 mg.	100-250 mg.
Riboflavin (B2)	1.7 mg.	1.3 mg.	50-250 mg.
Niacin/niacinamide (B3)	19 mg.	15 mg.	50-250 mg.
Pantothenic acid (B5)	4-7 mg.	4-7 mg.	60-2,000 mg.
B6 (pyridoxine)	2 mg.	1.6 mg.	25-250 mg.
B12 (cobalamine)	2 mcg.	2 mcg.	500-2,000 mcg.
Folic Acid	200 mcg.	180 mcg.	800-2,000 mcg.
Lycopene	5 mg.	5 mg.	15-30 mg.
Beta-carotene	none	none	25,000-100,000 IU
Biotin	30-100 mcg.	30-100 mcg.	200-800 mcg.
C	60 mg.	60 mg.	675-3,000 mg.
D	5 mcg. (200 IU)	5 mcg. (200 IU)	200-1,000 IU
E	10 mg. (15 IU) *	8 mg. (12 IU) *	400-1,600 IU **

The natural abundance of these 2x4=8 components of the Vitamin E family varies from plant to plant [2]. **Table 4** illustrates some natural abundances.

Table 4 – Typical Vitamin E content of selected foods (based on α -tocopherol activity)

	Vitamin E	
	mg/100g food portion	IU/100g food portion
Wheat germ oil	119	178
Sunflower oil	49	73
Peanut oil	19	28
Soybean oil	8.1	12
Butter	2.2	3.2
Sunflower seeds, raw	50	74
Almonds	27	41
Peanuts, dry roasted	7.4	11
Asparagus, fresh	1.8	2.7
Spinach, fresh	1.8	2.7

1 mg α -tocopherol equivalent to 1.49 IU.

1.6 The role of Vitamin E in Cardiovascular Diseases as an Oxidative Protector of LDL

Lipids travel from the small intestine all through the bloodstream to every cell to be used as fuel. They are ‘packaged’ and ‘repackaged’ along the way. Each of the phases produces aggregates with varying degree of cholesterol content, which are globular micellelike particles.

Lipoprotein densities increase with decreasing particle diameter, since the density of their outer coating is greater than that of their inner core. Thus, the HDL, which are the most dense of the lipoproteins are also the smallest. Five distinctly different molecular aggregates exist (**Table 5**) and their inter-conversion scheme is as follows:



The protein components of lipoproteins are known as apolipoproteins or just apoproteins. At least nine apolipoproteins are distributed in different amounts in the human lipoproteins (**Table 5**). They form roughly a 20Å mono-layer wrapped around the surface as shown in **Figure 2**. Most of the apolipoproteins are water soluble and associate rather weakly with lipoproteins. These apolipoproteins have a high helix content which increases when they are incorporated into lipoproteins. Apparently, the helices are stabilized by a lipid environment, because helices fully satisfy the backbone’s hydrogen bonding potential in the lipoprotein’s water-free interior

Very often HDL is labelled as “good cholesterol” and LDL as “bad cholesterol”. Actually this is a misnomer as there is no “good” nor “bad” cholesterol. The reason for such designation comes from the fact that LDL is more susceptible for oxidation than the other forms. Thus the oxidative stress converts LDL to oxidized LDL, responsible for plaque formation, the source of all cardiovascular problems. Vitamin E, by virtue of the fact that it is lipid soluble, is accumulated in these lipoproteins. It should be noted that the higher the daily Vitamin E intake, the higher its concentration in lipoprotein.

In the August 7, 1997, issue of the New England Journal of Medicine, Marco Diaz, MD, wrote a review article² entitled, “Antioxidants and Atherosclerotic Heart Disease.” He concludes that antioxidants may very well reduce the risk of atherosclerosis by helping produce LDL resistance to oxidative modification and thus, reduce inflammation of the artery and the initial phase of atherosclerosis (the fatty streak). He goes on to state there may be other mechanisms by which antioxidants help reduce the risk of nonfatal heart attacks. This is probably by stabilizing the plaque where it is most likely to rupture, which is in the oxidized, LDL-laden, foam cell layer of the plaque. It may also reduce the size of the plaque. This means even individuals who have significantly advanced hardening of the arteries would benefit from supplementation with antioxidants such as Vitamin E.

Table 5: Characteristics of the Major Classes of Lipoproteins in Human Plasma

	Chylomicrons	VLDL	IDL	LDL	HDL
Density ($\text{g}\cdot\text{cm}^{-3}$)	<0.95	<1.006	1.006-1.019	1.019-1.063	1.063-1.210
Particle diameter (Å)	750-12,000	300-800	250-350	180-250	50-120
Particle mass (kD)	400,000	10,000-80,000	5,000-10,000	2,300	175-360
% Protein ^a	1.5-2.5	5-10	15-20	20-25	40-55
% Phospholipids ^a	7-9	15-20	22	15-20	20-35
% Free cholesterol ^a	1-3	5-10	8	7-10	3-4
% Triacylglycerols ^b	84-89	50-65	22	7-10	3-5
% Cholesteryl esters ^b	3-5	10-15	30	35-40	12
Major apolipoproteins	A-I, A-II, B-48, C-I, C-II, C-III, E	B-100, C-I, C-II, C-III, E	B-100, C-III, E	B-100	A-I, A-II, C-I, C-II, C-III, D, E

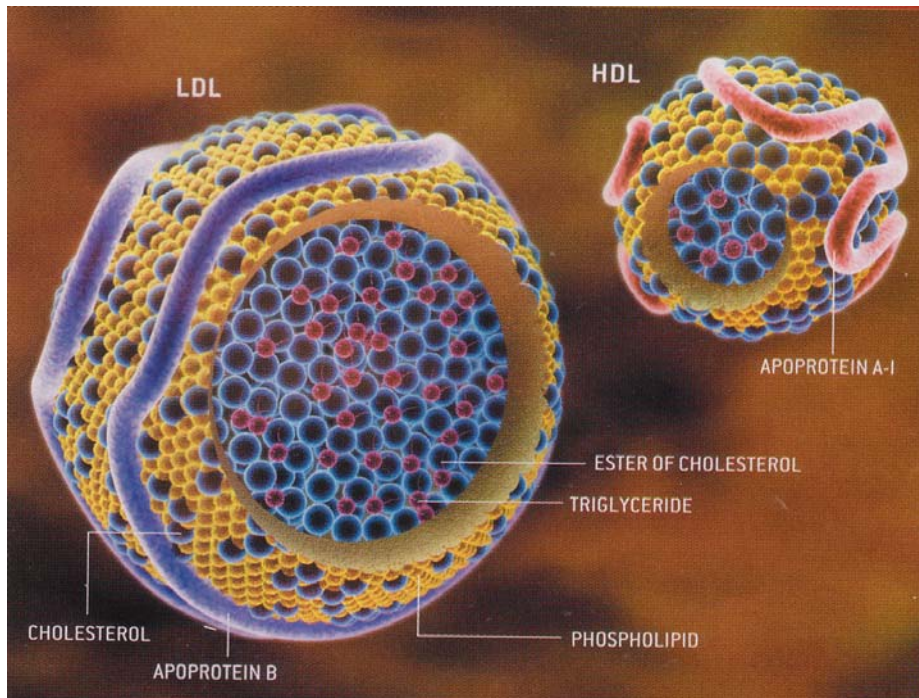
^a Surface Components^b Core Lipids

Figure 2 - Diagram of LDL, the major cholesterol carrier of the bloodstream. This spheroidal particle consists of some 1500 cholesteryl ester molecules surrounded by an amphiphilic coat of ~800 phospholipid molecules, ~500 cholesterol molecules and a single 550-kD molecule of apolipoprotein B-100.

2. CHOICE OF TOPIC

Vitamin E, a term introduced³ in 1922, does not represent a single compound but in fact includes two families of compounds: tocopherols and tocotrienols⁴. Both families consists of a chroman [benzpyran] ring structure and a sidechain. The sidechain has the characteristics, isoprenoid skeleton, typical of terpenes. Members of the tocopherol families have saturated sidechains but the same sidechain in the tocotrienol family has three non-conjugated double bonds. Such carbon – carbon double bonds are separated by $-\text{CH}_2-\text{CH}_2-$ units. For both families the carbon atom that carries the sidechain is stereo centre of *R* configuration; however the sidechain of the tocopherols have two additional stereo-centres at the branching points, both of which are of *R* configuration. The structural variations of the two families are shown in Figure 3 and Figure 4.

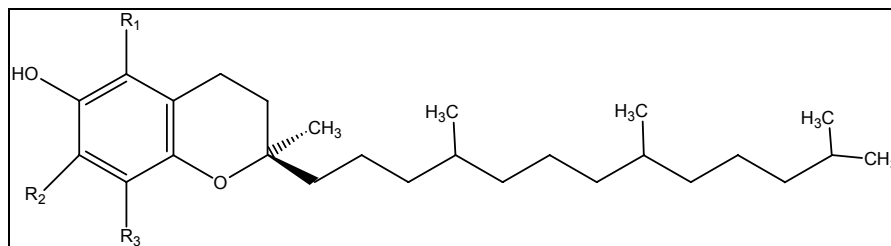


Figure 3 – The Structure of Tocopherol in *R* configuration

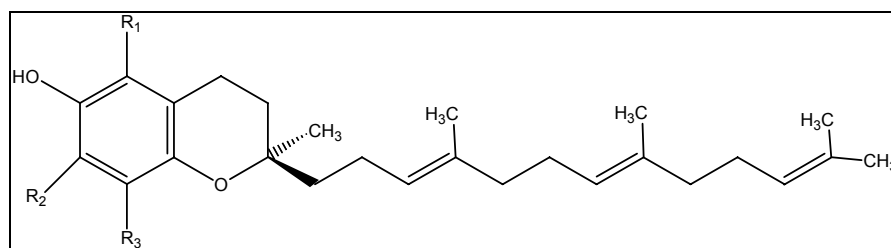


Figure 4 – The Structure of Tocotrienol

Each of these families has four homologous members, labelled as α , β , γ , and δ . They differ from each other in the extent of methyl substitution in the aromatic ring (R_1 , R_2 , R_3).

Table 6 - Methyl substituted homologues of Tocopherol and Tocotrienol

	R ₁	R ₂	R ₃
α	Me	Me	Me
β	Me	H	Me
γ	H	Me	Me
δ	H	H	Me

Thus these are two (2) families of compounds (tocopherol and tocotrienol) and each may come in four (4) homologous forms.

Of these 2x4=8 species, it is α -tocopherol which is most frequently used, partly due to the fact that it is commercially available in synthetic form. Of course the synthetic form is not a pure enantiomer but is instead a mixture of R- and S α - tocopherol acetate (see Table 7 and Figure 5). The effectiveness of the synthetic form has been traditionally questioned with no explanation at the molecular level, even though the primary function of Vitamin E is an antioxidant then undergoing an oxidation reaction *at the molecular level*. We now have more precise data to support the earlier assumption⁵.

Table 7 - Natural and synthetic compounds of the Vitamin E family

Natural derivatives	Activity %
RRR- α -tocopherol	100
RRR- β -tocopherol	57
RRR- γ -tocopherol	37
RRR- δ -tocopherol	1.4
R- α -Tocotrienol	30
R- β -tocotrienol	5
Synthetic derivatives	Activity %
RRR- α -tocopheryl acetate	100
RRS- α -tocopheryl acetate	90
RSS- α -tocopheryl acetate	73
SSS- α -tocopheryl acetate	60
RSR- α -tocopheryl acetate	57
SRS- α -tocopheryl acetate	37
SRR- α -tocopheryl acetate	31
SSR- α -tocopheryl acetate	21

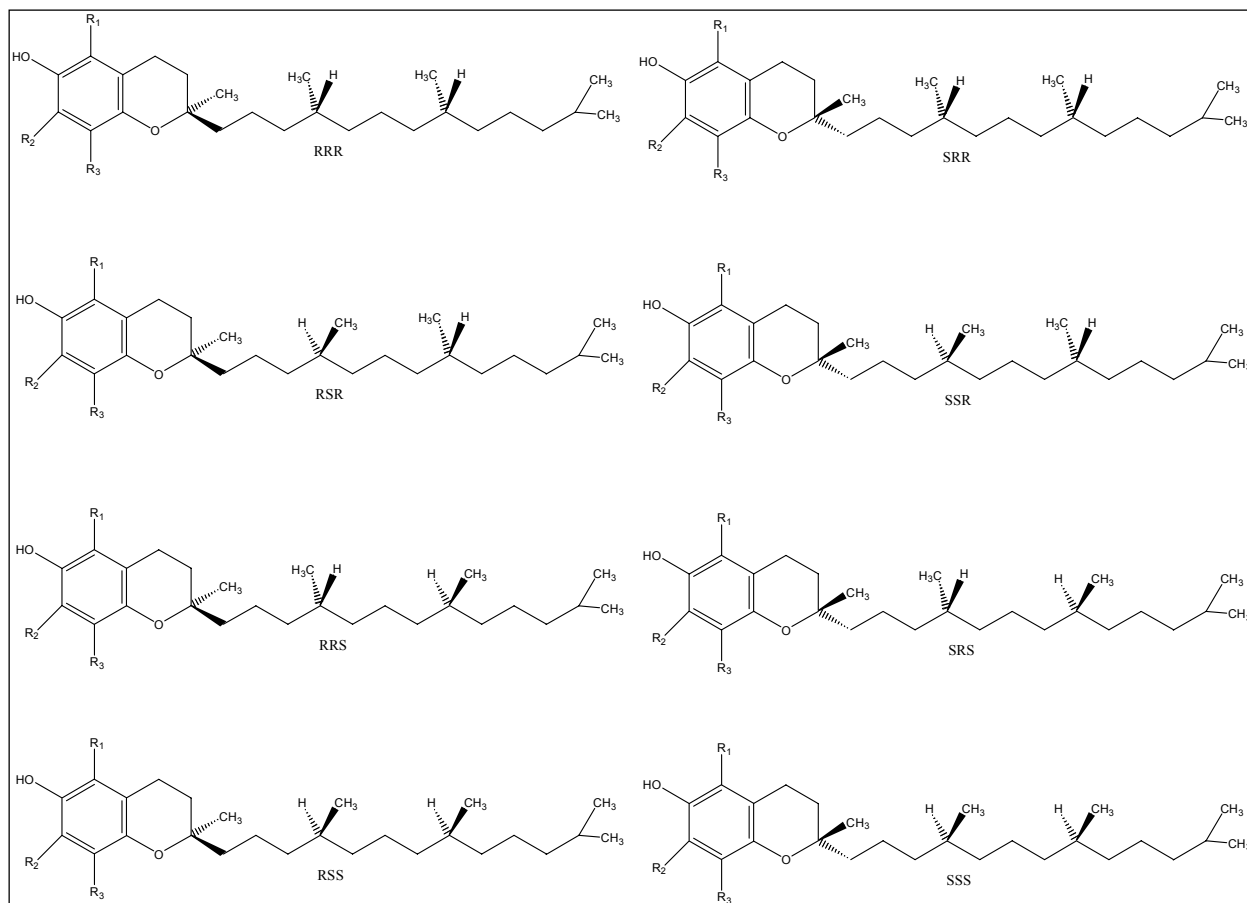


Figure 5 - Stereoisomers of tocopherols

Recently it has been suggested⁶ that the selenium congener of α -tocopherol (**Figure 6**) may be a very effective antioxidant.

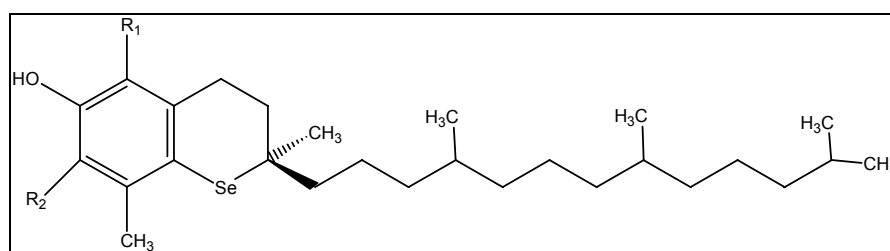


Figure 6 - The Structure of Seleno-tocopherol

This raises the question of whether the sulphur (S) and selenium (Se) congeners of Vitamin E may be more effective antioxidants than Vitamin E itself. The answer to such a question may be decided by quantitatively characterizing the redox mechanism of the three congeners containing O, S and Se, respectively.

3. INTRODUCTION

3.1 The Consequences of Oxidative Stress

One of the major current theories of aging as well as of the origin of numerous degenerative diseases is associated with a variety of free radical reactions within the human body⁷. These reactions are collectively referred to as oxidative stress.

The free radicals are generated as by-products of redox reactions associated with the metabolism⁸. The free radicals include the superoxide anion (O_2^-), the hydroperoxyl radical (HOO), hydrogen peroxide (H_2O_2) and the hydroxyl radical (HO). These are collectively referred to as "reactive oxygen species" (ROS). They are all very reactive in the body and therefore short-lived. Normally there are natural mechanisms defending against the free radicals within the body⁹, which may be enzymatic or non-enzymatic. However, if for some reason, these defence mechanisms become weakened, then the free radicals can react with cellular structures like DNA as well as proteins or destroy membranes through lipid peroxidation^{10,11,12}. It is generally believed that through these processes, aging and other age related degenerative diseases such as cardiovascular disorders and cancer, are induced⁷. Recently, oxidation of a methionine residue, as a result of oxidative stress has been implicated¹³ in the initiation of Alzheimer disease.

Vitamin E is a potent antioxidant that helps prevent cancer by blocking lipid peroxidation; the oxidation of polyunsaturated fats into free radicals. Lipid peroxidation is potentially important in all cancers but is especially significant as a cause of breast and colon cancers.

Vitamin E also serves a crucial role in immune system function. A low level of the vitamin leads to impaired antibody production, the inability to manufacture T and B lymphocytes and reduced resistance to cancer and infection.

Vitamin E works synergistically with Vitamin C and the mineral selenium (Se), with which it has a special affinity. Selenium and Vitamin E combined, constitute a 'one-two punch' against cancer. Since it is not possible to obtain optimally protective quantities of Vitamin E from diet alone, supplements of 400 to 1,600 international units daily are recommended.

3.2 Structural Background

One of the structural problems of the compounds and their basis of activity is associated with the saturated heterocyclic ring fused to the benzene ring. This ring cannot be considered to be cyclohexane or its heterocyclic analogue in a boat or chair conformation since it has, at least formally, one carbon-carbon double bond.

The so-called "half-chair" conformation had been considered to be the most likely structure, before experimental observation provided strong support for that assumption.

The ring is expected to exist in to two interconvertible enantiomeric forms. The transition state for such a ring-flip is expected to show some symmetry. It is tempting to consider the

planar structure to be a good candidate for the transition state but such a conformation could be a higher order critical point. It is more likely that the transition state is a boat conformation. (**Figure 7**)

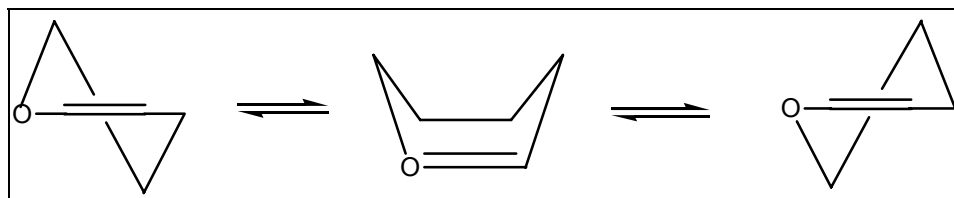


Figure 7 - Ring flip in dihydropyran

Tetralin may be regarded as the hydrocarbon analogue of such a heterocyclic ring. Of the four CH₂ groups in tetralin, the two allylic CH₂ exhibit quasiaxial or pseudoaxial (a') and, quasi-equatorial or pseudo-equatorial (e') orientation while the orientation of the central CH₂-CH₂ moiety is expected to be close to non-cyclic molecules such as ethane or butane. This is illustrated in the case of cyclohexene ¹⁴. (**Figure 8**)

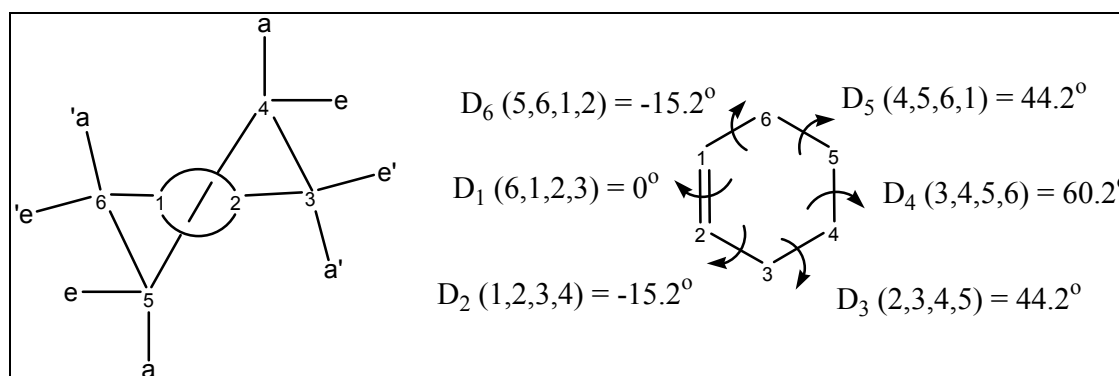


Figure 8 - Conformation and dihedral angles of cyclohexene previously obtained on the basis of molecular modelling

Thus, the further away we go from the double bond, the closer we get to the ideal situation. Estimated dihedral angles (D_i) may look like the following.

While we cannot extrapolate in a blindfolded way to the stereochemistry of the tetralin from the conformations of cyclohexene, nevertheless some analogy is expected.

4. AIM OF STUDY

In the *first phase* of the Project the structure of the chroman ring together with its S and Se congeners were studied. Naturally, one may wish to compare chroman with its hydrocarbon analog (tetralin). Tetralin(I), chroman(II) and its sulphur(III) and selenium(IV) congeners are shown below. (Figure 9)

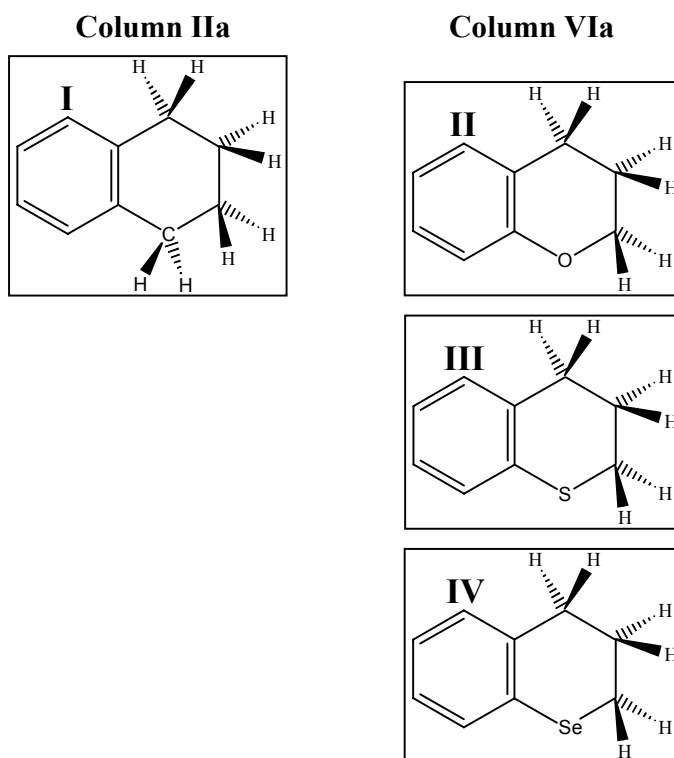


Figure 9 – Tetralin as well as chroman and its congeners, with their respective Groups in the periodic table.

In the *second phase* of the project, the conformational intricacy of a shortened model of α -tocopherol has been investigated.

In the *third phase*, the stabilization or destabilization effect of the subsequent methyl substitution on the benzene rings has been investigated with special emphasis on the α , β , γ and δ -tocopherol models.

In the *fourth phase*, an oxidative mechanistic study has been carried out on α -tocopherol, as well as α -thiotocopherol and α -selenotocopherol models to some extent.

The corresponding models are depicted in **Figure 10**.

5. METHOD

5.1 Computational Background

Since it is generally believed that the tail ends of tocopherols are only needed to enhance fat solubility¹⁵, it is appropriate to concentrate on the fused ring systems.

Due to the large size of tocopherols ($C_{28}H_{50}O_2$) and current limitations of computational resources, only model compounds were studied. The size of the various models investigated are shown below (**Figure 10**) with respect to the full tocopherol structure. Computations were carried out using the Gaussian 98 program¹⁶ “package”.

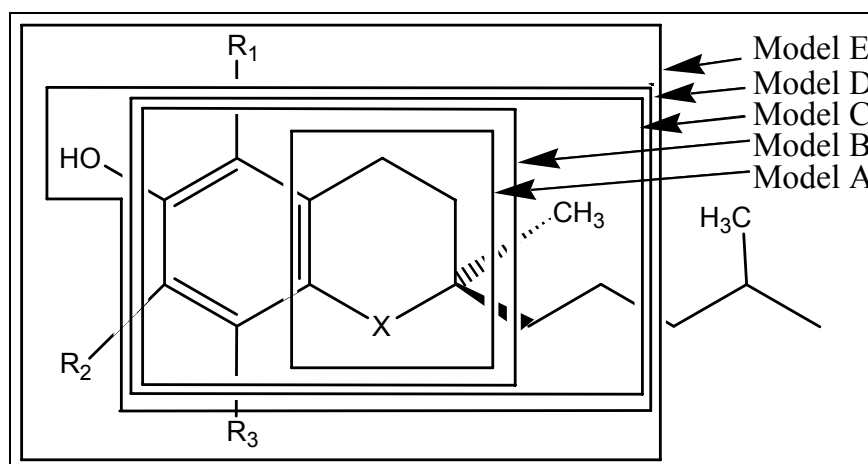


Figure 10 – Models of tocopherols

The structural stabilities were investigated on going from **Model A** through **Model E**. The redox mechanism was investigated in the case of the α -tocopherol model (**Model E**).

Convergence criteria of 3.0×10^{-4} , 4.5×10^{-4} , 1.2×10^{-3} , and 1.8×10^{-3} were used for the gradients of the RMS (root mean square) Force, Maximum Force, RMS Displacement and Maximum Displacement vectors, respectively.

Although computations have been carried out at several levels of theory, only the results obtained at the highest level [B3LYP/6-31G(d)] are reported in this dissertation.

5.2 Models A and B

Molecular computations were carried out on the following four compounds: tetralin (**I**), chroman (**II**), thiochroman (**III**), and selenochroman (**IV**) as shown in **Figure 11**. No visualization tool was used for this purpose.

For the sake of convenience, the variations of geometrical and energetic parameters from O to S to Se were fitted to quadratic functions, even though no quadratic relationships are assumed to be operative. For such graphical presentation the optimized parameters were plotted against the covalent atomic radii: O = 0.745Å, S = 1.040Å and Se = 1.163Å^{15,16}.

5.3 Models C and D

Corresponding to **Model A** through **Model D**, four families (**A**, **B**, **C**, **D**) of the four compounds (**I**, **II**, **III**, **IV**) were studied as shown in **Figure 4**. Altogether, sixteen compounds were studied. Compound **III** and **IV** are sulphur and selenium congeners of **II**.

No visualization tool was used for any computational purpose of this work. It should be noted that there are two extra hydrogen atoms in the carbon congeners (i.e. X=CH₂) of **IA**, **IB**, **IC** and **ID**. Key dihedral angles are defined in **Figure 5**.

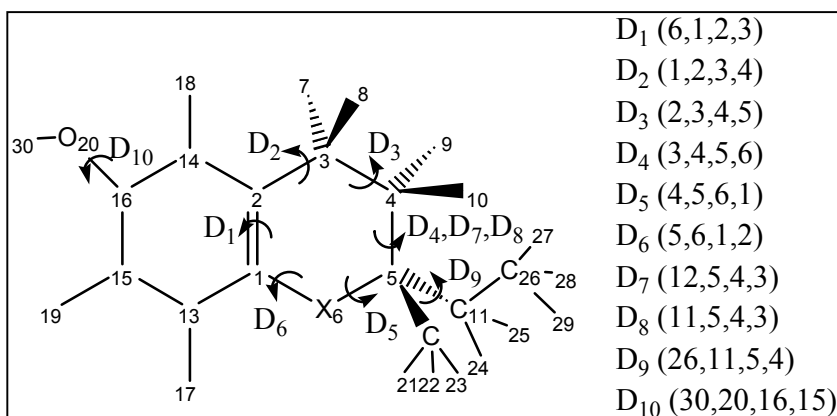
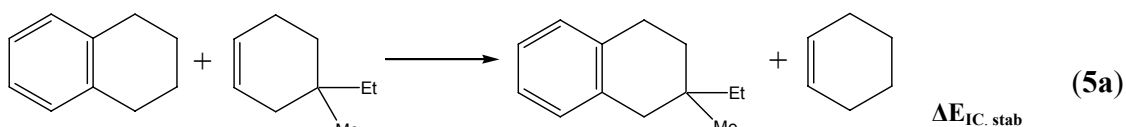
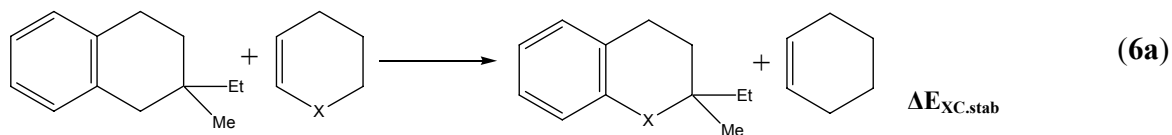


Figure 11 - Definition of key dihedral angles.

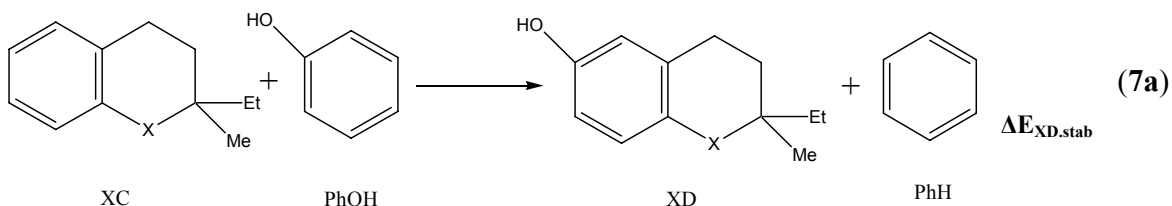


$$\Delta E_{IC,stab} = [E (IC) + E (C_6H_{10})] - [E (IB) + E (C_6H_8EtMe)] \quad (5b)$$

In order to compare the relative stabilities of the X=O, S and Se congeners, the following three isodesmic reactions were applied.



$$\Delta E_{XC.stab} = [E(XC) + E(IA)] - [E(IC) + E(XA)] \quad (6b)$$



$$\Delta E_{Total.stab} = \Delta E_{XD.stab} + \Delta E_{XC.stab} \quad (7b)$$

The overall stabilization energy is the sum of the two individual stabilization energies.

$$\Delta E_{XD.stab} = [E(XD) + E(PhH)] - [E(XC) + E(PhOH)] \quad (8)$$

For the sake of convenience, the variations of geometrical and energetic parameters from O to S and Se were fit to quadratic functions, even though no quadratic relationships are assumed to be operative. For such graphical presentation the optimized parameters were plotted against the covalent atomic radii: O = 0.745Å, S = 1.040Å and Se = 1.163Å^{17, 18}.

5.4 Model E

Eight structures, the unsubstituted and seven methyl substituted ring structures, were considered for oxygen (**II**), sulphur (**III**), and selenium (**IV**) heteroatoms in the ring. Thus, a total of 3x8=24 structures are reported on this model E. Of the seven substituted structures four are Vitamin E models (α , β , γ , δ while the remaining three (E, E*, F), two single (E, E*) and one double (F) methylated ring respectively, have no relation to Vitamin E.

The stabilization or destabilization exerted by the methyl groups attached to the aromatic ring were studied through isodesmic reactions in which the Me group was transferred from toluene to the aromatic ring of the chroman skeleton, as well as its sulphur and selenium congeners. The following B3LYP/6-31G(d) energy values were used for toluene and benzene: (-271.56662) and (-232.248659) hartrees respectively.

5.5 Redox Reaction Mechanisms

The definition of the spatial orientation as well as the numbering of the constituent atomic nuclei are shown in **Figure 3**. The input files were numerically generated. No visualization tool was used for this purpose. Abinitio Molecular orbital calculations, completed using the Gaussian as program package calculations are reported at the B3LYP/6-31G(d) levels of theory.

For the hydride abstraction, three different cations were investigated correspondingly to mild, medium and strong hydride affinity. The computed energies necessary for balanced reactions are summarized in **Table 8**. On the basis of the computed hydride affinities (**Table 8**) it seems that the $H^{(-)}$ affinity of pyridinium ion is numerically close to that of $Li^{(+)}$. For this reason, rather than NADH, Li-H may be used as a hydride donor in its place at least on energetic grounds. The computed total energies for both radical and ionic reactions are listed in **Table 9**.

Table 8 - Energy Components and hydride affinities for hydride abstraction as computed at the B3LYP/6-31G(d) level of theory

Cation	E(Hartree)	Neutral	E(Hartree)	Hydride Affinity (Kcal/mol)
Li(+)	-7.284544	LiH	-8.081922	210.57
C ₅ H ₆ N(+)	-248.656978	C ₅ H ₇ N	-249.455315	211.17
CH ₃ (+)	-39.480388	CH ₄	-40.518383	361.56

Table 9 - Energy Components, necessary to balance the redox reactions, computed at the B3LYP/6-31G(d) level of theory

Species	E(Hartree)	Species	E(Hartree)
E(H [•])	-0.461817	E(HOO [•])	-150.899156
E(HO [•])	-75.723455	E(HOO ⁻)	-150.462597
E(H ₂ O)	-76.408953	E(HOOH)	-151.532085
E(H ₃ O ⁺)	-76.685908	E(HOOLi)	-158.503570

6. RESULTS AND DISCUSSION

6.1 Molecular Structures

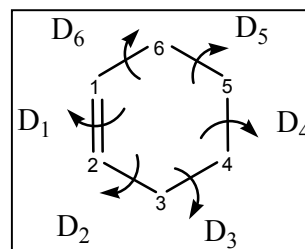
One of the structural problems of Vitamin E is associated with the saturated ring fused to the benzene ring. This ring cannot be considered to be cyclohexane, nor any of its heterocyclic analogues in the chair conformation, because it has, at least formally, one carbon-carbon double bond. The so-called “half-chair” conformation had been considered to be the most likely structure and was confirmed by experiment^{14, 19-24}.

Of the four CH₂ groups found in tetralin, the two allylic CH₂ groups exhibit quasixial or pseudoaxial (a') and quasi-equatorial or pseudo-equatorial (e') orientations. The orientation of the central CH₂-CH₂ moiety is expected to be close to non-cyclic molecules such as ethane or butane. Thus, the further one moves away from the double bond, the closer one comes to the ideal situation. Optimized dihedral angles (D_i) are shown in **Table 10**.

Table 10 – Previously reported and presently optimized dihedral angles of cyclohexene, computed at the B3LYP/6-31G(d) level of theory

Dihedrals *	Previously Reported	Present Optimized
D ₁	0.00	-1.61
D ₂	-15.20	-13.87
D ₃	44.20	44.11
D ₄	-60.20	-60.47
D ₅	44.20	44.14
D ₆	-15.20	-13.90

* as defined in **Figure 8**



The ring is expected to exist in two inter-convertible enantiomeric forms with the transition state for such a ring-flip expected to show some molecular symmetry; interconnecting the two non-super-imposable mirror image (enantiomer) minima on either side. It is tempting to consider the planar structure to be a good candidate for the transition state, but such a conformation could be a higher order critical point. It is more likely that the transition state is a boat conformation. The ring-inversion has been studied computationally only in the cases of tetralin as well as its oxygen, sulphur and selenium congeners²⁵.

6.1.1 Ring Conformations of Vitamin E models (Models A and B)

The optimized bond lengths show no deviations from expected structural behaviour. The greatest change is expected in the C-X-C region. The C-X bond length, involving the aromatic carbon is slightly shorter than the other one, involving the aliphatic carbon. These optimized bond lengths correlate linearly with the covalent radii of O, S and Se.

The C-X-C and the X-C-C bond-angles are of greatest interest as X is changed from O to S and Se. Values show that the C-X-C bond-angle is undergoing the greatest change, as O is changed to S and Se, the C-X-C bond-angle moves from a value larger than tetrahedral towards 90°, typical of S and Se. In contrast to this, the X-C-C bond-angle is compensating for such a dramatic closing in C-X-C, through a modest opening in the X-C-C values. These changes at the DFT level are evaluated as moving from 111.8°, for (X = Oxygen) to 113.5° (X = Selenium).

For the torsion of the heterocyclic ring, dihedral angles behave in an interesting way. Some dihedral angle pairs behave in non-routine fashion, as if the influence of the X nucleus on these two dihedrals was inconsequential. Other dihedral angles are similar in magnitude while others are nearly identical.

6.1.1.1 Molecular geometries at transition structures

The ring inversion (**Figure 7**) was studied in the cases of compounds **I**, **II**, **III** and **IV**. For compound **II** (X = Oxygen) the initial state, the transition state and the final states are shown in **Figure 12**. Clearly the fused heterocyclic ring exhibits a highly distorted boat arrangement (**Figure 12**) in comparison to the idealized case given in **Figure 7**.

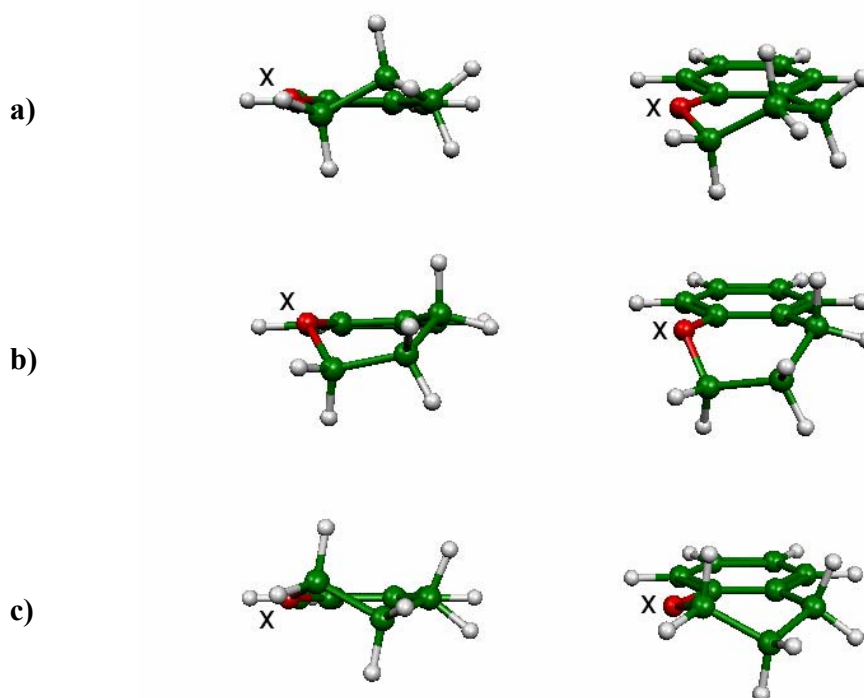


Figure 12 - Optimized minimum energy (a, c) and transition (b) structures for chroman (X=O). The sulphur (X=S) and selenium (X=Se) congeners have analogous geometries.

6.1.1.2 Energetics of Ring inversion

The energies of activations (E_a) values for the $X = [O, S, Se]$ containing molecules (**II**, **III** and **IV**, respectively) were plotted against the covalent radii of X . The difference between O and S is large while the difference between S and Se is small.

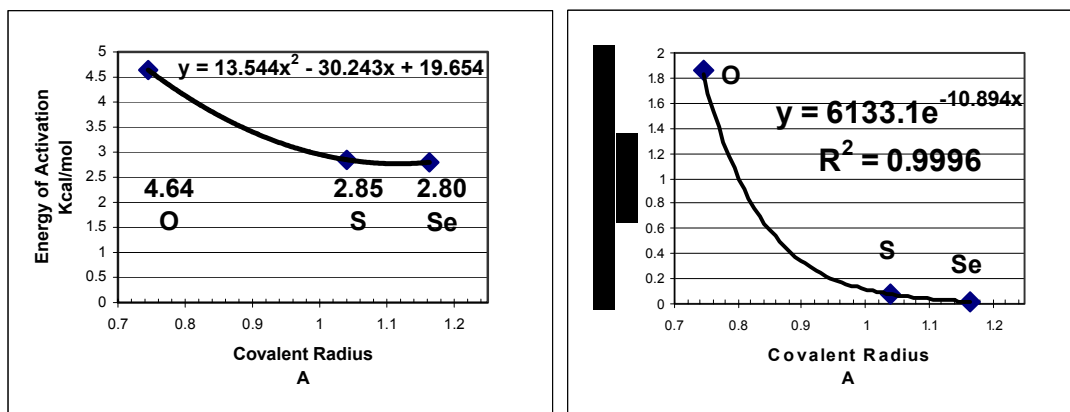


Figure 13 – Variation of ring inversion energy of activation with the size of the heteroatom

The left hand side plot shows a quadratic fit while the right hand side plot shows an exponential fit only after it was determined that the exponential function converges to $2.78 \text{ Kcal}\cdot\text{mol}^{-1}$.

6.1.2 Ring Substitutions of Vitamin E models (Models C and D)

6.1.2.1 Molecular Geometry of Stable Structures

The geometry exhibited changes with heteroatom substitution. The increasing atomic size created by the progression from oxygen to sulphur, then to selenium made a noticeable difference for selected bond length, bond angles and dihedral angles.

Changes in C-C bond lengths and bond angles about a carbon atom are influenced slightly by the nearby O, S or Se. However, the changes are not large and their change is not necessarily monotonic, as one would expect on the basis of the periodic table ($O \rightarrow S \rightarrow Se$). Very often the parameter in question for sulphur is either smaller or larger than that for the oxygen and selenium-containing compound.

Take for example the bond angle between the three saturated carbon atoms C-C-C* (where C* is the stereocentre) in **Model D** the following non-monotonic change was observed.

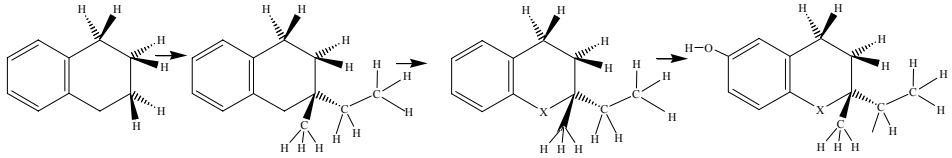


On going from the single heterocyclic ring (**A**) to the next larger system where a benzene ring is fused to the heterocycle (**B**), large amplifications in dihedral angles were noticed. This amplification was followed by two consecutive attenuations on going from **B** to **C** and subsequently, from **C** to **D**. The final system (**D**) did not differ much from the original (**A**) ring structure.

6.1.2.2 Molecular Energetics

The computed total energies are not comparable since each of the sixteen molecular systems has a different number of electrons. In order to make an energetic comparison of the sixteen molecular structures, some isodesmic reaction energy calculation should be made in order to determine the relative stabilization or destabilization exerted by the substituents on the basic structures. The calculations were carried out according to equations given in the Method Section: (3) – (6). Stabilization energies are summarized in **Table 6**.

Table 11 – Computed stabilization energies resulting from sequential substitution, computed at the B3LYP/6-31G(d)



IB	IB → IC	X	IC → XC	XC → XD	Total	O → X
0.00	0.344	O	-6.412	1.592	-4.820	0.000
		S	0.428	0.759	+1.188	6.008
		Se	-5.293	0.566	-4.726	0.094

The stabilization energies reveal that oxygen and selenium substitutions stabilize the ring system more or less to the same extent; -4.8 and -4.7 $\text{Kcal}\cdot\text{mol}^{-1}$, respectively. However, sulphur destabilizes the same ring system marginally ($+1.2$ $\text{Kcal}\cdot\text{mol}^{-1}$)

It is clear from the plot of $\Delta E_{\text{total stabilization energy}}$ against the covalent radii that O and Se are similar but S is completely different. (**Figure 14**)

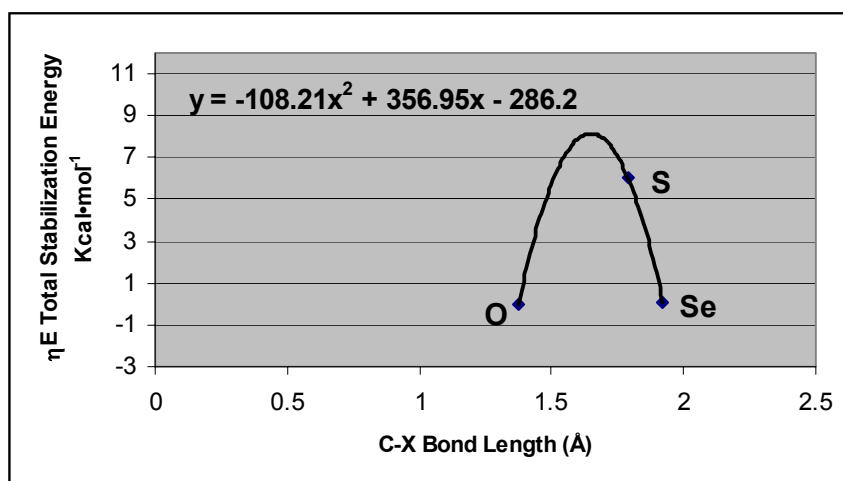


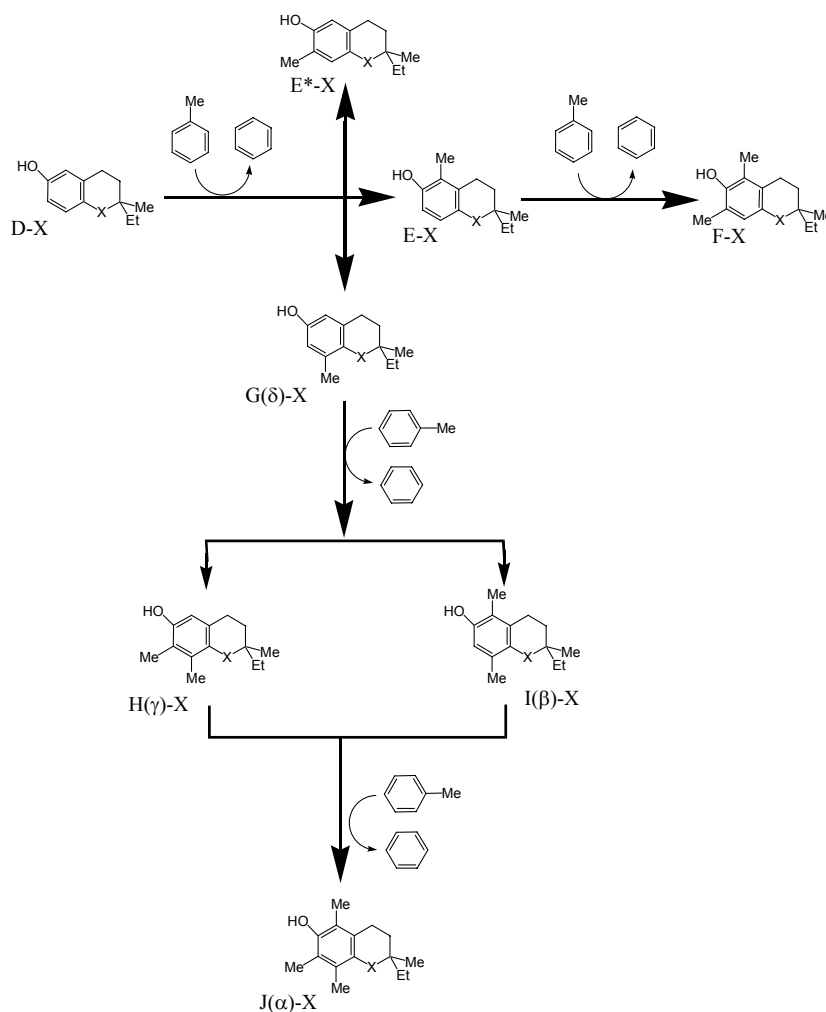
Figure 14 – Variation of total stabilization energy with C-X bond length (X=O, S, Se)

6.1.3 Aromatic Methyl Substitution of Vitamin E models (Models E)

6.1.3.1 Molecular Geometries

A total of twenty-four compounds were subjected to geometry optimizations. Of that total, each of the oxygen, sulphur, and selenium containing rings each had 8 homologues containing 0, 1, 2 and 3 methyl groups attached to the aromatic ring.

The structures of the 8 homologues are shown in **Figure 15**.



The structures of the triple methylated aromatic ring ($J(\alpha)$ -homologues) for the O, S and Se congeners computed at the B3LYP/6-31G(d) level of theory, are shown in **Figure 16**.

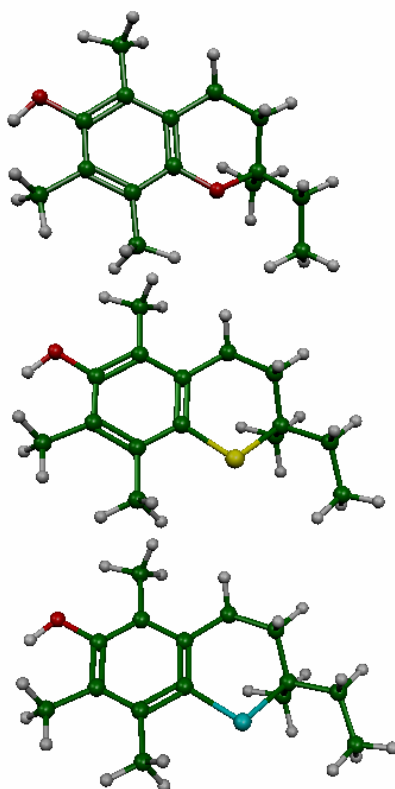


Figure 16 - Three optimized structures of the shortened sidechain model of the α -tocopherol computed at the B3LYP/6-31G(d). X=O (top), X=S (middle), X=Se (bottom)

The hydroxyl group (OH) was almost always coplanar with the aromatic ring (within $\pm 3^\circ$), deviating at most up to $\pm 7^\circ$ as a result of the steric ‘congestion’ arising from the six-fold substitution on the benzene ring. The orientation of the OH was such that it pointed away from the adjacent CH_3 group, whenever the structure would permit.

There were some structural trends, whereby the C-C bonds adjacent to the C carrying the Me substitution are lengthened, irrespective of heteroatom substitution. In contrast, the bond angles changed extensively with heteroatom substitution, irrespective of Me substitution. Several other structural trends of smaller magnitude are also apparent but not elaborated upon here.

6.1.3.2 Molecular Energetics

The computed total energies are summarized in **Table 12**. The energies of stabilization calculated according to the scheme given in **Figure 15** are tabulated in **Table 13**. The graphical representation of these results is shown in **Figure 17**.

Table 12 – Total energies (Hartrees) computed for the 24 optimized structures computed at the B3LYP/6-31G(d) level of theory

	II(O)	III(S)	IV(Se)
D	-617.36422	-940.33278	-2941.52972
E	-656.68052	-979.64832	-2980.84517
E*	-656.68287	-979.65164	-2980.84873
F	-695.99823	-1018.96614	-3020.16312
G(δ)	-656.68269	-979.65015	-2980.84932
H(γ)	-695.99754	-1018.96431	-3020.16386
I(β)	-695.99890	-1018.96543	-3020.16461
J(α)	-735.31221	-1058.27721	-3059.47685

Table 13 – Energy of stabilization associated with single or multiple methyl group transfers computed at the B3LYP/6-31G(d) level of theory

	II(X=O)		III(X=S)		IV(X=Se)	
	single step	accumulated steps	single step	accumulated steps	single step	accumulated steps
XD->XE	1.043	1.043	1.520	1.520	1.576	1.576
XD->XE*	-0.430	-0.430	-0.562	-0.562	-0.658	-0.658
XE->XF	0.161	1.204	0.090	1.610	0.007	1.583
XD->XG(δ)	-0.320	-0.320	0.372	0.372	-1.028	-1.028
XG(δ)->XH(γ)	1.952	1.633	2.386	2.759	2.147	1.118
XG(δ)->XI(β)	1.100	0.781	1.684	2.056	1.676	0.648
XI(β)->XJ(α)	2.918	3.699	3.879	5.934	3.587	4.235

Non-Natural Models of Vitamin E

α, β, γ, δ-Tocopherol

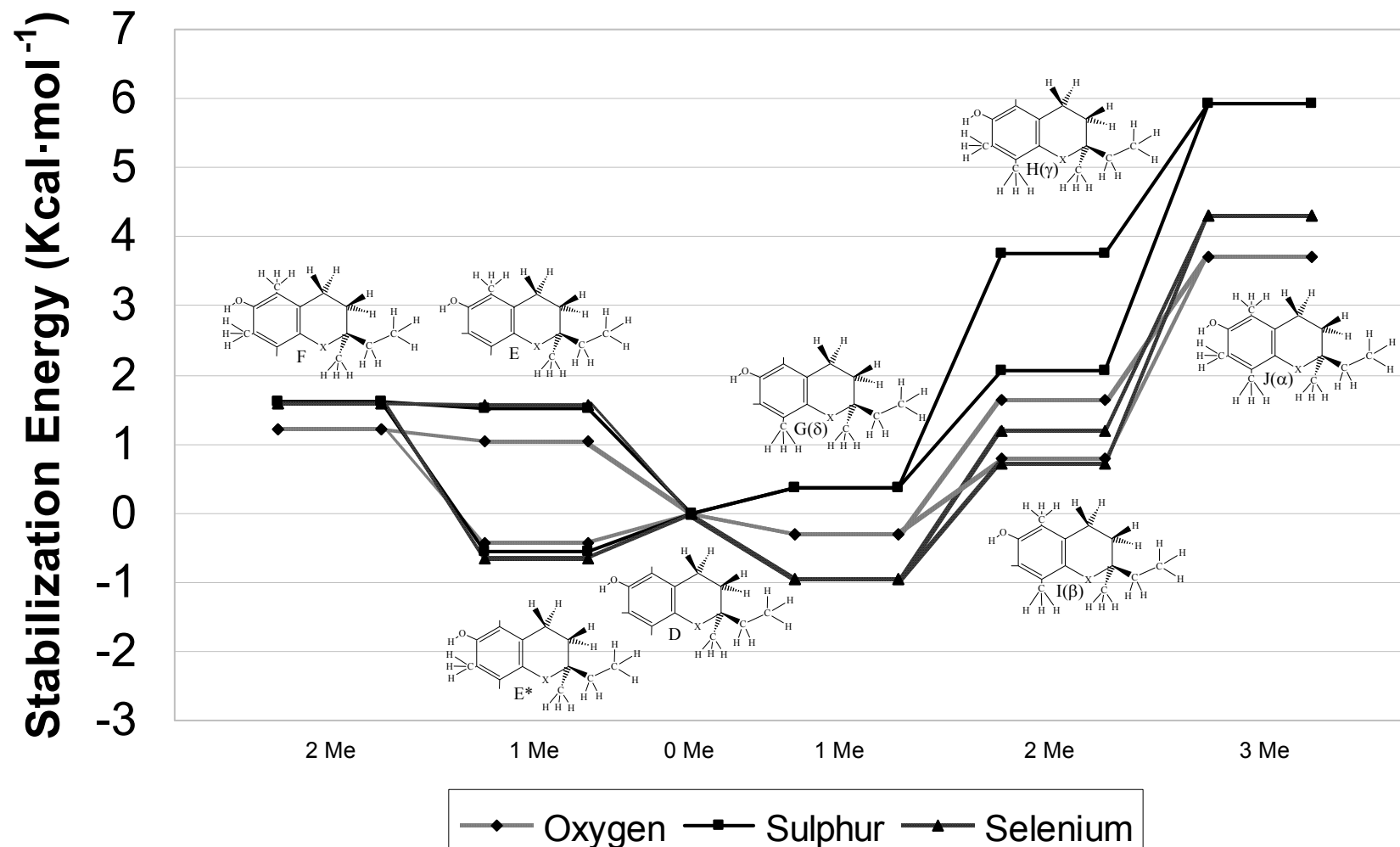


Figure 17 - Computed stabilization energies, determined at the B3LYP/6-31G(d) level of theory.

The extent of the naturally occurring (α , β , γ , δ) tocopherol are shown below in **Figure 18**.

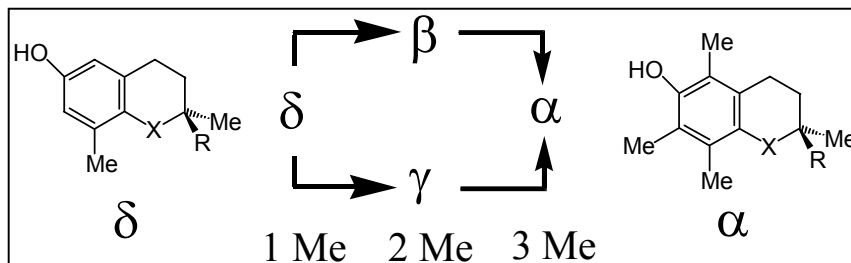


Figure 18 – Aromatic methyl substitution of α , β , γ and δ tocopherol

A comparison of the relative activity of z-tocopherols ($z = \alpha, \beta, \gamma, \delta$), as measured by $\ln\{[A_z]/[A_\alpha]\}$, may be envisaged as a functional dependence using the calculated energy of stabilization (ΔE_z) as an independent variable.

$$\ln \{[A_z]/[A_\alpha]\} = F(\Delta E_z) \quad (10)$$

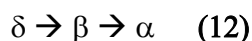
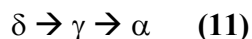
The numerical values are given in **Table 14**.

Table 14 – Relative biological activity of tocopherols and computed stabilization energy values of model compounds, determined at the B3LYP/6-31G(d) level of theory.

Relative Activity *			Computed Stabilization Energy		
z-tocopherol	$[A_z]/[A_\alpha]$	$\ln\{[A_z]/[A_\alpha]\}$	$1 - \ln\{[A_z]/[A_\alpha]\}$	ΔE_z	$\Delta\Delta E_z = \Delta E_\alpha - \Delta E_z$
α	1.000	0.000	0.000	3.698	0.000
β	0.570	-0.562	1.562	0.780	2.918
γ	0.370	-0.994	1.994	1.634	2.054
δ	0.014	-4.269	5.269	-0.318	4.016

* Activities were taken from Reference [3], also quoted in **Table 3** of Reference [13]

Plotting the above equation yielded graphs that suggested that there may exist an exponential relationship interconnecting either one, or both, of the paths shown below:



For this reason the relationship is converted to the following form:

$$y = 1.0 - \ln\{[A_z]/[A_\alpha]\} = f(\Delta\Delta E_z) = f(x) \quad (13)$$

where $x = \Delta\Delta E_z = \Delta E_\alpha - \Delta E_z$

The exponential function obtained for the first ($\delta \rightarrow \gamma \rightarrow \alpha$) of these two paths is shown in **Figure 19**. While the fit shown in **Figure 19** was fairly good ($R^2=0.99$), the other path ($\delta \rightarrow \beta \rightarrow \alpha$) did not allow a fit to a reasonably good exponential function. With respect to the exponential fit obtained for the $\delta \rightarrow \gamma \rightarrow \alpha$ path, it seemed that β was estimated to be less stable by 1.750 Kcal/mol.

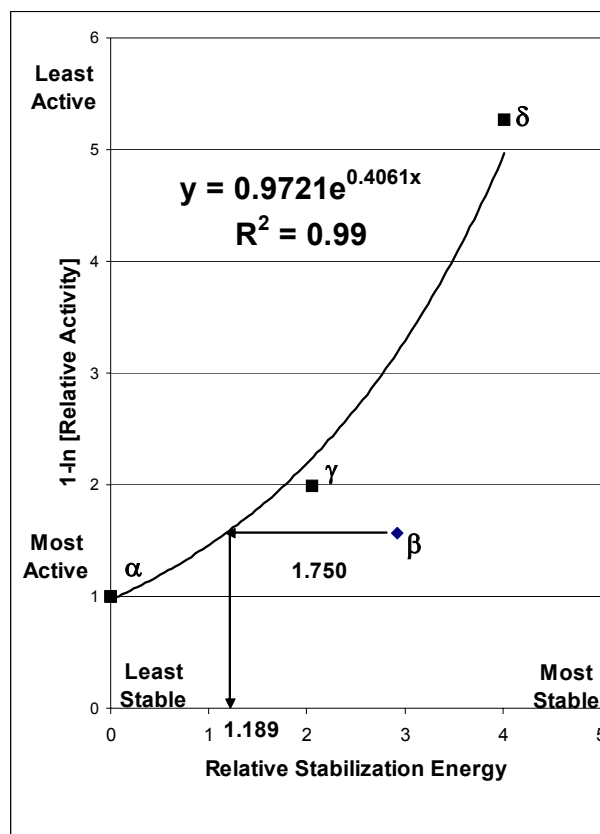


Figure 19 - Modified relative activity of tocopherol vs relative stabilization energies of tocopherol model

While we have no explicit structured explanation for this derivation, it should be pointed out that the two methyl groups in the β form are in *para*-position with respect to each other. This would suggest that any electronic effects the Me-groups might exert on the aromatic ring would be cancelled, or nearly cancelled, by vectorial addition. For this reason, all the dipole moments were computed, revealing a reduction in polarity when the two *para* Me groups were present.

This data showed that homologous E, F, I(β), and J(α) have dipole moments less than 1 debye due to partial cancellation of electronic effects while homologous D, E*, G(δ) and H(γ) have dipoles over 2 debye. This is the case for all three congeners. Note that the J(α), I(β), H(γ), G(δ) homologues are Vitamin E compounds while D, E, E* and F homologues are not members of the Vitamin E family.

The question of arithmetical additivity in the stabilization or destabilization effects of these Me-groups on the chroman ring and its congeners has to be examined at least in passing. The results are shown in **Table 15**.

Table 15 – Energies of stabilizations calculated as a sum of components or through direct computations

	II(X=O)		III(X=S)		IV(X=Se)	
	Sum of Components	Directly Calculated	Sum of Components	Directly Calculated	Sum of Components	Directly Calculated
XE + XE* -> XF	0.613	1.205	0.958	1.613	0.918	1.581
XG(δ) + XE* -> XH(γ)	-0.750	1.634	-0.190	3.758	-1.094	1.183
XG(δ) + XE -> XI(β)	0.723	0.780	1.892	2.055	0.548	0.712
XI(β) + XE* -> XJ(α)	0.350	3.698	1.494	5.933	-0.010	4.301

It appears that the stabilization energies are not additive, indicating that in addition to the electronic effects, steric ‘congestion’ occurs when the methyl groups are proximally introduced. Such an observation has been noted by Hammett [16] in studying chemical reactivity. When the substituents were far away from the reaction site, good correlation was observed between reactivity and structure. Alternatively, when substituents were placed in an *ortho*-position, the points scattered randomly and did not correlate at all. Thus, the Hammett linear free-energy relationship is valid only when the substituents are far away from the reaction site.

For the I(β) isomers, where the two Me-groups are in *para*-position with respect to each other, the discrepancy is within 0.2 Kcal* mol^{-1} . For the F isomers, where the Me groups are in *meta*-position with respect to each other, the discrepancy is within 0.7 Kcal/ mol^{-1} . In these two cases the Me groups are virtually independent of each other. However, when two Me groups are in an *ortho*-orientation, the discrepancy is 4.3 Kcal* mol^{-1} , indicating that steric destabilizing congestion dominates over electronic stabilizing effects.

6.2 Redox Reaction Mechanism

6.2.1 The dichotomy of anti-oxidant and pro-oxidant nature of Vitamin E

It is generally accepted that reduction of morbidity and mortality from cardiovascular disease is associated with an increased intake of antioxidant Vitamin E and Vitamin C. This apparent cause-causality relationship has been explained on the basis of oxidative modification of low density lipoprotein (LDL). The corollary of this assumption is that the inhibition of lipid peroxidation in LDL, by Vitamin E, leads to the reduction of myocardial infarction and stroke. Numerous papers testify along this line^{26, 27, 28}.

However, not only does Vitamin E behave as a non-anti-oxidant²⁹, but pro-oxidant³⁰ effects of Vitamin E have also been demonstrated. The fact that Vitamin E can act as both anti-oxidant and pro-oxidant has led to the point that Vitamin E is known as a “Janus molecule”³¹.

The free radical oxidation products of α -tocopherol have been analyzed by Liebler et al³² in 1996, showing other more extensively oxidized products than the quinoidal structure. The ionic mechanism was suggested by Roseman et al;³³ in 1999 which has led to the quinoidal structure. These mechanisms were also reviewed recently by Brigelius-Flohe and Traber³⁴.

Under strong oxidative conditions Vitamin E may undergo progressively more extensive oxidation that could lead to irreversible metabolization of the tocopherol molecule. Such a destructive oxidation³², leading to a variety of epoxides, which may metabolize even further is shown in **Figure 20**. Note that the steps in the left hand column in **Figure 20** are non-destructive as it corresponds to the formation of quinone-hydroquinone analogues of Vitamin E. Nevertheless, there exists an ionic oxidative mechanism of α -tocopherol leading to a quinoidal or even to a hydroquinone structure³³ shown in **Figure 21**. However, some side reactions may occur with the left hand column of **Figure 21** showing the non-destructive process.

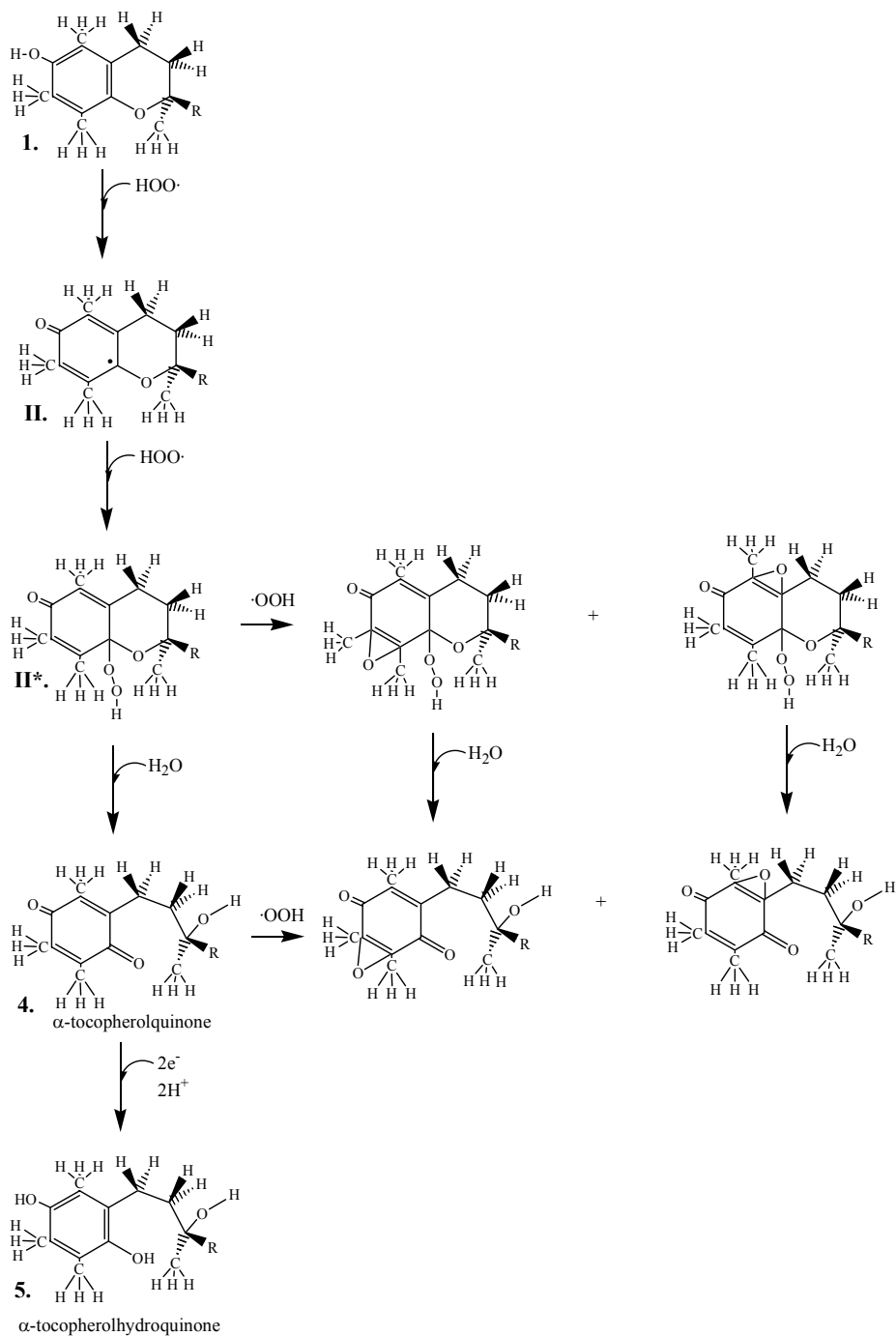


Figure 20: A schematic mechanistic representation of non-destructive (left column) and destructive (right column) free radical oxidation of α -tocopherol by $\text{HOO}\cdot$.

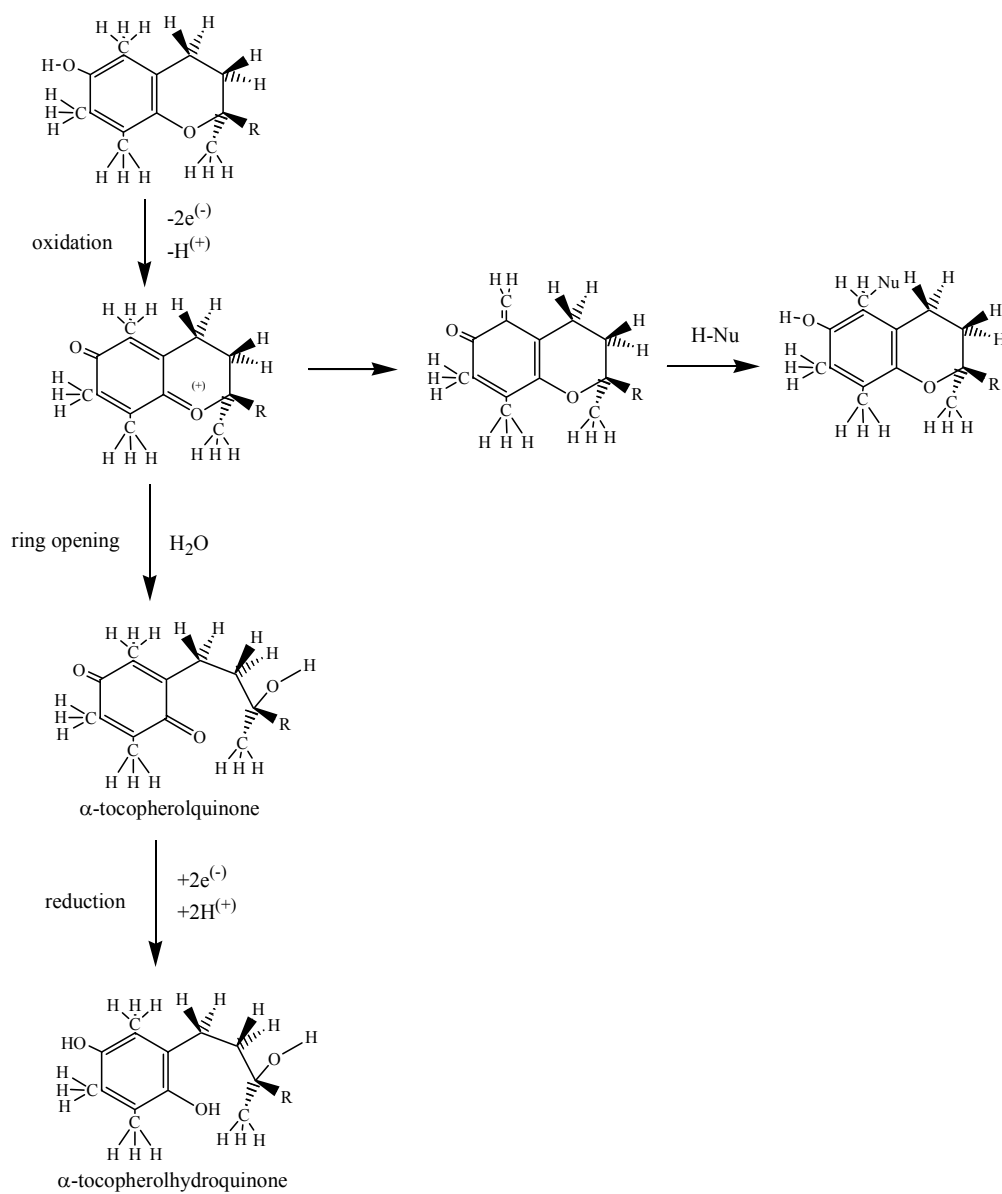


Figure 21 - A schematic mechanistic representation of non-destructive (left side) and destructive (right side) ionic oxidation of α-tocopherol.

The free radical as well as an ionic mechanism studied in the present dissertation is shown in **Figure 22**.

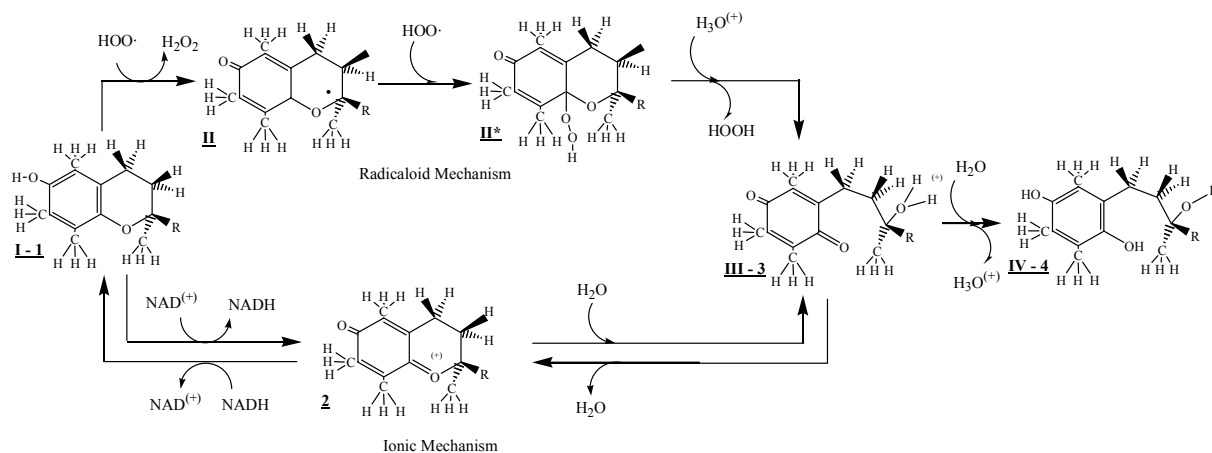


Figure 22 – Radical and ionic mechanism of α-tocopherol oxidation.

At this time several questions may be raised and some putative answers may be provided, in relation to the dichotomy of the anti-oxidant as well as pro-oxidant nature of Vitamin E.

Of course one may argue that the anti-oxidant and pro-oxidant nature of Vitamin E depends on the redox potential. In turn, the redox potential varies accord to the Nernst equation (14).

$$E = E^0 - \frac{RT}{v} \ln \left\{ \frac{[\text{Red}]}{[\text{Ox}]} \right\} \quad (14)$$

where v is the number of electrons transferred and the expression $[\text{Red}]/[\text{Ox}]$ measures the ratio of reduced to oxidized forms.

Nevertheless, it seems plausible to seek explanation at the molecular level concerning the “traffic” which is passing through the overall reduction presented in Figure 22.

Sufficient computed results are presented to provide theoretical backing to the merit of the questions to be asked along with some suggested putative mechanistic answers.

6.2.2 Molecular geometries

In the ionic mechanism, only compounds labelled **1** and **5**, have unsaturated benzenoid rings. The intermediates labelled as **2** and **3** and the product molecule labelled as **4**, have quinoidal bonding. However, the quinoidal structure for **4** can clearly be seen in **Figure 5** and compared to the original Vitamin E model **1**. In the free radical mechanisms reactant is labelled as **I**, intermediates as **II** and **II***, while the products are specified as **III** and **IV**. Clearly **1=I**, **3=III** and **4=IV**. Reduced and oxidized structures are shown in **Figure 23**.

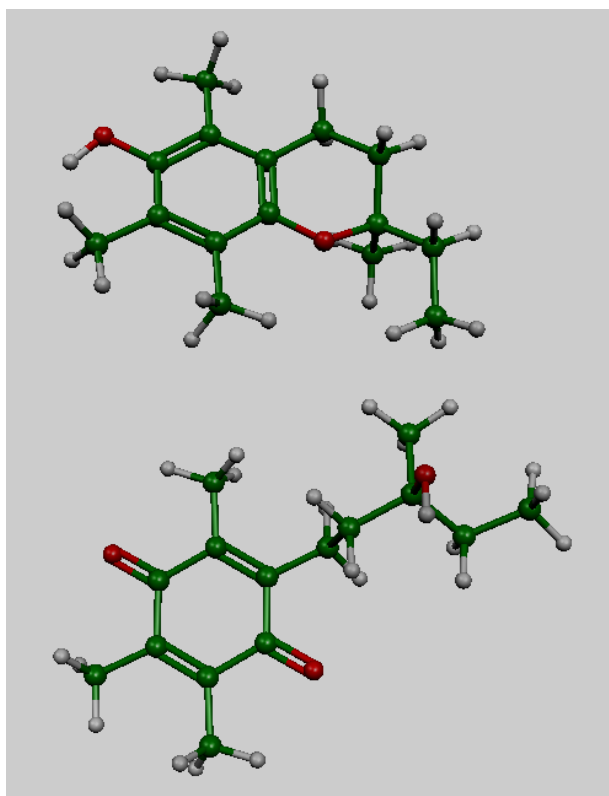


Figure 23 - Structures of α -tocopherol (top) and α -tocopherolquinone, geometry optimized at the B3LYP/6-31G(d) level of theory, corresponding to reduced [Red] and oxidized [Ox] forms, respectively, in equation (2), optimized at the B3LYP/6-31G(d) level of theory. All aromatic CC bond lengths in the top structure are in the vicinity of 1.40Å. The single and double bond lengths in the ring of the bottom structures are in the vicinity of 1.49Å and 1.35Å respectively

6.2.3 Free radical oxidative ring opening mechanism for α -tocopherol

Figure 24 shows the energy profile for the free radical mechanism on the basis of the data presented in **Tables 16 and 17**. The energies of water and oxonium ions necessary for the mechanism are shown in **Table 9** in the **Method** section. The thermodynamic reaction profile showing only energy minima, allows a down-hill process in the thermodynamic sense. Consequently, the radical scavenging ability of α -tocopherol is well established on energetic grounds.

Table 16 - Total energy values of α -tocopherol model and its oxidized forms computed at the B3YP/6-31G(d) level of theory

reactant, intermediates, product	E (Hartree)			
	Free Radical Route		Ionic Route	
reactant	I	-735.31212	1	-735.31212
closed ring intermediate	II	-734.69317	2	-734.45881
closed ring intermediate	II*	-885.63012		-
open ring intermediate	III	-810.84221	3	-810.84221
product	IV	-810.51082	4	-810.51082

Table 17- Total and relative energies for the free radical mechanism

Route	State	E(Hartree)	ΔE (Kcal·mol ⁻¹)	$\Delta\Delta E$ (Kcal·mol ⁻¹)
Neutral	I + 2HOO· + H ₃ O ⁺ + H ₂ O	-1190.205294	0.000	0.000
	II + HOO· + HOOH + H ₃ O ⁺ + H ₂ O	-1190.219272	-8.771	-8.771
	II* + HOOH + H ₃ O ⁺ + H ₂ O	-1190.257066	-32.487	-23.716
	III + 2HOOH + H ₂ O	-1190.315332	-69.050	-36.563
	IV + 2HOOH + H ₃ O ⁺	-1190.260897	-34.892	34.159

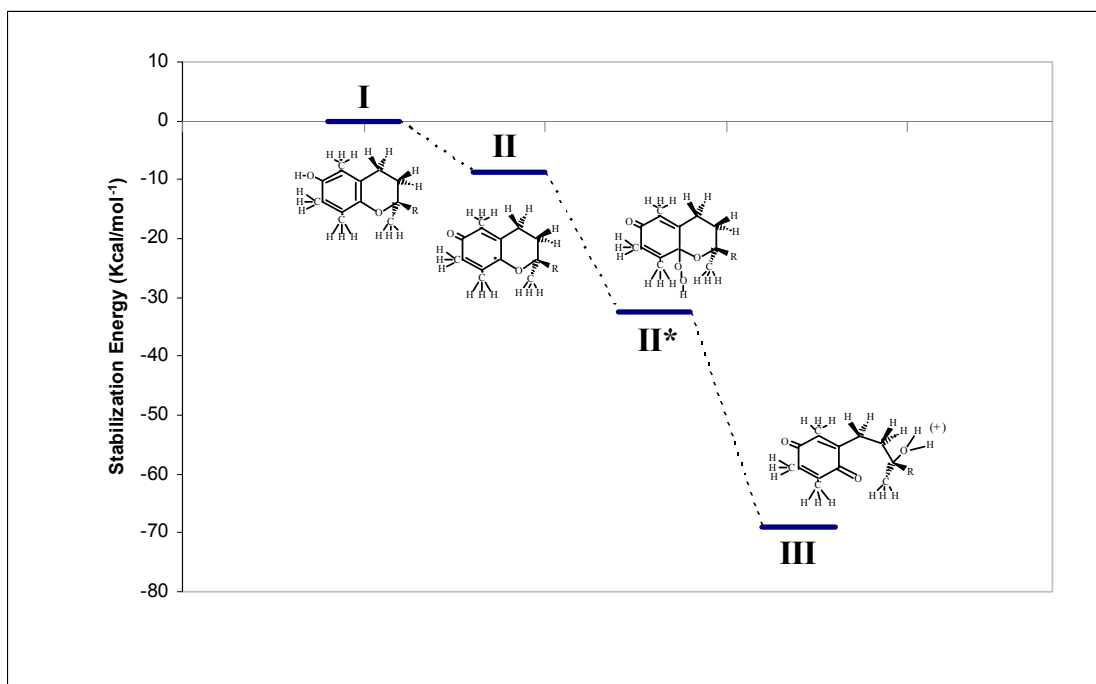
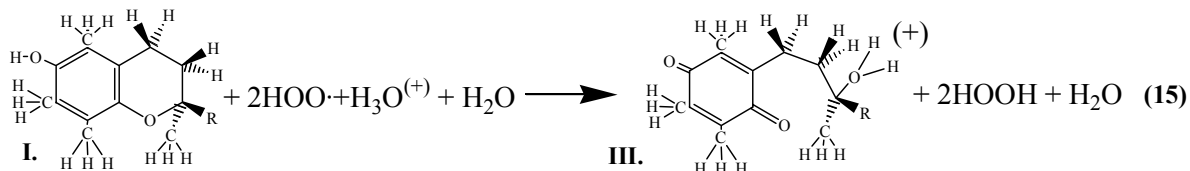


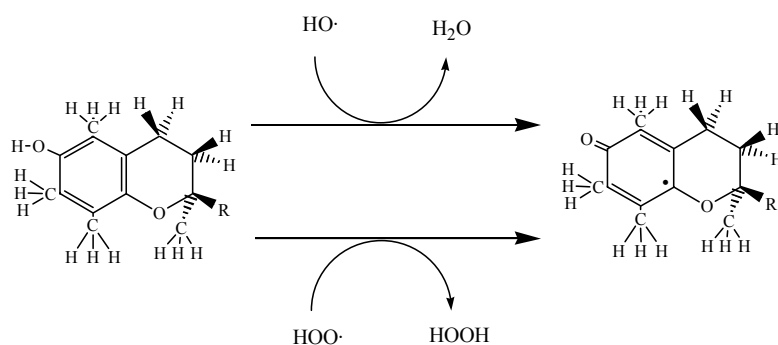
Figure 24 - Reaction profile of non-destructive free radical oxidation of α -tocopherol model by HOO·.

The reaction is balanced from reactant (**I**) to the first ionic product (**III**) as shown in equation (3).



The overall amount of energy released is $-32.49 \text{ Kcal}\cdot\text{mol}^{-1}$.

While the first step (hydrogen abstraction), may occur by either $\text{HO}\cdot$ or $\text{HOO}\cdot$ attack, the energetics are expected to be considerably more exothermic, by about $-32.4 \text{ Kcal}\cdot\text{mol}^{-1}$, with the $\text{HO}\cdot$ radical than with the $\text{HOO}\cdot$ radical.



This would only underline the validity of the conclusion reached when the $\text{HOO}\cdot$ radical is used.

6.2.4 Ionic Oxidative Ring Opening Mechanism for α -tocopherol

The relative energies necessary to construct a thermodynamic reaction profile for the ionic reactions are summarized in **Table 16** and **18**. The thermodynamic reaction profile (only energy minima, without the appropriate transition states) is shown in **Figure 25** for α -tocopherol. The energies of water and oxonium ions necessary for the mechanism are shown in **Table 9**.

Table 18- Total and relative energies for the ionic mechanism

Hydride Abstraction Initiator	State	E(Hartree)	$\Delta E \text{ (Kcal}\cdot\text{mol}^{-1})$	$\Delta\Delta E \text{ (Kcal}\cdot\text{mol}^{-1})$
Li^+	1 + Li^+ +2 H_2O	-895.414570	0.000	0.000
	2 + LiH +2 H_2O	-895.358638	35.098	35.098
	3 + LiH + H_2O	-895.333085	51.133	16.035
	4 + LiH + H_3O^+	-895.278650	85.291	34.159

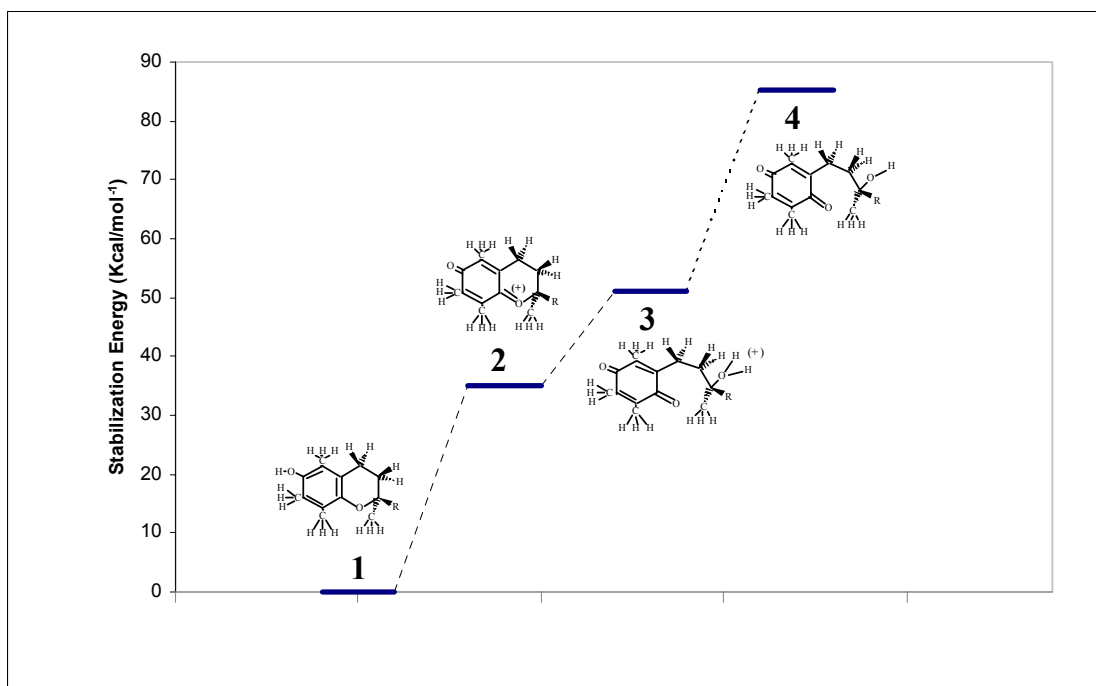
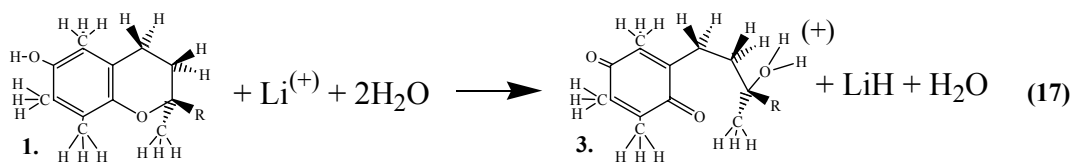


Figure 25 - Reaction profile for ionic oxidation mechanism using $\text{Li}^{(+)}$, a hydride abstractor modeling $\text{NAD}^{(+)}$

It should be emphasized that the first step involves a hydride acceptor; in biological systems it is $\text{NAD}^{(+)}$. However no full computations have been accomplished at the DFT level for the $\text{NAD}^{(+)}/\text{NADH}$ system due to its large size. Protonated pyridine gives hydride affinity close to that of $\text{Li}^{(+)}$ therefore this model appears to be fairly realistic for $\text{NAD}^{(+)}$, at least on energetic grounds.

The reaction was balanced from the reactant (**1**) to the first ionic product (**3**) as shown in (17), using $\text{Li}^{(+)}$ instead of $\text{NAD}^{(+)}$.



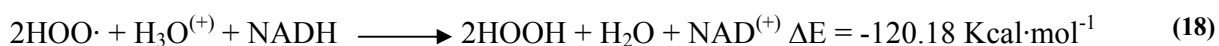
The overall amount of energy change is $+85.35 \text{ Kcal}\cdot\text{mol}^{-1}$.

6.2.5 Ionic Reductive Ring Closing Mechanism in α -Tocopherol

It is clear from **Figure 25** that the steps are all endothermic. This indicates that the ionic mechanism is unlikely to occur. However, the reverse process, namely the reduction back from the oxidized α -tocopherol (i.e. α -tocopherolquinone) to the original α -tocopherol, would be expected to be an exothermic process. Thus, it seems that the oxidation proceeds by a free radical mechanism while the reductive conversion, back to α -tocopherol, would be expected to proceed *via* the ionic mechanism. This combined mechanism is shown in **Figure 26**.

It is believed that the coupled nature of the radical and ionic redox process is shown in **Figure 26** for the first time. The energy profile for the combined mechanism is illustrated in **Figure 27**.

Since α -tocopherol has been used but not consumed in the coupled reaction, α -tocopherol may be regarded as a catalyst for the following overall processes.



The essential point is, however, that α -tocopherol can convert the peroxyradical only to hydrogen peroxide [H_2O_2] but not further. From that point outward, it is the duty of the enzyme glutathione peroxidase $\text{GP}_x(\text{Se})$ or catalase(Fe) to carry the process further through the full reduction, to H_2O .

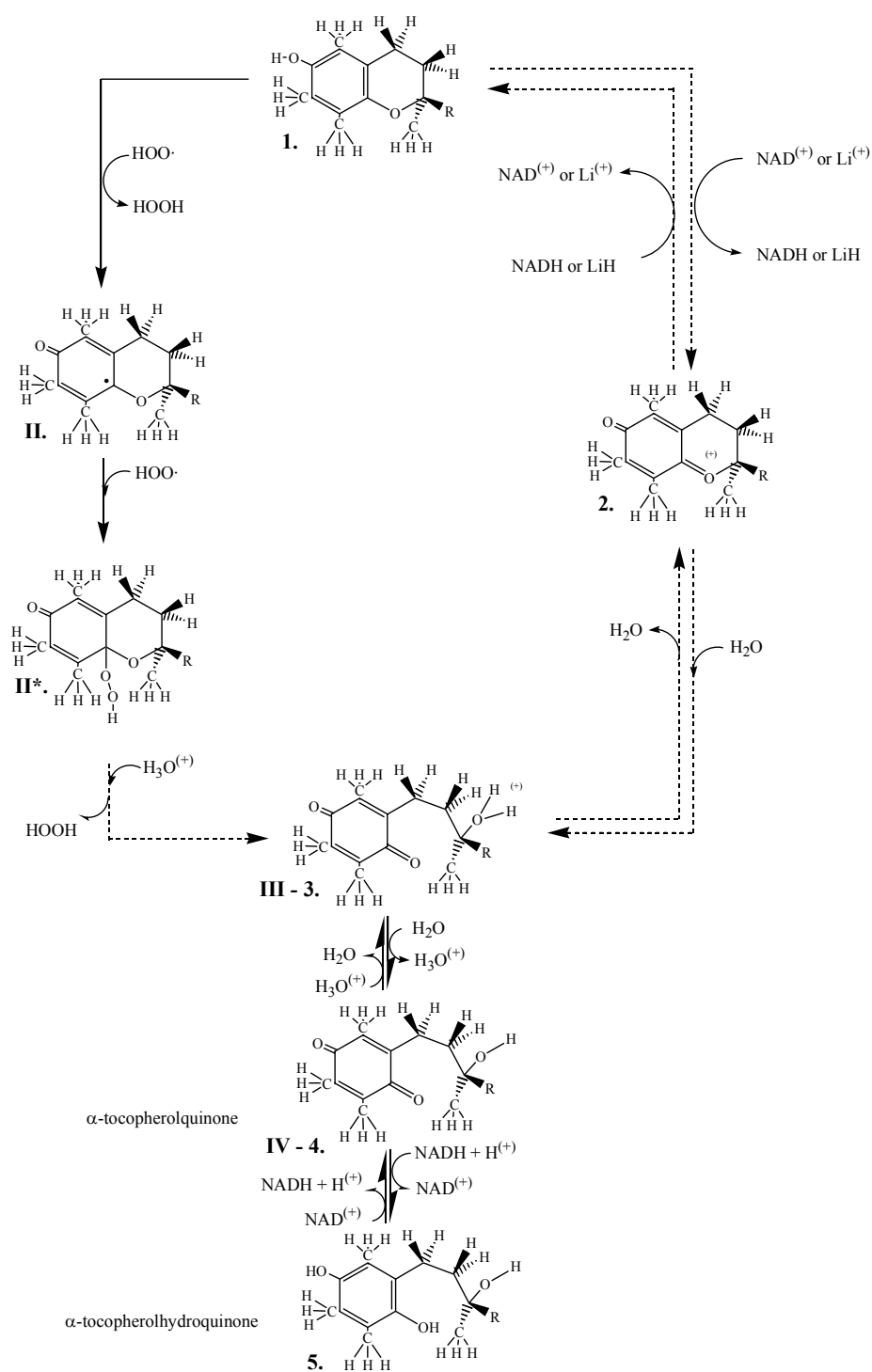


Figure 26 - The connection of a combined non-destructive free-radical and reversible ionic mechanism of oxidation of α -tocopherol quinone. Note the reversible nature of the ionic process.

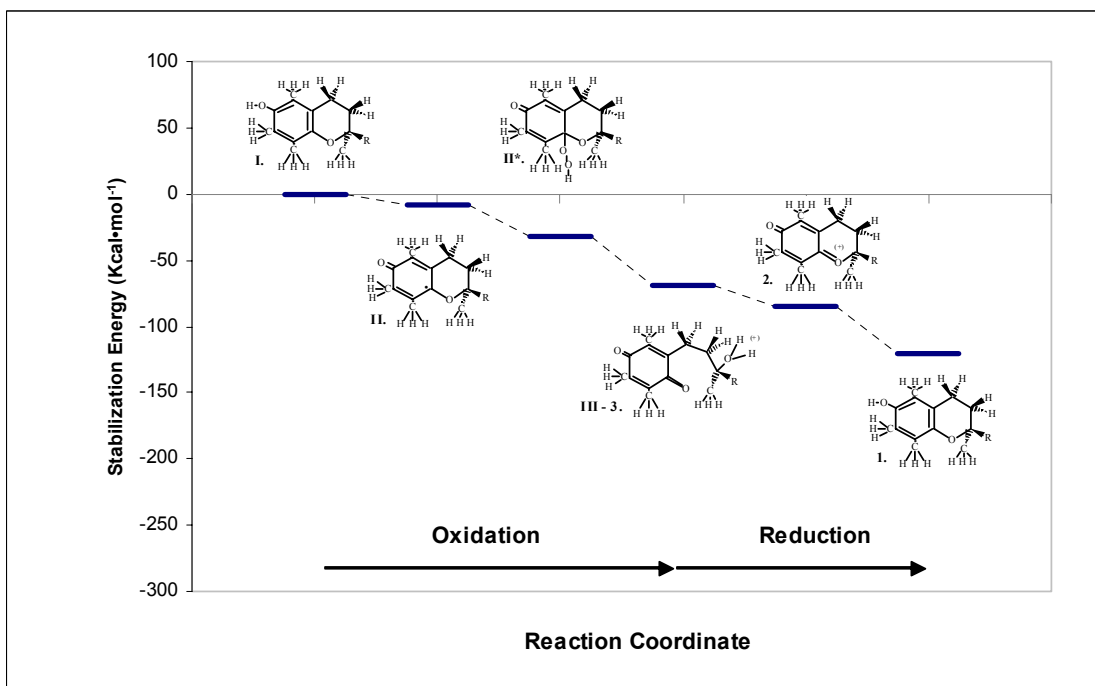


Figure 27 - Full cycle of reaction mechanism involving free radical open shell oxidation and closed shell recovery of α -tocopherol. The energy difference between initial and final states is related to the process: $2\text{HOO}\cdot + \text{Li-H} \rightarrow \text{HOOH} + \text{HOOLi}$

A schematic illustration of the overall process involving the various enzymes and non enzymatic anti-oxidants is shown in **Figure 28**.

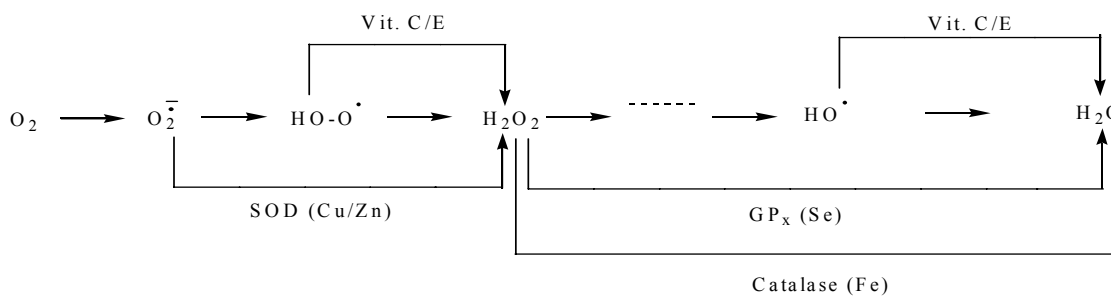


Figure 28 – The role of various enzymes and antioxidants in the reduction of concentration of Reactive Oxygen Species (ROS)

The catalytic nature of Vitamin E is illustrated in **Figure 29**. Clearly, if Vitamin E was destroyed at the end of the first step it could not produce more peroxide. Thus, under such condition its pro-oxidant nature perhaps would not have been ever observed. However, Vitamin E is recycled, biologically, as **Figure 29** indicates and a single α -tocopherol molecule may convert numerous $\text{HOO}\cdot$ radical to H_2O_2 which is accumulated if not removed at the same rate enzymatically with the participation of catalase(Fe) or glutathione peroxidase, $\text{GP}_x(\text{Se})$. This accumulation of peroxide, which may be referred to as a “peroxide traffic jam”, may well be the reason of the pro-oxidant effect of Vitamin E.

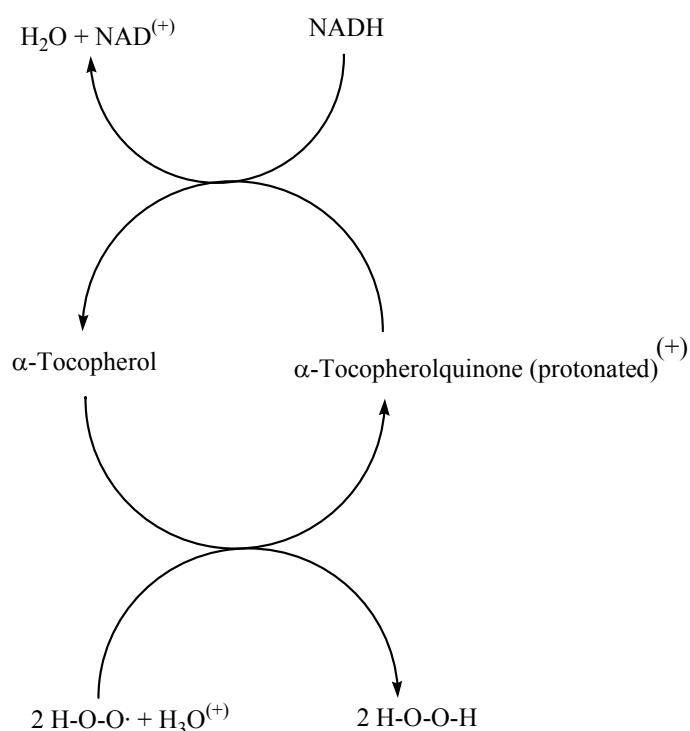


Figure 29 - Overall representation of the catalytic effect of α -tocopherol

6.2.6 Mechanistic comparison of O, S and Se congeners

In closing it may be appropriate to return to the question whether the sulphur or selenium congeners of α -tocopherol might exhibit better Vitamin E-like activity. The results obtained for the radicaloid oxidative ring opening as well as for the ionic reductive ring closing is shown in **Figure 30** which is based on the data presented in **Tables 19-23**. It clearly shows that the overall energetics with respect to thermodynamics are the same for O, S and Se congeners of α -tocopherol, since they are only catalysts which are being used but not consumed in the process. The central intermediate in the process (structure **III-3** in **Figure 30**) shows some difference in thermodynamic stabilities. However, for full assessment, the transition states must be more thoroughly investigated.

Table 19 - Total energy values of α -tocopherol and its congeners and its oxidized forms computed at the B3YP/6-31G(d) level of theory

reactant, intermediates, product	E (Hartree)			
		O	S	Se
reactant	1	-735.31212	-1058.27672	-3059.47561
closed ring intermediate	2	-734.45881	-1057.41808	-3058.61790
open ring intermediate	3	-810.84221	-1133.79773	-3134.99031
product	4	-810.51082	-1133.46666	-3134.65787

Table 20 - Total and relative energies for the ionic mechanism of α -tocopherol and its congeners, computed at the B3LYP/6-31G(d) level of theory

Congener	State	E(Hartree)	ΔE (Kcal·mol ⁻¹)	$\Delta\Delta E$ (Kcal·mol ⁻¹)
O	<u>1</u> +Li ⁺ +2H ₂ O	-895.414570	0.000	0.000
	<u>2</u> +LiH+2H ₂ O	-895.358638	35.098	35.098
	<u>3</u> +LiH+H ₂ O	-895.333085	51.133	16.035
	<u>4</u> +LiH+H ₃ O ⁺	-895.278650	85.291	34.159
S	<u>1</u> +Li ⁺ +2H ₂ O	-1218.379172	0.000	0.000
	<u>2</u> +LiH+2H ₂ O	-1218.317904	38.447	38.447
	<u>3</u> +LiH+H ₂ O	-1218.288605	56.832	18.385
	<u>4</u> +LiH+H ₃ O ⁺	-1218.234492	90.788	33.956
Se	<u>1</u> +Li ⁺ +2H ₂ O	-3219.578057	0.000	0.000
	<u>2</u> +LiH+2H ₂ O	-3219.517725	37.859	37.859
	<u>3</u> +LiH+H ₂ O	-3219.481190	60.785	22.926
	<u>4</u> +LiH+H ₃ O ⁺	-3219.425701	95.605	34.820

Table 21 – Total energies for free radical mechanism of α -tocopherol and its congeners, computed at the B3LYP/6-31G(d) level of theory

reactant, intermediates, product	E (hartree)			
		O	S	Se
reactant	I	-735.31212	-1058.27672	-3059.47561
closed ring intermediate	II	-734.69317	-1057.65619	-3058.85517
closed ring intermediate	II*	-885.63012	-1208.59280	-3209.79780
open ring intermediate	III	-810.84221	-1133.79773	-3134.99031
product	IV	-810.51082	-1133.46666	-3134.65787

Table 22 - Total and relative energies for the free radical mechanism of α -tocopherol and its congeners, , computed at the B3LYP/6-31G(d) level of theory

Congener	State	E(Hartree)	ΔE (Kcal \cdot mol $^{-1}$)	$\Delta\Delta E$ (Kcal \cdot mol $^{-1}$)
O	<u>I</u> + 2HOO \cdot + H ₃ O $^{+}$ + H ₂ O	-1190.205294	0.000	0.000
	<u>II</u> + HOO \cdot + HOOH + H ₃ O $^{+}$ + H ₂ O	-1190.219272	-8.771	-8.771
	<u>II*</u> + HOOH + H ₃ O $^{+}$ + H ₂ O	-1190.257066	-32.487	-23.716
	<u>III</u> + 2HOOH + H ₂ O	-1190.315332	-69.050	-36.563
	<u>IV</u> + 2HOOH + H ₃ O $^{+}$	-1190.260897	-34.892	34.159
S	<u>I</u> + 2HOO \cdot + H ₃ O $^{+}$ + H ₂ O	-1513.169896	0.000	0.000
	<u>II</u> + HOO \cdot + HOOH + H ₃ O $^{+}$ + H ₂ O	-1513.182291	-7.778	-7.778
	<u>II*</u> + HOOH + H ₃ O $^{+}$ + H ₂ O	-1513.219751	-31.284	-23.506
	<u>III</u> + 2HOOH + H ₂ O	-1513.270852	-63.351	-32.067
	<u>IV</u> + 2HOOH + H ₃ O $^{+}$	-1513.21674	-29.395	33.956
Se	<u>I</u> + 2HOO \cdot + H ₃ O $^{+}$ + H ₂ O	-3514.368781	0.000	0.000
	<u>II</u> + HOO \cdot + HOOH + H ₃ O $^{+}$ + H ₂ O	-3514.381273	-7.838	-7.838
	<u>II*</u> + HOOH + H ₃ O $^{+}$ + H ₂ O	-3514.424750	-35.121	-27.282
	<u>III</u> + 2HOOH + H ₂ O	-3514.463437	-59.398	-24.277
	<u>IV</u> + 2HOOH + H ₃ O $^{+}$	-3514.407949	-24.578	34.820

Table 23 – Full mechanistic relative energies for O, S, Se congeners, computed at the B3LYP/6-31G(d) level of theory

Model	E(kcal \cdot mol $^{-1}$)					
	O		S		Se	
	$\Delta\Delta E$	ΔE	$\Delta\Delta E$	ΔE	$\Delta\Delta E$	ΔE
I	0.000	0.000	0.000	0.000	0.000	0.000
II	-8.771	-8.771	-7.778	-7.778	-7.838	-7.838
II*	-23.716	-32.487	-23.506	-31.284	-27.282	-35.120
III	-36.563	-69.050	-32.067	-63.351	-24.277	-59.397
2	-16.035	-85.085	-18.385	-81.736	-22.926	-82.323
1	-35.098	-120.183	-38.447	-120.183	-37.859	-120.182

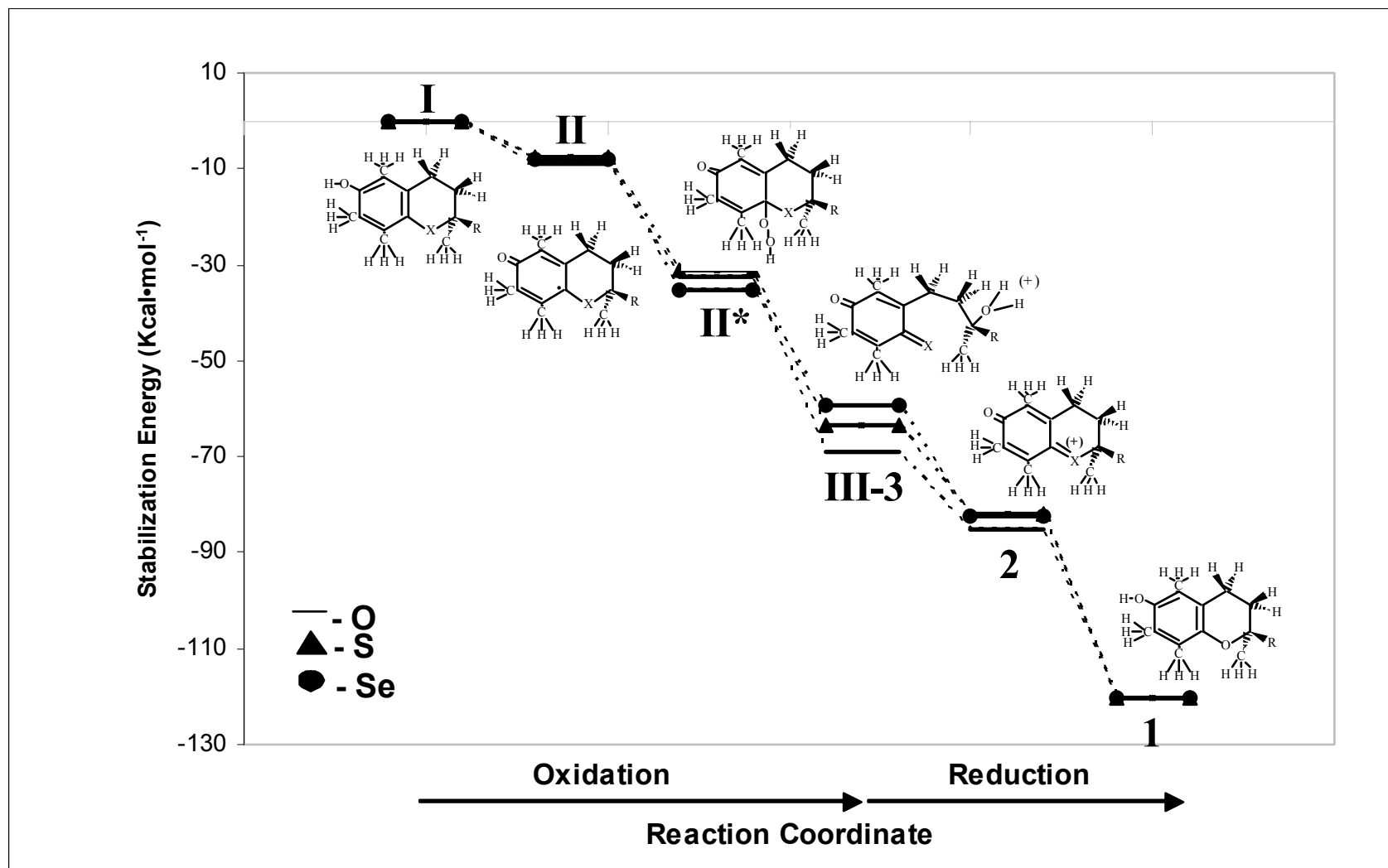


Figure 31 – Ionic reaction profile for X=O, S, and Se oxidative ring opening and reductive ring closing mechanism using LiH, a hydride donor modeling NADH, completed at the B3LYP/6-31G(d) level of theory.

6.3. Furthur study of Vitamin E Models

6.3.1. Full conformational space of tocopherol models

Furthur investigation leads to the study of the full conformational space of the tocopherol model.

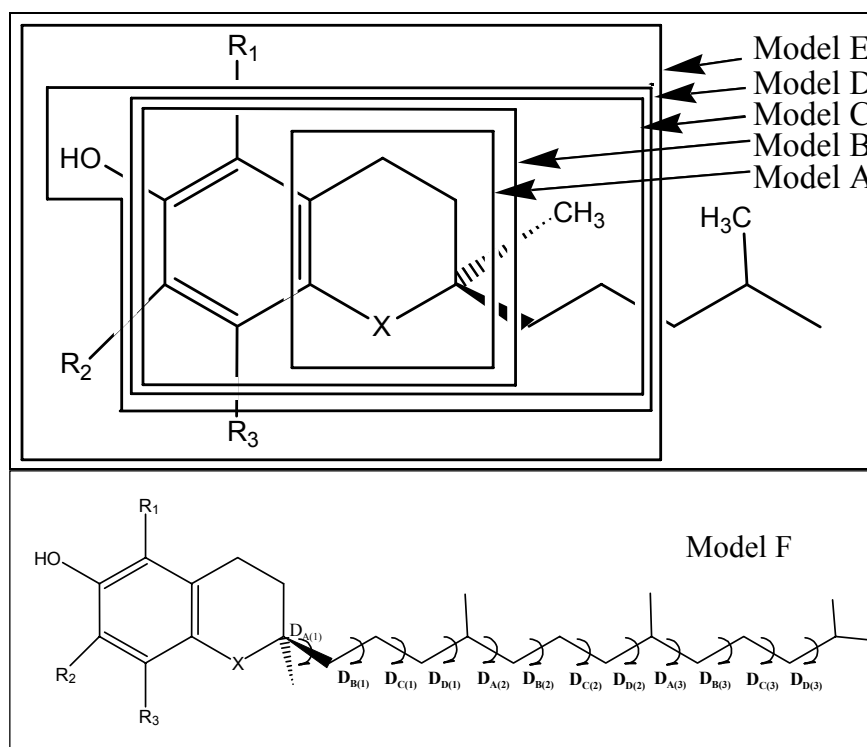


Figure 32 – Models of tocopherols

In this computational study, the complete Vitamin E called Model F with full methyl substitution (**Table 6**) is investigated. The full model of α -tocopherol was considered for oxygen (**II**), sulphur (**III**), and selenium (**IV**) heteroatoms in the ring. These structures, with a fully extended chain with each chain dihedral in the *anti* position are shown. Futhurmore, the chain is investigated with all chain dihedrals set to either *gauche*⁺ or *gauche*⁻ conformations.

6.3.2 Preliminary Results

Comparison of the sequence of stabilities shows a non-monotonic change which concurs with the results from Model E. The R-C-Me bond angles at the ring stereocenter varied the following way: 112.2°(O), 111.6°(S), 112.2°(Se).

Table 24 – Presently optimized dihedral angles of the α -tocopherol sidechain and its congeners. (Definition of dihedral angles are shown in **Figure 34**)

X	Level of Theory	DA ₁	DB ₁	DC ₁	DD ₁	DA ₂	DB ₂	DC ₂	DD ₂	DA ₃	DB ₃	DC ₃	DD ₃	Total E (Har)
O	B3LYP/6-31G(d)	176.520	185.552	184.653	171.764	189.305	175.397	184.248	170.883	188.584	175.106	183.208	171.703	-1285.6982304
S	B3LYP/6-31G(d)	175.525	179.987	184.029	169.900	187.985	174.808	183.402	170.396	188.464	175.627	183.661	172.020	-1608.6628400
Se	B3LYP/6-31G(d)	174.469	181.136	183.823	170.226	188.012	174.758	183.640	170.871	188.329	175.019	183.256	171.883	-3609.8618088

These dihedrals have been separated into three segments corresponding to the chain steric centres. It is important to note the non-monotonic nature of the dihedrals especially nearest and furthest away from the ring structure.

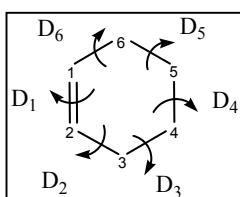


Table 25 – Presently optimized ring dihedral angles for O, S, Se compounds.

X	Level of Theory	D1	D2	D3	D4	D5	D6
O	B3LYP/6-31G(d)	0.702	-18.976	47.058	-58.683	42.520	-13.673
S	B3LYP/6-31G(d)	-0.278	-14.213	43.633	-65.652	52.021	-15.059
Se	B3LYP/6-31G(d)	-1.936	-10.399	40.386	-66.641	56.581	-16.402

Further computations were made with the sidechain of the O, S, Se congeners in the *gauche*- and *gauche*⁺ conformations. Figure 33, 34 show optimized minimum energy structures in the fully extended and *gauche*⁻ conformations. Further information, including a comparison of the relative energies of these conformers can be found in the appendices.

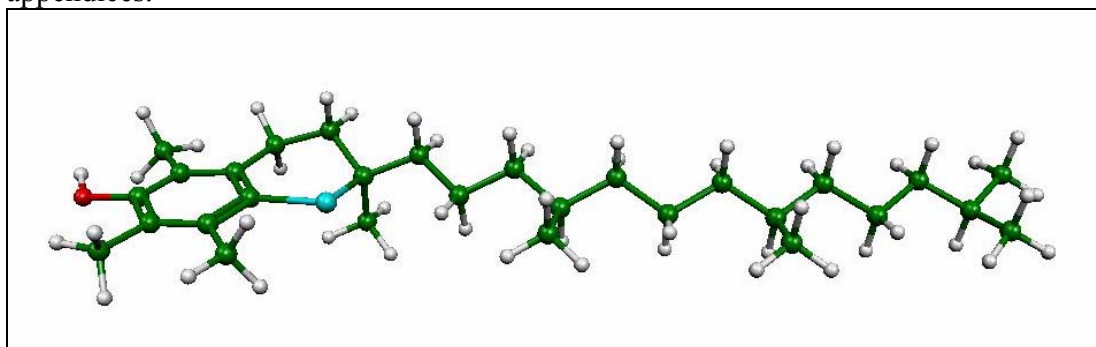


Figure 33 – B3LYP/6-31G(d) optimized minimum energy structure for fully extended tail of Selenium congener.

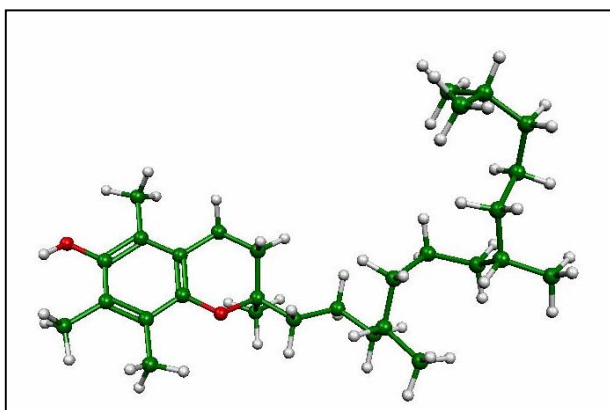


Figure 34 - B3LYP/6-31G(d) optimized minimum energy structure for *gauche*⁻ trend of α -tocopherol.

7. CONCLUSIONS

7.1 Model A and Model B

It is in human nature to wonder if “Mother Nature” did the best possible structural arrangement or whether we can improve upon it. The question has been asked^{12, 13} in general about antioxidants and in particular about Vitamin E^{35, 36}.

From the present study, one can see that the influence of **X = S (III)** and **X = Se (IV)** are analogous to one another other but that they are very much different from the **X = O** congener (**II**). On the basis of this result, one may expect the Sulphur and the Selenium containing compounds to be either much weaker or much stronger antioxidants than the Oxygen containing one. Further research is needed in this area, in order to quantify the anti-oxidant characteristics of all topologically probable stable conformers, for each of these molecular systems.

7.2 Model C and Model D

The present work shows that O and Se stabilize the fused ring system of Tocopherols more or less to the same extent, while S destabilizes it slightly.

The stabilization is of the following order:

$$\begin{array}{ccccccc} \text{O} & \approx & \text{Se} & >> & \text{S} & & \\ -4.82 & & -4.73 & & +1.19 & (\text{Kcal}\cdot\text{mol}^{-1}) \end{array}$$

It remains to be seen if the energies of the red-ox reaction mechanism follow the same sequence.

7.3 Model E

Both Me and heteroatom substitution change the molecular structure of Vitamin E, in terms of bond lengths, bond angles and dihedral angles. The effect of Me substitution was observed predominantly in the case of adjacent bond lengths, while heteroatom substitution influenced bond angles and dihedral angles.

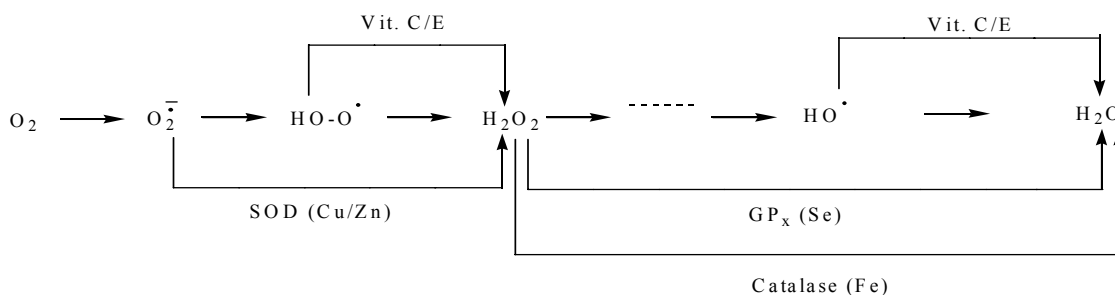
With the exception of the model of β -tocopherol, where the 2 introduced Me groups (*para*-orientation) nearly cancel their electronic contribution and provide little steric congestion, a general trend was observed with increasing substitution in the following sequence $\delta \rightarrow \gamma \rightarrow \alpha$. The structural contribution is measured by the relative stabilities in $\text{Kcal}\cdot\text{mol}^{-1}$ units, with δ being the most stable and α being the least stable. This trend correlated with the logarithmic relative activity of the Vitamin E homologues δ , γ and α , respectively.

This clearly indicates that there is a structural basis for the differing biological activity of the naturally occurring tocopherol homologues.

7.4 Mechanism

If Vitamin E reacts with $\text{HO}\cdot$ radical then the radical is converted to H_2O which represents no further biological detriment, as it is the last structure in the overall reductive process starting with O_2 . However, when Vitamin E reacts with $\text{HOO}\cdot$ then the peroxyradical is converted to hydrogen peroxide (H_2O_2) which could cause oxidative damage.

The present investigation has shown that a substantial fraction of the oxidized Vitamin E may be reduced back to active Vitamin E which could, in turn, produce more hydrogen peroxide. The responsibility of removal of the hydrogen peroxide from the system is bestowed upon two enzymes: the iron containing catalase (Fe) and the selenium containing glutathione peroxidase, $\text{GP}_x(\text{Se})$. If there is a noticeable concentration reduction of these enzymes, then the peroxides accumulate, leading to a “peroxide traffic-jam”. This can happen for example if the Se supply is low, as discussed at the beginning of this dissertation. Of course, the accumulated H_2O_2 , produced by Vitamin E, can make a great deal of damage and thus consequently Vitamin E may well be misjudged to be a pro-oxidant, while the phenomenon may be due to the low level of selenium (Se).



It now appears that future clinical studies, designed to investigate the efficacy (the anti-oxidant effect) and the toxicity of the accumulated peroxide (*via* the pro-oxidant effect) of Vitamin E should include the monitoring of other participating components of the detoxification process of ROS. Such studies should include the monitoring of the level of catalase (Fe or Mn) as well as glutathione peroxidase (Se). Nutritionists³⁷ and Biochemists³⁸ have already questioned whether the imbalance of these enzymes could be a significant contributor to the damages originated from oxidative stress.

8. REFERENCES

1. James A. Joseph *et. al.*; Free Radical Biology & Medicine **30** (2001) 583-594
2. Marco N. Diaz, MD, et al. "Antioxidants and atherosclerotic heart disease." New England journal of Medicine 337 (August 7, 1997): 408-416.
3. Evans M, Bishop K. S. Science 1922;55:650.
4. Bauernfeind JB. In: Vitamin E: a comprehensive treatise. New York. Marcel Dekker, 1980. p. 99-167.
5. Weimann B, Weiser H. Am. Clin. Nutr. 1991;53:1056S-60S
6. Al-Maharik N, Engman L., Malmstrom J., Schiesser C. Intramolecular Homolytic Substitution at Selenium: Synthesis of Novel Selenium-Containing Vitamin E Analogues. J. Org Chem. 2001, 66, 6286-6290.
7. Aubrey D. N. G. de Grey *The Mitochondrial Free Radical Theory of Aging* R. G. Landes Company, Austin, Texas, USA, 1999.
8. B. Chance, H. Sies, and A. Boveris, Physiological Review 1979 [59] 527.
9. B. N. Ames, M. K. Shigenaga, in *Molecular Biology of Free Radical Scavenging Systems*. Ed. J. G. Scandalios, Cold Spring Harbor Laboratory Press, New York, 1992, 1.
10. S. Steenken, Chem. Rev. 1979 [89] 503.
11. K. L. Fong, P. B. McCay, J. L. Poyer, B. H. Misra, B. Keele, J. Biol. Chem. 1973 [248] 7792.
12. T. I. Mak, W. B. Weglicki, J. Clin. Invest. 1985 [75] 58.
13. S. Varadarajan, J. Kanski, M. Aksenova, C. Lauderback, D. A. Butterfield, J. Am. Chem. Soc. 123 (2001) 5625.
14. Anet, F. A. L. (1989), "Conformational Analysis of Cyclohexenes," see reference to Rabideau, P. W., Ed. (1989), p. 1.
15. G.W. Burton and K. U. Ingold, Acc. Chem. Res. 19 (1986) 194.
16. M. J. Frisch, G. W. Trucks, H. B. Schlegel, G. E. Scuseria, M. A. Robb, J. R. Cheeseman, V. G. Zakrzewski, J. A. Montgomery, Jr., R. E. Stratmann, J. C. Burant, S. Dapprich, J. M. Millam, A. D. Daniels, K. N. Kudin, M. C. Strain, Ö. Farkas, J. Tomasi, V. Barone, M. Cossi, R. Cammi, B. Mennucci, C. Pomelli, C. Adamo, S. Clifford, J. Ochterski, G. A. Petersson, P. Y. Ayala, Q. Cui, K. Morokuma, D. K. Malick, A. D. Rabuck, K. Raghavachari, J. B. Foresman, J. Cioslowski, J. V. Ortiz, A. G. Baboul, B. B. Stefanov, G. Liu, A. Liashenko, P. Piskorz, I. Komaromi, R. Gomperts, R. L. Martin, D. J. Fox, T. Keith, M. A. Al-Laham, C. Y. Peng, A. Nanayakkara, M. Challacombe, P. M. W. Gill, B. Johnson, W. Chen, M. W. Wong, J. L. Andres, C. Gonzalez, M. Head-Gordon, E. S. Replogle, and J. A. Pople, Gaussian, Inc., Pittsburgh PA, 1998.
17. C. Glidwell. Inorg. Chim. Acta 20 (1976) 113.
18. C. Glidwell. Inorg. Chim. Acta. 36 (1979) 135.

19. Auf der Heyde, W. and Luttke, W. (1978), Chem. Ber., 111, 2384
20. Chiang, J. F. and Bauer, S. H. (1969), J. Am. Chem. Soc., 91, 1898.
21. Geise, H. J. and Buys, H. R. (1970), Recl. Trav. Chim. Pays-Bas, 89, 1147
22. Naumov, V. A., Dashevskii, V. G., and Zaripov, N. M. (1970), J. Struct., Chem. USSR 11, 793 (Engl. Transl. P. 736)
23. Ogata, T. and Kozima, K. (1969), Bull. Chem. Soc. Jpn., 42, 1263
24. Scharpen, L. H., Wollrab, J. E., and Ames, D. P. (1986), J. Chem. Phys., 49, 2368
25. D. H. Setiadi, G. A Chass, L. L. Torday, A. Varro, and J. Gy. Papp, THEOCHEM (2002) in press. *
26. I, Jialal, C.F. Fuller, B.A. Huet, Thrombosis and Vascular Biology 15(1995) 190
27. H.M.G. Princen, W. Van Dwyvenroorde, R. Buytenhek, A. VanderLaarse, G. Van Poppel, J.A. Gevers Leuven, V.W.M. VanHinsbergh, Thrombosis and Vascular Biology 15(1995) 325
28. P. Weber, A.Bendich, L.J. Machlin, Nutrition 13(1997)
29. A. Azzo, A. Stocker, Progressin Lipid Research 39(2000) 231
30. J.M. Upston, A.C. Terentis, R. Stocker, FASEB J. 13(1999) 977
31. R. Ricciarelli, J-M. Zingg, A. Azzi, FASEBJ. 15(2001) 2314
32. D.C. Lieber, J.A. Burr, L. Philips and A.J. Harm, Anal Biochem 236(1996) 27-34.
33. T. Roseman, H. WD, Tetrahedron 51(1995) 7917-7926
34. R. Brigelius-Flohe and M.G. Traber, FASEB J. 13(1999) 1145-1155.
35. J. S. Wright, E. R. Johnson and G. A. DiLabio, J. Am. Chem. Soc. 123 (2001) 1173-1183.
36. C. H. Schiesser, From Marco Polo to chiral stannanes – radical chemistry for the new millennium, Arkivoc (2001).
37. C. C. Lai, W. H. Huang, A. Askari, L. M. Klevay and T. H. Chiu, J. Nutr. Biochem 6(1995) 256
38. P. Amsad, A. Peskin, G. Shah, M. Mirault, R. Moret, I. Zbindeu, and P. Cerutti, Biochemistry, 30(1991) 9305

APPENDICES OF PUBLISHED PAPERS:

1. **David H. Setiadi**, Gregory A. Chass, Ladislaus L. Torday, Andras Varro and Julius Gy. Papp, Vitamin E Models. Conformational Analysis and Stereochemistry of Tetralin, Chroman, Thiochroman and Selenochroman, THEOCHEM **2002**, **594**, 161-172.
2. **David H. Setiadi**, Gregory A. Chass, Ladislaus L. Torday, Andras Varro and Julius Gy. Papp, Imre G. Csizmadia, Vitamin E Models. The effect of heteroatom substitution in 2-ethyl-2-methyl chroman and 2-ethyl-2-methyl-6-hydroxychroman, Eur. Phys. J. D **2002**, **20**, 609-618.
3. **David H. Setiadi**, Gregory A. Chass, Ladislaus L. Torday, Andras Varro and Julius Gy. Papp, Vitamin E Models. Shortened Sidechain Models of α , β , γ and δ Tocopherol and Tocotrienol. A Density Functional Study, J. Mol. Struct. THEOCHEM **2003**, **637**, 11-26.
4. **David H. Setiadi**, Gregory A. Chass, Ladislaus L. Torday, Andras Varro and Julius Gy. Papp, Vitamin E Models. Can the anti-oxidant and pro-oxidant dichotomy of α -tocopherol be related to an ionic ring closing and ring opening redox reaction. THEOCHEM **2003**, **620**, 93-106.
5. **David H. Setiadi**, Gregory A. Chass, Joseph C. P. Koo, Botond Penke and Imre G. Csizmadia, Exploratory study on the full conformation space of α -tocopherol and its selected congeners. THEOCHEM **2003**, **666-667**, 439-443.

Vitamin E models. Conformational analysis and stereochemistry of tetralin, chroman, thiochroman and selenochroman

David H. Setiadi^{a,*}, Gregory A. Chass^a, Ladislaus L. Torday^b, Andras Varro^b,
Julius G. Papp^{b,c}

^aGlobal Institute of Computational Molecular and Materials Science, VELOCET 210 Dundas Street W., Suite 810, Toronto, Ont.,
Canada M5G 2E8

^bDepartment of Pharmacology and Pharmacotherapy, Szeged University, Domter12, Szeged 6701, Hungary

^cDivision of Cardiovascular Pharmacology, Hungarian Academy of Sciences and Szeged University, Domter12, Szeged 6701, Hungary

Received 15 March 2002; accepted 24 April 2002

Abstract

Tetralin, chroman as well as its S and Se containing congeners were subjected to ab initio (RHF/3-21G and RHF/6-31G(d)) and DFT (B3LYP/6-31G(d)) computation. Molecular geometries and the activation energies for ring inversions were determined with full geometry optimizations. © 2002 Elsevier Science B.V. All rights reserved.

Keywords: Tocopherol models; Tocotrienol models; Vitamin E as an antioxidant; Molecular structure; Ring inversion; HF and DFT computations

1. Preamble

Vitamin E, a term [1] introduced in 1922, does not represent a single compound but in fact includes two families of compounds; mainly tocopherols and tocotrienols. Both families consist of a chroman (benzopyrane) ring structure and a sidechain, the latter having the characteristic isoprenoid skeleton, typical of terpenes. Members of the tocopherol family have saturated sidechains but the same sidechain in the tocotrienol family has three non-conjugated double bonds. Such

carbon–carbon double bonds are separated by $-\text{CH}_2-\text{CH}_2-$ units. For both families, the carbon atom that carries the sidechain is a stereocenter of *R* configuration, however, the sidechain of the tocopherols has two additional stereocenters, at the branching points both of which are of *R* configuration. The structural variations of the two families are shown in Fig. 1.

Each of these families have four homologous members (Table 1), labeled as α , β , γ , and δ . They differ from each other in the extent of the methyl substitution in the aromatic ring. Overall, these two (2) families of compounds (tocopherol and tocotrienol) and each may come in four (4) homologous forms. The natural abundance of these $2 \times 4 = 8$ components of the vitamin E family varies from plant to plant [2] as summarized in Table 2.

* Corresponding author.

E-mail addresses: david_setiadi@hotmail.com (D.H. Setiadi), gchass@fixy.org (G.A. Chass), pyro@phcol.szote.u-szeged.hu (L.L. Torday), varro@phcol.szote.u-szeged.hu (A. Varro), papp@phcol.szote.u-szeged.hu (J.G. Papp).

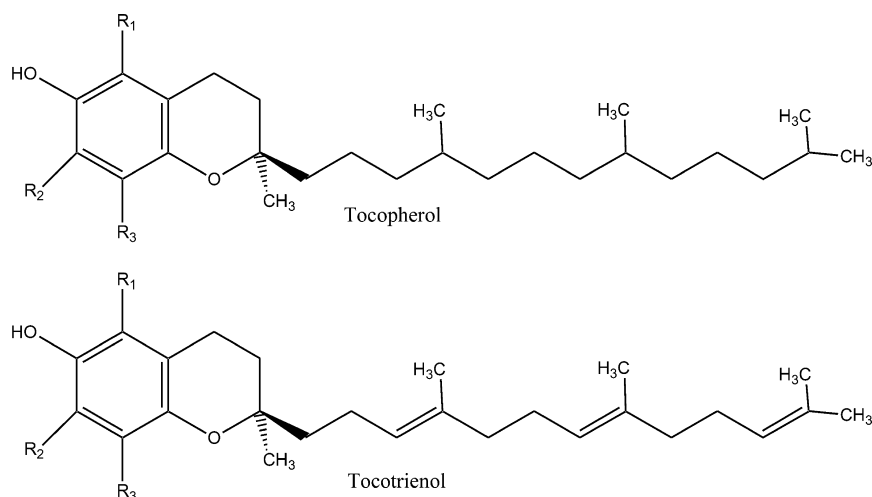


Fig. 1. Structures of tocopherols and tocotrienols. Substituents R_1 , R_2 and R_3 are specified in Table 1.

Of these eight species, it is α -tocopherol which is most frequently used partly because it is commercially available in synthetic form, which does not come as a pure enantiomeric mixture. The effectiveness of the synthetic racemic mixture has traditionally been questioned, lacking an explanation at the molecular level. The primary function of vitamin E is, however, as an antioxidant, undergoing an oxidation reaction at the molecular level. Presently, we have more precise data to support this traditional assumption [3], as shown in Table 3.

Recently it has been suggested [4] that the selenium congener of α -tocopherol (Fig. 2) may be a very effective antioxidant. For this reason, we wish to study the structure of the chroman ring together with its S and Se congeners. We also wish to compare chroman with its hydrocarbon analog (tetralin).

Table 1
Extent of methyl substitutions of the tocopherol and tocotrienol families

	R_1	R_2	R_3
α	Me	Me	Me
β	Me	H	Me
γ	H	Me	Me
δ	H	H	Me

All of these compounds (**I**, **II**, **III**, and **IV**) are depicted in Section 3 below.

2. Introduction

2.1. Oxidative stress and vitamin E

One of the major current theories of aging as well as of the origin of numerous degenerative diseases is

Table 2
Typical vitamin E content of selected foods (based on α -tocopherol activity)

	Vitamin E	
	mg/100 g food portion	IU/100 g food portion ^a
Wheat germ oil	119	178
Sunflower oil	49	73
Peanut oil	19	28
Soybean oil	8.1	12
Butter	2.2	3.2
Sunflower seeds, raw	50	74
Almonds	27	41
Peanuts, dry roasted	7.4	11
Asparagus, fresh	1.8	2.7
Spinach, fresh	1.8	2.7

^a 1 mg α -tocopherol equivalent to 1.49 IU.

Table 3

Relative activity of tocopherol and tocotrienol stereoisomers and their acetates

Natural vitamin E derivatives	Activity (%)	Synthetic vitamin E derivatives	Activity (%)
RRR- α -tocopherol	100	RRR- α -tocopheryl acetate	100
RRR- β -tocopherol	57	RRS- α -tocopheryl acetate	90
RRR- γ -tocopherol	37	RSS- α -tocopheryl acetate	73
RRR- δ -tocopherol	1.4	SSS- α -tocopheryl acetate	60
R- α -tocotrienol	30	RSR- α -tocopheryl acetate	57
R- β -tocotrienol	5	SRS- α -tocopheryl acetate	37
		SRR- α -tocopheryl acetate	31
		SSR- α -tocopheryl acetate	21

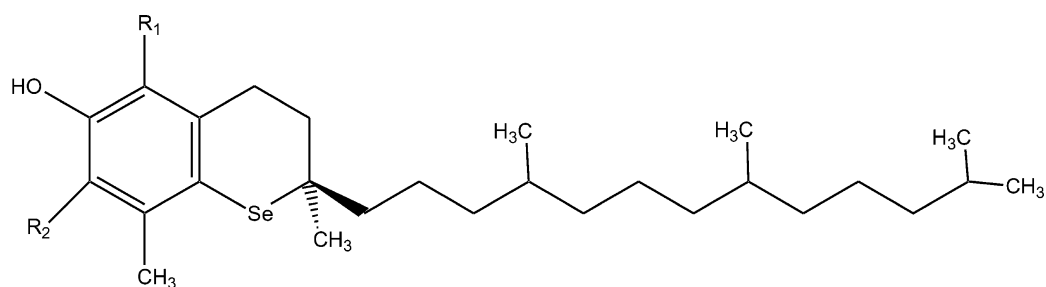
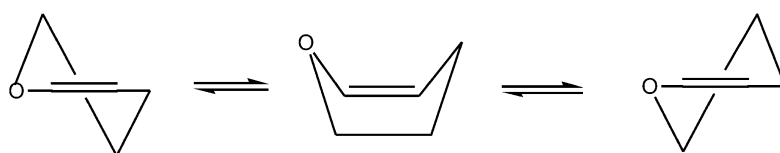
Fig. 2. Seleno-congener of α -tocopherol.

Fig. 3. Ring-flip in dihydropyran.

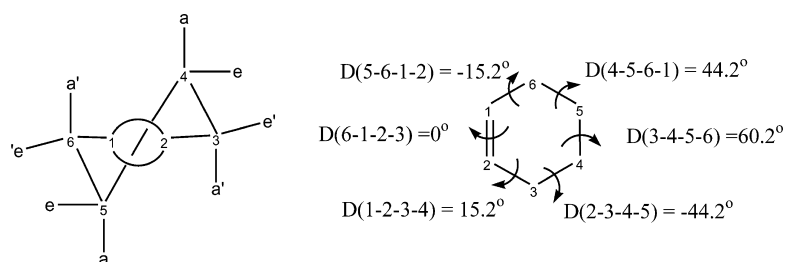


Fig. 4. Conformation and dihedral angles of cyclohexene as part of the tetralin ring system. The ring may exist in two enantiomeric forms. The signs in one of the enantiomers are as shown in the figure. In the other enantiomer, the dihedral angles are of opposite sign.

associated with a variety of free radical reactions within the human body [5]. These reactions are collectively referred to as oxidative stress.

Free radicals are generated as by-products of redox reactions associated with metabolism [6]. These include the superoxide anion (O_2^-), the hydroperoxyl radical (HOO), hydrogen peroxide (H_2O_2) and the hydroxyl radical (HO). These are collectively referred to as ‘reactive oxygen species’ (ROS) and are all very reactive in the body and therefore short-lived. Normally, there are natural mechanisms defending against the free radicals within the body [7], which may be enzymatic or non-enzymatic. However, if for some reason, these defense mechanisms become weakened then the free radicals can react with cellular structures such as DNA as well as proteins, or even destroy membranes through lipid peroxidation [8–10]. It is generally believed that through these processes, aging and other age-related degenerative diseases such as cardiovascular disorders and cancer are induced [1]. Recently, oxidation of a methionine residue has been implicated [11] in Alzheimer’s disease as a result of oxidative stress.

Vitamin E is a potent antioxidant that helps prevent cancer by blocking lipid peroxidation, as well as the oxidation of polyunsaturated fats into free radicals. Lipid peroxidation is potentially important in all cancers but is especially significant as a cause of breast and colon cancers.

Vitamin E also serves a crucial role in the function of the immune system. A low level of this vitamin leads to impaired antibody production, inability to manufacture T and B lymphocytes and reduced resistance to cancer and infection.

Vitamin E works synergistically with vitamin C and the mineral selenium, with which it has a special affinity. Selenium and vitamin E combined, constitutes a double defense against cancer. As it is not possible to obtain optimally protective quantities of E from diet alone, supplements of 40–1600 international units (IU) are recommended daily.¹

2.2. Structural background

One of the structural problems of vitamin E is associated with the saturated ring fused to the benzene

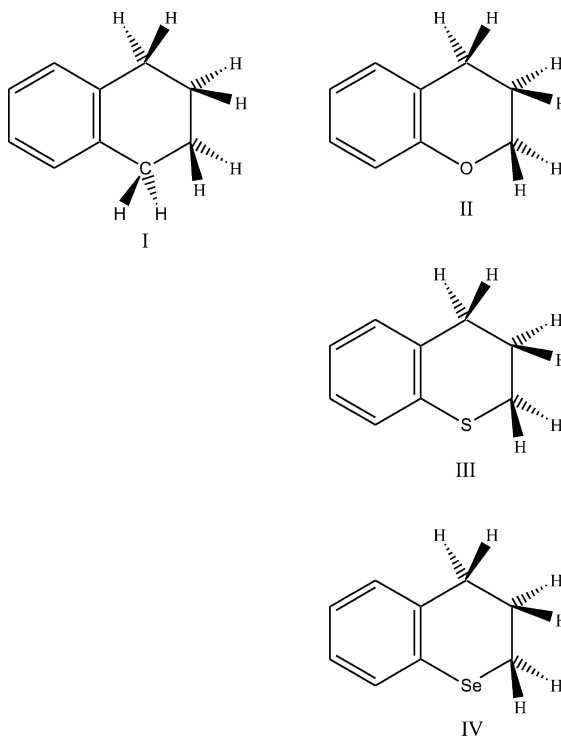


Fig. 5. Tetraline, chroman and its S and Se congeners.

ring. This ring cannot be considered to be cyclohexane or its heterocyclic analogues in a boat conformation because it has, at least formally, one carbon–carbon double bond. The so-called ‘half-chair’ conformation had been considered to be the most likely structure, before experimental observation provided strong support for that assumption.

The ring is expected to exist in two interconvertible enantiomeric forms, with the transition state for such a ring-flip expected to show some symmetry. It is tempting to consider the planar structure to be a good

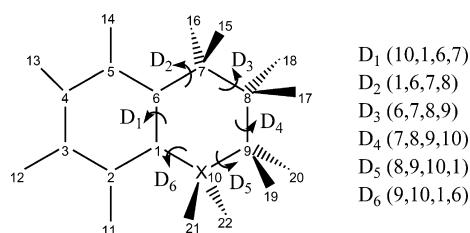
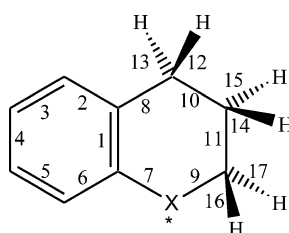


Fig. 6. Definition of the spatial orientation of atomic nuclei used for molecule including the numeric definition of relevant dihedral angles.

¹ 1 mg α -tocopherol = 1.49 IU.

Table 4

Optimized bond lengths for the stable conformers ($\lambda = 0$) of compounds **I**, **II**, **III**, and **IV** obtained at three levels of theory

	X	1	2	3	4	5	6	7	8	9	10
HF/3-21G	CH ₂	1.3900	1.3912	1.3790	1.3855	1.3790	1.3912	1.5241	1.5241	1.5374	1.5374
	O	1.3855	1.3880	1.3800	1.3872	1.3774	1.3860	1.3772	1.5197	1.4451	1.5396
	S	1.3843	1.3918	1.3787	1.3848	1.3782	1.3865	1.8356	1.5208	1.8872	1.5374
	Se	1.3862	1.3868	1.3821	1.3828	1.3814	1.3832	1.9231	1.5125	1.9950	1.5459
HF/6-31G(d)	CH ₂	1.3927	1.3940	1.3799	1.3879	1.3799	1.3940	1.5191	1.5191	1.5283	1.5283
	O	1.3895	1.3923	1.3802	1.3895	1.3786	1.3906	1.3550	1.5155	1.4079	1.5283
	S	1.3924	1.3942	1.3795	1.3872	1.3786	1.3943	1.7823	1.5186	1.8133	1.5265
	Se	1.3926	1.3890	1.3843	1.3843	1.3835	1.3882	1.9073	1.5106	1.9692	1.5346
B3LYP/6-31G(d)	CH ₂	1.4066	1.4026	1.3920	1.3970	1.3920	1.4027	1.5203	1.5203	1.5339	1.5338
	O	1.4054	1.4005	1.3930	1.3984	1.3908	1.4004	1.3717	1.5163	1.4306	1.5338
	S	1.4072	1.4024	1.3920	1.3965	1.3907	1.4044	1.7884	1.5182	1.8364	1.5321
	Se	1.4053	1.3996	1.3945	1.3956	1.3935	1.3998	1.9150	1.5101	1.9970	1.5421
		11	12	13	14	15	16	17	18	19	
HF/3-21G	CH ₂	1.5368	1.0847	1.0871	1.0844	1.0855	1.0855	1.0844	1.0871	1.0847	
	O	1.5286	1.0836	1.0865	1.0833	1.0833	1.0837	1.0781	–	–	
	S	1.5268	1.0836	1.0870	1.0855	1.0830	1.0787	1.0791	–	–	
	Se	1.5339	1.0829	1.0865	1.0852	1.0825	1.0796	1.0791	–	–	
HF/6-31G(d)	CH ₂	1.5268	1.0861	1.0889	1.0861	1.0881	1.0881	1.0861	1.0889	1.0861	
	O	1.5188	1.0853	1.0881	1.0856	1.0860	1.0878	1.0808	–	–	
	S	1.5234	1.0852	1.0887	1.0866	1.0853	1.0835	1.0828	–	–	
	Se	1.5251	1.0842	1.0886	1.0868	1.0850	1.0806	1.0804	–	–	
B3LYP/6-31G(d)	CH ₂	1.5327	1.0977	1.1011	1.0968	1.0993	1.0993	1.0968	1.1010	1.0977	
	O	1.5245	1.0969	1.1002	1.0963	1.0971	1.1009	1.0932	–	–	
	S	1.5272	1.0967	1.1011	1.0977	1.0967	1.0955	1.0942	–	–	
	Se	1.5261	1.0956	1.1009	1.0982	1.0963	1.0924	1.0921	–	–	

candidate for the transition state but such a conformation could be a higher order critical point. It is more likely that the transition state is a boat conformation (Fig. 3).

Of the four CH₂ groups found in tetralin, the two allylic CH₂ exhibit quasiaxial or pseudoaxial (a') and quasiequatorial or pseudoequatorial (e') orientation, while the orientation of the central

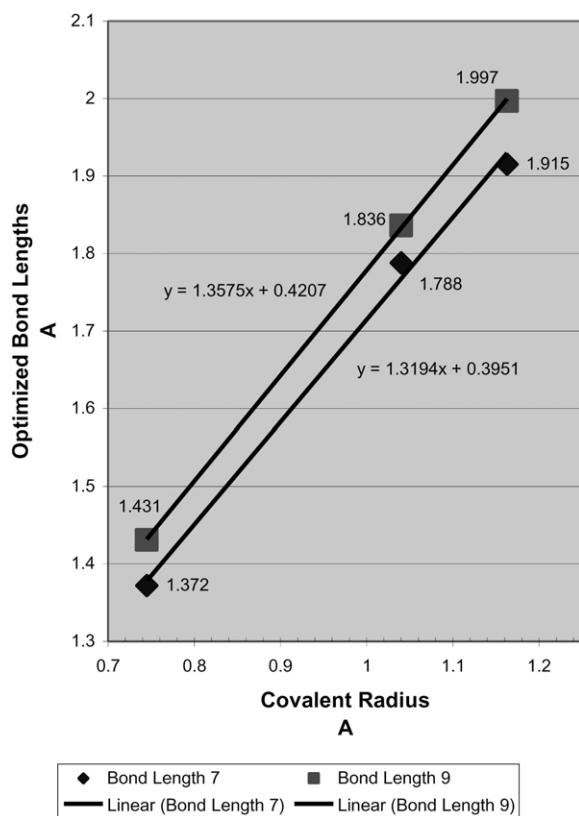


Fig. 7. Variation of selected bond lengths as a function of atomic radii.

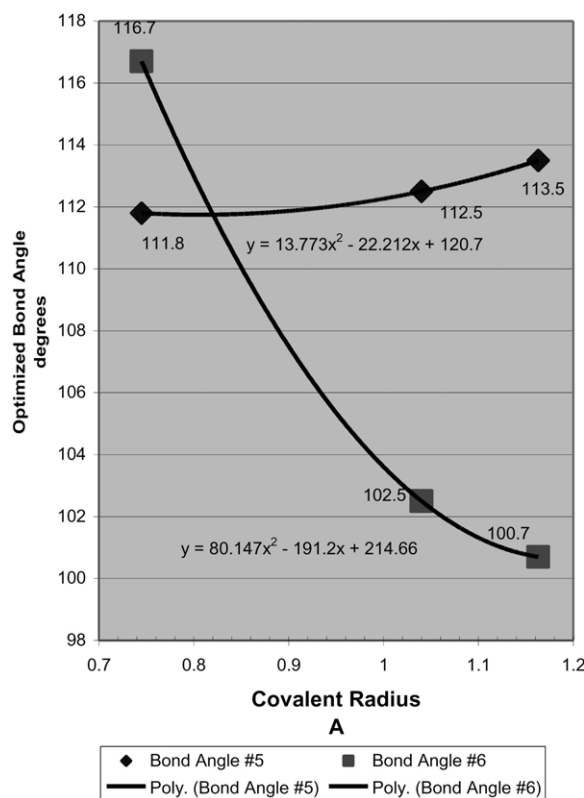


Fig. 8. Variation of selected bond-angles as a function of atomic radii.

CH₂–CH₂ moiety is expected to be close to non-cyclic molecules such as ethane or butane (Fig. 4).

Thus, the further away one moves away from the double bond, the closer one comes to the ideal planar situation. Estimated dihedral angles (D_i) are shown in Fig. 4. While we cannot extrapolate in a blindfolded way to the stereochemistry of tetralin from the conformations of cyclohexene, some analogy is nevertheless expected.

3. Method

Molecular orbital computations were carried out, using the GAUSSIAN98 program package [13], on the following four compounds: tetralin (**I**), chromane (**II**),

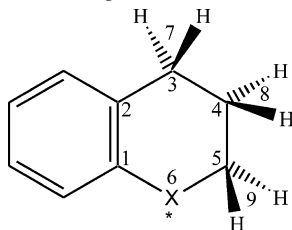
thiochroman (**III**), and selenochroman (**IV**) as shown in Fig. 5.

Two methods and two split-valence basis sets were used, mainly the RHF/3-21G, RHF/6-31G(d) and the B3LYP/6-31G(d) levels of theory. Convergence criteria of 3.0×10^{-4} , 4.5×10^{-4} , 1.2×10^{-3} , 1.8×10^{-3} are used for the gradients of the RMS (root mean square) force, maximum force, RMS displacement and maximum displacement vectors, respectively.

Since it is generally believed that the tail end of tocopherols are only needed to enhance fat solubility [12] it is appropriate to concentrate on the fused ring systems (**II**, **III**, and **IV**). Compounds **III** and **IV** are congeners of **II**. All of these compounds lack the symmetry, which is present in **I**.

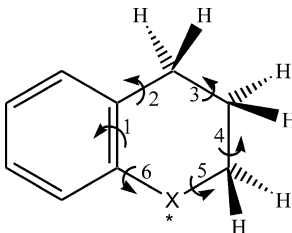
The definition of the spatial orientation of the

Table 5

Optimized bond-angles for the stable conformers ($\lambda = 0$) of compounds **I**, **II**, **III**, and **IV** obtained at three levels of theory

	X	1	2	3	4	5	6	7	8	9	10
HF/3-21G	CH ₂	121.746	121.748	112.682	109.374	109.372	112.683	107.341	107.856	107.856	107.344
	O	122.827	120.267	110.538	108.812	110.519	118.565	106.667	108.627	109.3	–
	S	124.136	123.089	113.721	110.859	111.423	102.205	107.263	108.13	109.581	–
	Se	121.362	120.21	110.281	112.012	113.889	99.633	107.824	107.89	109.018	–
HF/6-31G(d)	CH ₂	121.624	121.623	113.133	110.229	110.222	113.133	106.163	106.876	106.879	106.159
	O	122.703	120.505	110.574	109.16	111.16	117.51	106.54	107.649	108.289	–
	S	124.228	123.424	114.721	111.359	112.054	102.191	106.143	107.342	107.798	–
	Se	121.434	120.45	111.626	112.671	113.646	101.09	106.964	107.06	108.663	–
B3LYP/6-31G(d)	CH ₂	121.478	121.474	113.377	110.288	110.291	113.385	105.707	106.735	106.735	105.716
	O	123.14	120.367	110.734	109.179	111.805	116.747	106.132	107.498	108.246	–
	S	124.43	123.008	114.512	111.518	112.445	102.512	105.813	107.232	107.869	–
	Se	121.524	120.5	111.714	112.709	113.499	100.694	106.843	107.001	108.92	–

Table 6

Optimized dihedral angles for the stable conformers ($\lambda = 0$) of compounds **I**, **II**, **III**, and **IV** obtained at three levels of theory

	X	1	2	3	4	5	6
HF/3-21G	CH ₂	2.846	– 18.423	48.888	– 65.027	48.887	– 18.423
	O	0.412	– 20.849	49.302	– 60.512	41.697	– 11.236
	S	1.199	– 31.5	65.183	– 64.182	31.667	– 1.341
	Se	– 4.002	– 51.068	76.461	– 42.076	– 4.838	29.465
HF/6-31G(d)	CH ₂	2.78	– 17.803	47.322	– 62.972	47.335	– 17.821
	O	0.557	– 16.368	44.563	– 61.353	47.083	– 16.406
	S	2.811	– 24.168	56.637	– 65.581	39.916	– 10.067
	Se	– 3.821	– 47.803	74.718	– 44.392	– 0.755	25.879
B3LYP/6-31G(d)	CH ₂	3.264	– 18.123	47.228	– 62.512	47.172	– 18.068
	O	0.228	– 17.573	45.834	– 61.223	44.939	– 14.149
	S	2.654	– 27.094	59.079	– 64.009	36.08	– 6.74
	Se	– 3.888	– 47.917	75.163	– 44.71	– 0.484	25.773

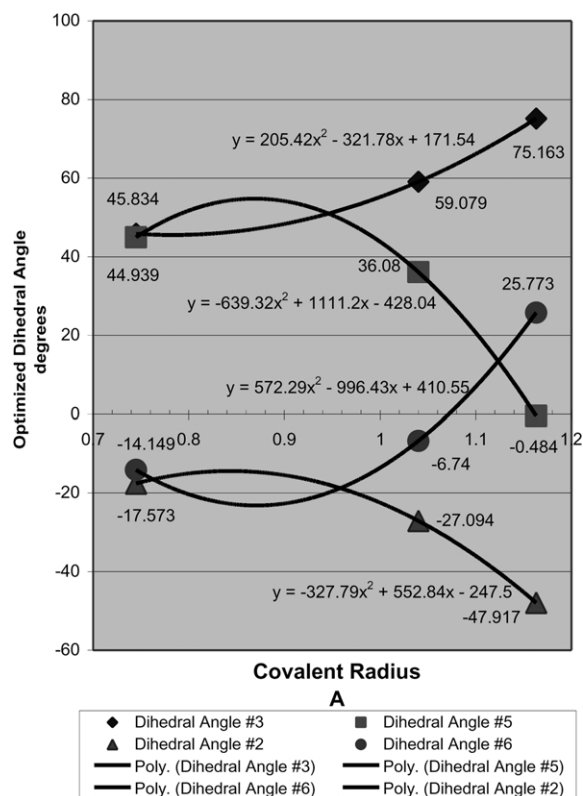


Fig. 9. Variation of selected dihedral angles as a function of atomic radii.

constituent atomic nuclei, shown in Fig. 6, was used in numerically generating the input files. No visualization tool was used for this purpose. It should be noted that H₂₁ and H₂₂ are present only in tetralin (I) but they are absent in chroman (II) and its higher congeners (III and IV).

For the sake of convenience, the variations of geometrical and energetic parameters from O to S to Se were fitted to quadratic functions, even though no quadratic relationships are assumed to be operative. For such graphical presentation the optimized parameters were plotted against the covalent atomic radii: O = 0.745 Å, S = 1.040 Å, and Se = 1.163 Å [14,15].

4. Results and discussion

Higher levels of theory are more reliable, therefore



Fig. 10. RHF/6-31G(d) optimized minimum energy and transition structures for chroman. The sulphur and selenium congeners have analogous geometries.

the majority of the discussion will be focused on the results obtained at the DFT level.

4.1. Molecular geometry of stable structures

The optimized bond lengths show no deviations from expected structural behavior. The greatest

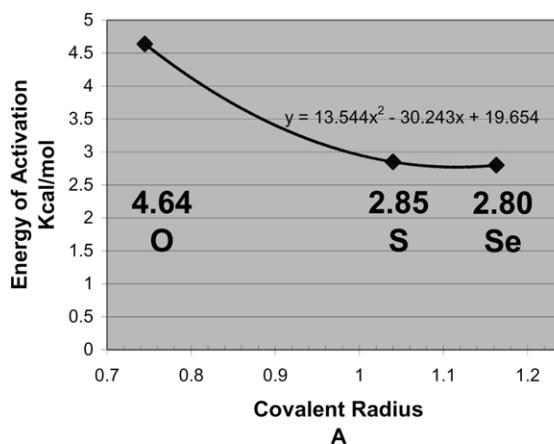
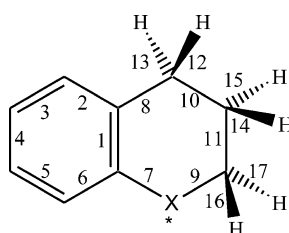


Fig. 11. Variation of energy of activation for ring inversion of chroman as well as S and Se congeners.

Table 7

Optimized bond lengths for the ring inversion transition structure ($\lambda = 1$) of compounds **I**, **II**, **III**, and **IV** obtained at three levels of theory

	X	1	2	3	4	5	6	7	8	9	10
HF/3-21G	CH ₂	1.3909	1.3872	1.3829	1.3832	1.3830	1.3861	1.5149	1.5213	1.5406	1.5656
	O	1.3836	1.3842	1.3845	1.3848	1.3826	1.3796	1.3839	1.5153	1.4542	1.5629
	S	1.3844	1.3924	1.3794	1.3848	1.3792	1.3844	1.8296	1.5265	1.8836	1.5624
	Se	1.3852	1.3930	1.3784	1.3844	1.3780	1.3861	1.9231	1.5289	1.9724	1.5617
HF/6-31G(d)	CH ₂	1.3909	1.3889	1.3847	1.3846	1.3848	1.3882	1.5113	1.5166	1.5405	1.5533
	O	1.3888	1.3855	1.3870	1.3855	1.3860	1.3821	1.3591	1.5096	1.4139	1.5454
	S	1.3930	1.3929	1.3818	1.3862	1.3811	1.3910	1.7786	1.5207	1.8135	1.5510
	Se	1.3918	1.3942	1.3811	1.3863	1.3805	1.3908	1.9063	1.5237	1.9466	1.5521
B3LYP/6-31G(d)	CH ₂	1.4069	1.3996	1.3949	1.3957	1.3949	1.3988	1.5119	1.5169	1.5374	1.5602
	O	1.4021	1.3961	1.3972	1.3970	1.3960	1.3942	1.3760	1.5085	1.4388	1.5496
	S	1.4069	1.4027	1.3930	1.3965	1.3921	1.4018	1.7864	1.5208	1.8360	1.5568
	Se	1.4051	1.4040	1.3926	1.3963	1.3918	1.4006	1.9171	1.5239	1.9726	1.5580
		11	12	13	14	15	16	17	18	19	
HF/3-21G	CH ₂	1.5420	1.0860	1.0834	1.0840	1.0834	1.0844	1.0839	1.0873	1.0836	
	O	1.5393	1.0848	1.0825	1.0819	1.0831	1.0775	1.0826	–	–	
	S	1.5263	1.0851	1.0831	1.0818	1.0851	1.0792	1.0788	–	–	
	Se	1.5278	1.0832	1.0854	1.0854	1.0820	1.0796	1.0807	–	–	
HF/6-31G(d)	CH ₂	1.5344	1.0875	1.0847	1.0857	1.0850	1.0861	1.0864	1.0897	1.0851	
	O	1.5368	1.0866	1.0842	1.0844	1.0853	1.0802	1.0855	–	–	
	S	1.5242	1.0864	1.0842	1.0837	1.0864	1.0829	1.0831	–	–	
	Se	1.5219	1.0842	1.0865	1.0871	1.0834	1.0812	1.0817	–	–	
B3LYP/6-31G(d)	CH ₂	1.5393	1.0996	1.0962	1.0968	1.0960	1.0968	1.0976	1.1017	1.0964	
	O	1.5459	1.0990	1.0953	1.0953	1.0962	1.0924	1.0984	–	–	
	S	1.5271	1.0986	1.0959	1.0950	1.0981	1.0941	1.0952	–	–	
	Se	1.5236	1.0960	1.0987	1.0990	1.0949	1.0929	1.0929	–	–	

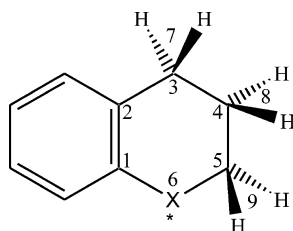
change is expected in the C–X–C region, specifically bond lengths labeled as 7 and 9, as shown in Table 4. The C–X involving the aromatic carbon (7) is slightly shorter than the other one involving the aliphatic

carbon (9). These optimized bond lengths correlate linearly with the covalent radii of O, S, and Se, as shown in Fig. 7.

The C–X–C and the X–C–C bond-angles,

Table 8

Optimized bond-angle lengths for the ring inversion transition structure ($\lambda = 1$) of compounds **I**, **II**, **III**, and **IV** obtained at three levels of theory



	X	1	2	3	4	5	6	7	8	9	10
HF/3-21G	CH ₂	118.481	120.394	115.204	113.747	109.880	108.287	106.723	107.160	108.039	107.814
	O	119.054	118.148	113.933	112.397	111.421	112.618	107.247	107.733	109.461	–
	S	120.569	124.084	118.153	114.424	109.213	106.717	106.677	107.545	109.861	–
	Se	121.210	124.870	119.284	114.852	109.795	92.215	106.533	107.393	109.128	–
HF/6-31G(d)	CH ₂	118.349	119.989	115.473	114.251	111.242	109.187	105.616	106.124	106.900	106.696
	O	118.525	116.941	112.612	112.228	112.666	112.839	106.495	106.730	108.159	–
	S	120.520	123.287	117.979	114.809	111.357	96.620	105.681	106.677	107.989	–
	Se	120.409	124.462	119.366	115.423	109.822	93.170	105.539	106.754	108.826	–
B3LYP/6-31G(d)	CH ₂	118.318	119.932	115.608	114.075	111.247	109.269	105.202	106.025	106.843	106.432
	O	118.847	116.619	112.609	112.047	113.735	112.492	106.344	106.758	108.125	–
	S	120.632	123.246	118.153	114.607	111.553	96.357	105.249	106.592	108.111	–
	Se	120.556	124.466	119.483	115.213	109.884	92.727	105.130	106.676	109.050	–

labeled **6** and **5**, respectively, are of greatest interest. The results are summarized in Table 5. Values show bond-angle **6** as undergoing the greatest change as the bond-angle (**6**) moves from a value larger than tetrahedral towards 90°, typical of S and Se. The diminishing of the C–C–C bond-angle is nearly exponential. In contrast to this, the X–C–C bond-angle (**5**) is compensating for such a dramatic closing in **6**, through a modest opening in the X–C–C (**5**) values. These changes at the DFT level are evaluated as moving from 111.8° for (X = oxygen) to 113.5° (X = selenium). The change is illustrated in Fig. 8.

For the torsion of the heterocyclic ring, dihedral angles behave in an interesting way as summarized in Table 6. The dihedral angles **1** and **4** behave in non-routine fashion, much as if the influence of the X nucleus on these two dihedrals was inconsequential. Dihedral

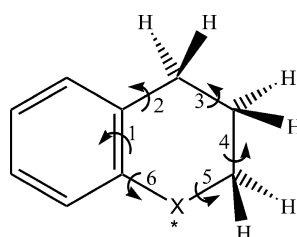
angles **2** and **6** are similar in magnitude and **3** and **5** are nearly identical. Yet they show deviation from one another as X = oxygen is replaced by sulfur and then by selenium. The variations of these dihedral angles are shown in Fig. 9.

4.2. Molecular geometries at transition structures

The ring inversion (Fig. 3) was studied in the cases of compounds **I**, **II**, **III**, and **IV**. For compound **II** (X = oxygen) the initial state, the transition state and the final states are shown in Fig. 10 as structures optimized at the RHF/6-31G(d) level of theory. Clearly, the fused heterocyclic ring exhibits a highly distorted boat arrangement (Fig. 10) in comparison to the idealized case given in Fig. 3. The optimized geometrical parameters, specifically bond lengths, bond-angles,

Table 9

Optimized dihedral angles lengths for the ring inversion transition structure ($\lambda = 1$) of compounds **I**, **II**, **III**, and **IV** obtained at three levels of theory



	X	1	2	3	4	5	6
HF/3-21G	CH ₂	− 5.450	29.194	− 3.496	− 41.810	64.682	− 41.565
	O	− 6.334	34.135	− 12.900	− 32.037	62.593	− 43.335
	S	− 5.213	26.268	8.548	− 56.141	65.340	− 36.158
	Se	5.727	− 25.247	− 10.899	57.659	− 63.418	33.606
HF/6-31G(d)	CH ₂	− 5.373	30.931	− 7.783	− 37.100	61.774	− 40.922
	O	− 4.317	38.477	− 22.512	− 23.716	60.899	47.071
	S	− 5.557	27.952	3.567	− 51.108	63.113	− 35.800
	Se	5.702	− 26.868	− 8.217	55.624	− 63.275	34.382
B3LYP/6-31G(d)	CH ₂	− 5.942	30.989	− 7.284	− 37.662	61.906	− 40.379
	O	− 4.454	41.093	− 27.214	− 19.083	57.513	− 46.097
	S	− 7.029	28.945	3.624	− 51.440	62.871	− 34.495
	Se	6.923	− 27.559	− 8.676	56.325	− 62.266	33.300

and dihedral angles are summarized in Tables 7–9, respectively.

4.3. Energetics of ring inversion

The energies of activations for the four compounds are tabulated in Table 10 at three levels of theory. The E_a values for the $X = [O, S, Se]$ containing molecules (**II**, **III**, and **IV**, respectively) were plotted against the covalent radii of X. The difference between O and S is large while the difference between S and Se is small (Fig. 11).

5. Conclusions

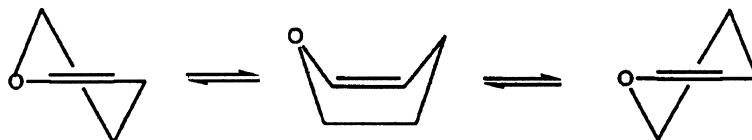
It is in human nature to wonder if ‘Mother

Nature’ did the best possible structural arrangement or whether we can improve upon it. The question has been asked [13,14] in general, about antioxidants and in particular about vitamin E [16,17].

From the present study, one can see that the influence of $X = S$ (**III**) and $X = Se$ (**IV**) are analogous to one another other but that they are very much different from the $X = O$ congener (**II**). On the basis of this result, one may expect the sulfur and the selenium containing compounds to be either much weaker or much stronger antioxidants than the oxygen containing one. Further research is needed in this area, in order to quantify the antioxidant characteristics of all topologically probable conformers, for each of these molecular systems.

Table 10

Optimized total energies for stable conformers ($\lambda = 0$) and ring inversion transition structure ($\lambda = 1$) as well as the associated energy of activation of compounds **I**, **II**, **III**, and **IV** obtained at three levels of theory



	<i>E</i> (hartree)		
X	Min	TS	<i>E</i> _a (kcal/mol)
HF/3-21G			
CH ₂	− 383.543851545	− 383.538891934	3.112205499
O	− 419.162508351	− 419.154678402	4.913371297
S	− 740.280616962	− 740.276189519	2.778264757
Se	− 2733.219289040	− 2733.212773800	4.088378253
<i>HF/6-31G(d)</i>			
CH ₂	− 385.686372822	− 385.680849545	3.465911550
O	− 421.501191382	− 421.493978702	4.526028827
S	− 744.156982123	− 744.152313980	2.929306414
Se	− 2744.222591050	− 2744.218050310	2.849359758
<i>B3LYP/6-31G(d)</i>			
CH ₂	− 388.306393922	− 388.301776427	2.897524287
O	− 424.203406366	− 424.196005393	4.644184567
S	− 747.177884971	− 747.173343996	2.849507222
Se	− 2748.368331440	− 2748.363874870	2.796542241

References

- [1] M. Evans, K.S. Bishop, *Science* 55 (1922) 650.
- [2] J.B. Bauernfeind, Vitamin E: A Comprehensive Treatise, Marcel Dekker, New York, 1980, pp. 99–167.
- [3] B. Weimann, H. Weiser, *Am. Clin. Nutr.* 53 (1991) 1056S–1060S.
- [4] N. Al-Maharik, L. Engman, J. Malmstrom, C. Schiesser, Intramolecular homolytic substitution at selenium: synthesis of novel selenium-containing vitamin E analogues, *J. Org. Chem.* 66 (2001) 6286–6290.
- [5] A.D.N.G. de Grey, *The Mitochondrial Free Radical Theory of Aging*, R.G. Landes Company, Austin, TX, 1999.
- [6] B. Chance, H. Sies, A. Boveris, *Physiol. Rev.* 59 (1979) 527.
- [7] B.N. Ames, M.K. Shigenaga, in: J.G. Scandalios (Ed.), *Molecular Biology of Free Radical Scavenging Systems*, Cold Spring Harbor Laboratory Press, New York, 1992, p. 1.
- [8] S. Steenken, *Chem. Rev.* 89 (1979) 503.
- [9] K.L. Fong, P.B. McCay, J.L. Poyer, B.H. Misra, B. Keele, *J. Biol. Chem.* 248 (1973) 7792.
- [10] T.I. Mak, W.B. Weglicki, *J. Clin. Invest.* 75 (1985) 58.
- [11] S. Varadarajan, J. Kanski, M. Aksenova, C. Lauderback, D.A. Butterfield, *J. Am. Chem. Soc.* 123 (2001) 5625.
- [12] G.W. Burton, K.U. Ingold, *Acc. Chem. Res.* 19 (1986) 194.
- [13] M.J. Frisch, G.W. Trucks, H.B. Schlegel, G.E. Scuseria, M.A. Robb, J.R. Cheeseman, V.G. Zakrzewski, J.A. Montgomery Jr., R.E. Stratmann, J.C. Burant, S. Dapprich, J.M. Millam, A.D. Daniels, K.N. Kudin, M.C. Strain, Ö. Farkas, J. Tomasi, V. Barone, M. Cossi, R. Cammi, B. Mennucci, C. Pomelli, C. Adamo, S. Clifford, J. Ochterski, G.A. Petersson, P.Y. Ayala, Q. Cui, K. Morokuma, D.K. Malick, A.D. Rabuck, K. Raghavachari, J.B. Foresman, J. Cioslowski, J.V. Ortiz, A.G. Baboul, B.B. Stefanov, G. Liu, A. Liashenko, P. Piskorz, I. Komaromi, R. Gomperts, R.L. Martin, D.J. Fox, T. Keith, M.A. Al-Laham, C.Y. Peng, A. Nanayakkara, M. Challacombe, P.M.W. Gill, B. Johnson, W. Chen, M.W. Wong, J.L. Andres, C. Gonzalez, M. Head-Gordon, E.S. Replogle, J.A. Pople, Gaussian Inc., Pittsburgh, PA, 1998.
- [14] C. Glidwell, *Inorg. Chim. Acta* 20 (1976) 113.
- [15] C. Glidwell, *Inorg. Chim. Acta* 36 (1979) 135.
- [16] J.S. Wright, E.R. Johnson, G.A. DiLabio, *J. Am. Chem. Soc.* 123 (2001) 1173–1183.
- [17] C.H. Schiesser, From Marco Polo to chiral stannanes—radical chemistry for the new millennium, *Arkivoc*, 2001.

Vitamin E models

The effect of heteroatom substitution in 2-ethyl-2-methyl chroman and 2-ethyl-2-methyl-6-hydroxychroman

D.H. Setiadi^{1,4,a}, G.A. Chass^{1,4,b}, L.L. Torday^{2,c}, A. Varro^{2,d}, J.Gy. Papp^{2,3,e}, and I.G. Csizmadia^{4,f}

¹ Global Institute of Computational Molecular and Materials Science @ VELOCET, 210 Dundas Street W., Suite 810, Toronto, Ontario, Canada M5G 2E8

² Department of Pharmacology and Pharmacotherapy, Szeged University, Domter12, Szeged, Hungary-6701

³ Division of Cardiovascular Pharmacology, Hungarian Academy of Sciences and Szeged University, Domter12, Szeged, Hungary-6701

⁴ Department of Chemistry, University of Toronto, 80 St. George St., Toronto, Ontario, Canada M5S 3H6

Received 9 May 2002 / Received in final form 9 July 2002

Published online 13 September 2002 – © EDP Sciences, Società Italiana di Fisica, Springer-Verlag 2002

Abstract. The molecular conformations of shortened molecular models of vitamin E (tocopherol and tocotrienol) and their sulfur and selenium congeners were studied computationally at the DFT level of theory [B3LYP/6-31G(d)]. The sequence of stabilization by the various heteroatoms was found to be the following: $O \sim Se > S$. On the basis of the present structural results it seems that the seleno-congener of vitamin E is a distinct possibility.

PACS. 31.15.Ar Ab initio calculations

1 Introduction

It is in human nature to wonder if “Mother Nature” always did the best possible structural arrangement for bioactive molecules, or whether we can improve upon it. The question has been asked in general about antioxidants, and in particular about vitamin E [1,2].

1.1 Vitamin E structures

Vitamin E, a term introduced in 1922 [3], does not represent a single compound but includes two families of compounds: tocopherols and tocotrienols. Both families consist of a chroman [benzopyrane] ring structure and a sidechain. The sidechain contains an isoprenoid skeleton, typical of terpenes. Members of the tocopherol family have saturated sidechains, but the same sidechain in the tocotrienol family has three non-conjugated double bonds. For both families, the carbon atom that carries the sidechain is a stereo centre of the *R* configuration. However, the sidechains of tocopherols have two additional

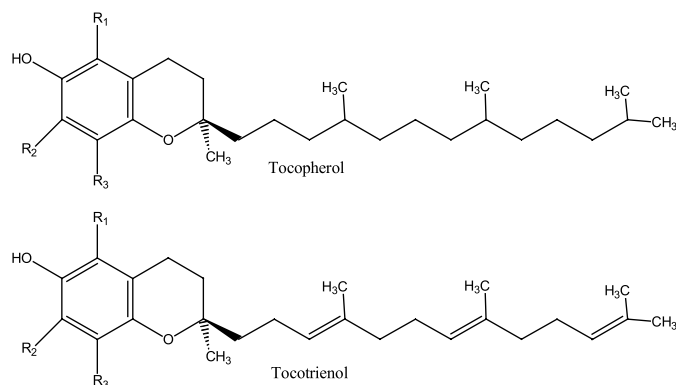


Fig. 1. Structures of tocopherols and tocotrienols. Substituents R₁, R₂, R₃ are hydrogens or methyl groups.

stereo-centres at their branching points, both of which are of *R* configuration. The structural variations of the two families are shown in Figure 1.

Each of these families has four homologous members, labeled as α , β , γ , and δ . They differ from each other in the extent of methyl substitution in the aromatic ring. Thus, these are two (2) families of compounds (tocopherol and tocotrienol) and each may come in four (4) homologous forms [4].

Of these $2 \times 4 = 8$ species, it is α -tocopherol which is most frequently used, partly because of its commercial

^a e-mail: dsetiadi@fixy.org

^b e-mail: gchass@fixy.org

^c e-mail: pyro@phcol.szote.u-szeged.hu

^d e-mail: varro@phcol.szote.u-szeged.hu

^e e-mail: papp@phcol.szote.u-szeged.hu

^f e-mail: icsizmad@alchemy.chem.utoronto.ca

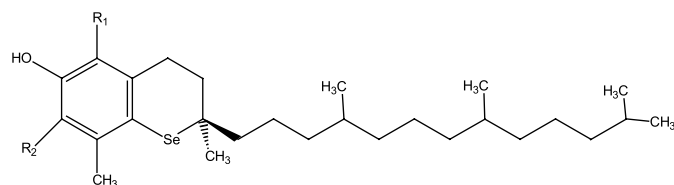


Fig. 2. Seleno-congener of α -tocopherol.

availability in synthetic form. Of course, the synthetic form is not a pure enantiomer. The effectiveness of the synthetic form has been questioned, without an explanation at the molecular level even though the primary function of vitamin E is an antioxidant rather than taking part in an oxidation reaction. Presently, we have more precise data to support the earlier assumption [5] that the different stereoisomers exhibit different effectiveness of biological activity.

It has recently been suggested [6] that the selenium congener of α -tocopherol [Fig. 2] may be a very effective antioxidant. Thus, one may ask if the sulphur (S) and selenium (Se) congeners of vitamin E might be more efficient antioxidants than vitamin E itself. The answer to such a question may be decided by studying the redox mechanism of the three congeners containing O, S and Se.

1.2 Conformational background

One of the structural problems of vitamin E is associated with the saturated ring fused to the benzene ring. This ring cannot be considered to be cyclohexane, nor any of its heterocyclic analogues in the chair conformation, because it has, at least formally, one carbon-carbon double bond. The so-called “half-chair” conformation had been considered to be the most likely structure and was confirmed by experiment [7–13].

Of the four CH_2 groups found in tetralin, the two allylic CH_2 exhibit quasiaxial or pseudoaxial (a') and quasi-equatorial or pseudo-equatorial (e') orientation. The orientation of the central $\text{CH}_2\text{--CH}_2$ moiety is expected to be close to non-cyclic molecules such as ethane or butane. Thus, the further one moves away from the double bond, the closer one comes to the ideal planar situation. Estimated dihedral angles (D_i) are shown in Figure 3.

The ring is expected to exist in two inter-convertible enantiomeric forms, with the transition state for such a ring-flip expected to show some molecular symmetry; interconnecting the two non-super-imposable mirror image (enantiomer) minima on either side. It is tempting to consider the planar structure to be a good candidate for the transition state, but such a conformation could be a higher order critical point. It is more likely that the transition state is a boat conformation. The ring-inversion has been studied computationally in the case of tetralin as well as its oxygen, sulfur and selenium congeners [14].

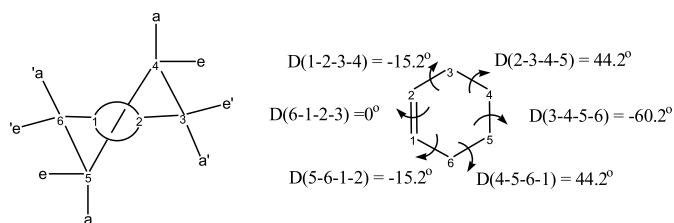


Fig. 3. Previously reported conformation and dihedral angles of cyclohexene.

2 Method

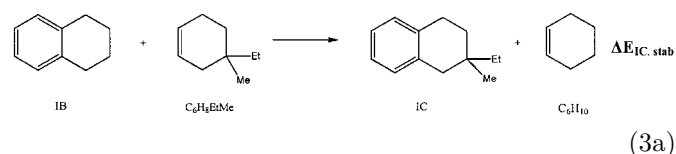
Since it is generally believed that the hydrocarbon tails of tocopherols are only necessary to enhance fat solubility [15] or “affinity” for hydrophobic environs, it is appropriate to concentrate an “activity”-related investigation (antioxidative character) on the fused ring systems, without the tail end.

Molecular orbital computations were carried out using the Gaussian 98 program package [16]. All computations were carried out at the B3LYP/6-31G(d) level of theory. Convergence criteria of 3.0×10^{-4} , 4.5×10^{-4} , 1.2×10^{-3} and 1.8×10^{-3} were used for the gradients of the RMS (root mean square) Force, Maximum Force, RMS Displacement and Maximum Displacement vectors, respectively.

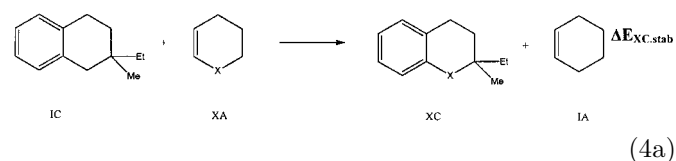
Four families (A, B, C, D) of the four compounds (I, II, III, IV) were studied as shown in Figure 4. All together, sixteen compounds were studied. Compound III and IV are sulfur and selenium congeners of II.

The definition of the spatial orientation of the constituent atomic nuclei shown in Figure 4 was used in numerically generating the input files. No visualization tool was used for any purpose for this work. It should be noted that there are two extra hydrogen atoms in the carbon congeners (*i.e.* $\text{X} = \text{CH}_2$) of IA, IB, IC and ID. The position of these two hydrogen atoms were optimized but omitted from the tabulated data. Key torsional angles are defined in Figure 5.

In order to compare the relative stabilities of the $\text{X} = \text{O}$, S and Se congeners, the following three isodesmic reactions were applied.



$$\Delta E_{\text{IC.stab}} = [E(\text{IC}) + E(\text{C}_6\text{H}_{10})] - [E(\text{IB}) + E(\text{C}_6\text{H}_8\text{EtMe})] \quad (3b)$$



$$\Delta E_{\text{XC.stab}} = [E(\text{XC}) + E(\text{IA})] - [E(\text{IC}) + E(\text{XA})] \quad (4b)$$

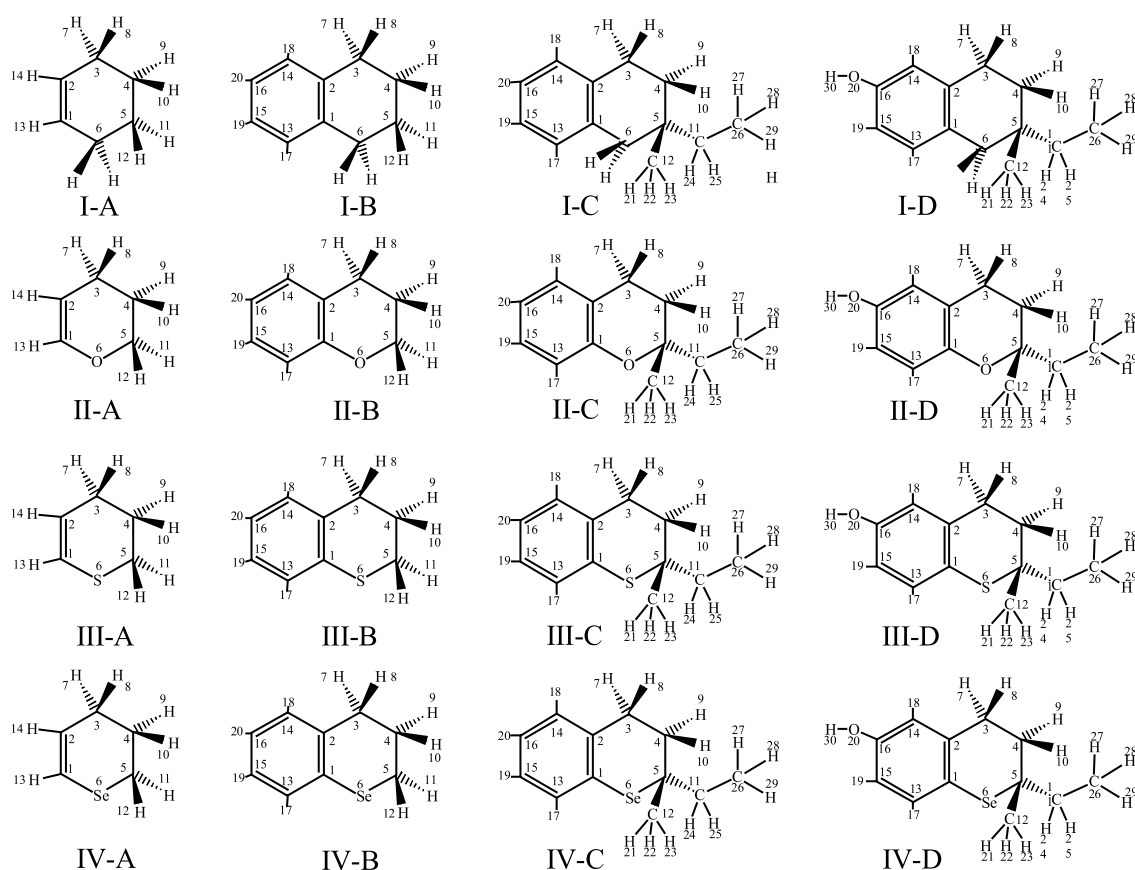
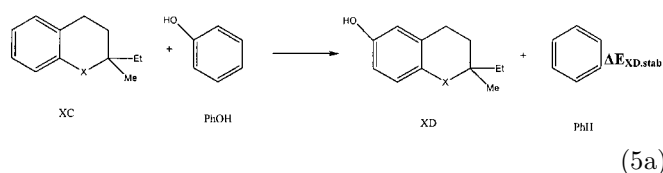


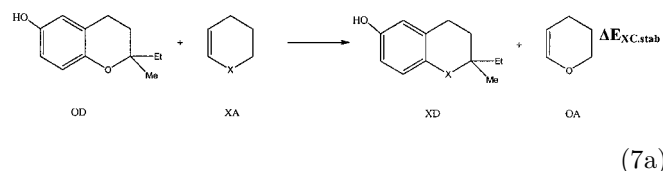
Fig. 4. Atomic numbering of the sixteen compounds studied.



The overall stabilization energy is the sum of the two individual stabilization energies

$$\Delta E_{\text{Total.stab}} = \Delta E_{\text{XD.stab}} + \Delta E_{\text{XC.stab}}. \quad (6)$$

Replacing oxygen (O) to sulfur (X = S) or selenium (X = Se). We may also obtain isodesmic energies as listed below in equations (7a, 7b)



Where X = S or Se

$$\Delta E_{\text{O} \rightarrow \text{X}} = [E(\text{XD}) + E(\text{OA})] - [E(\text{OD}) + E(\text{XA})]. \quad (7b)$$

For the sake of convenience, the variations of geometrical and energetic parameters from O to S to Se were fitted to

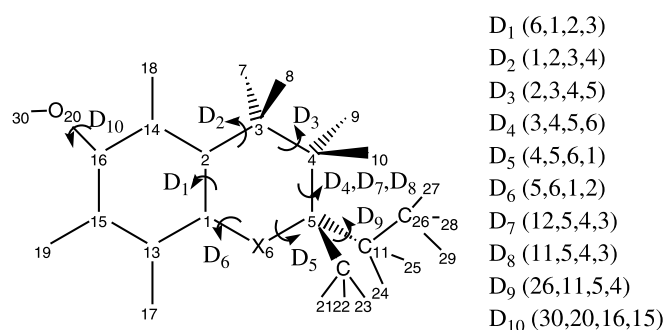


Fig. 5. Definition of key dihedral angles.

quadratic functions, even though no quadratic relationships are assumed to be operative. For such graphical presentation the optimized parameters were plotted against the covalent atomic radii: O = 0.745 Å, S = 1.040 Å and Se = 1.163 Å [8,9].

3 Results and discussion

Although computations have been carried out at several levels of theory, only the results obtained at the highest level [B3LYP/6-31G(d)] are reported in this work.

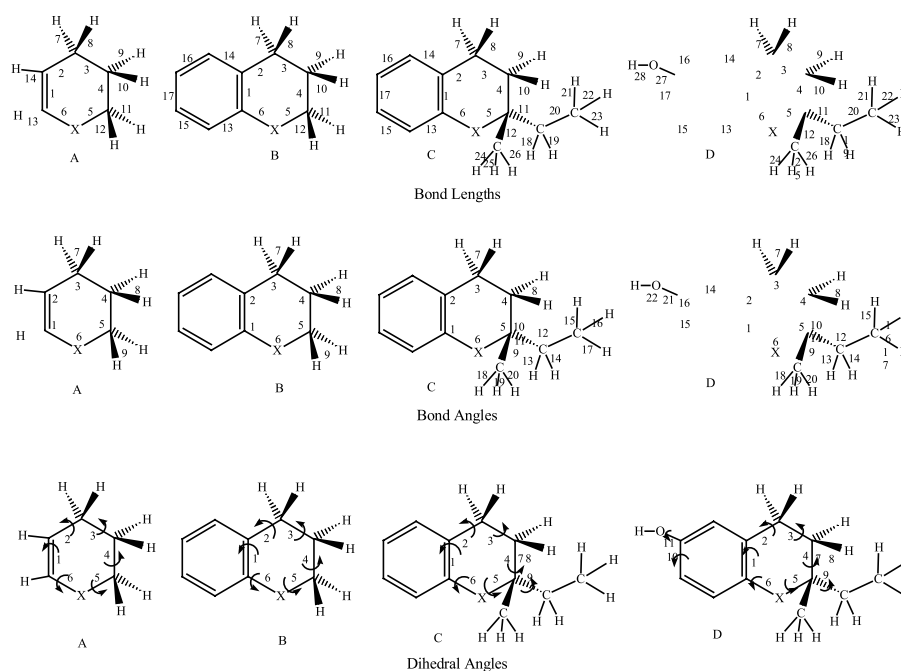


Fig. 6. Labeling of bonds, angles, and dihedrals.

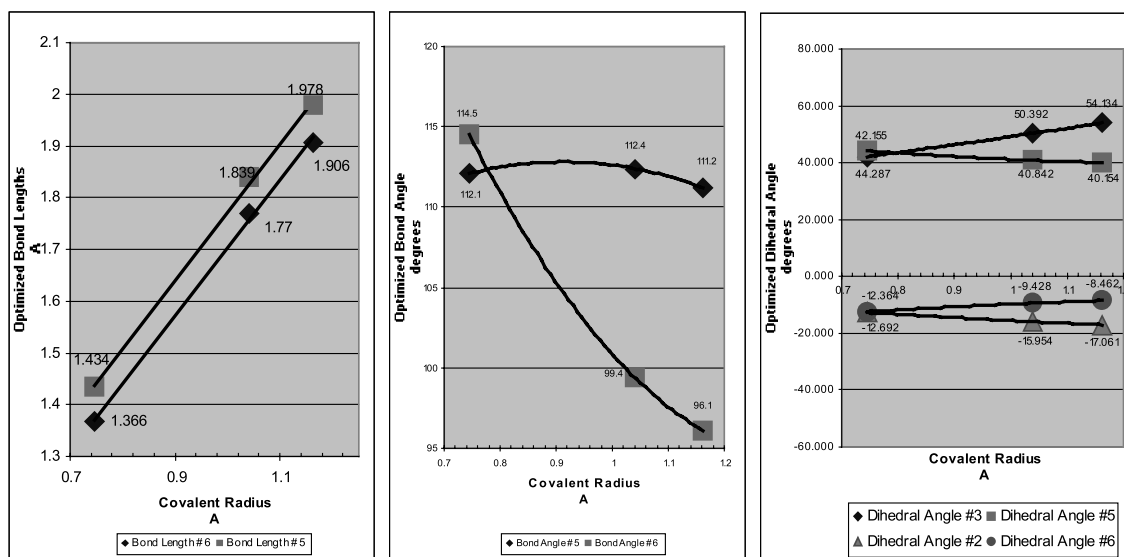


Fig. 7. Geometrical variation in cyclohexene as a result of oxygen, sulfur and selenium substitution. Atomic radii in angstrom on horizontal axis.

3.1 Molecular geometry of stable structures

The labeling of the bond lengths, bond angles and dihedral angles are given in Figure 6. The corresponding optimized parameters are summarized in Tables 1, 2 and 3, respectively.

The optimized dihedral angles of cyclohexene compare favourably to those reported earlier as shown in Table 4; the geometry changes with heteroatom substitution. The increasing atomic size created by the progression from oxygen to sulfur, then to selenium makes a noticeable difference, as is illustrated in Figure 7 for selected bond length, bond angles and dihedral angles.

When both substitutions by the heteroatoms within the ring, as well as alkyl and hydroxyl substitution on tetralin are considered, the changes are quite complex. Some of the tabulated results are shown in the form of a 3D-bar diagram in Figure 8.

Changes in C–C bond lengths and bond angles about a carbon atom are influenced slightly by the nearby O, S or Se. However, the changes are not large and their change is not necessarily monotonic, as one would expect on the basis of the periodic table (O→S→Se). Very often the parameter in question for sulfur is either smaller or larger

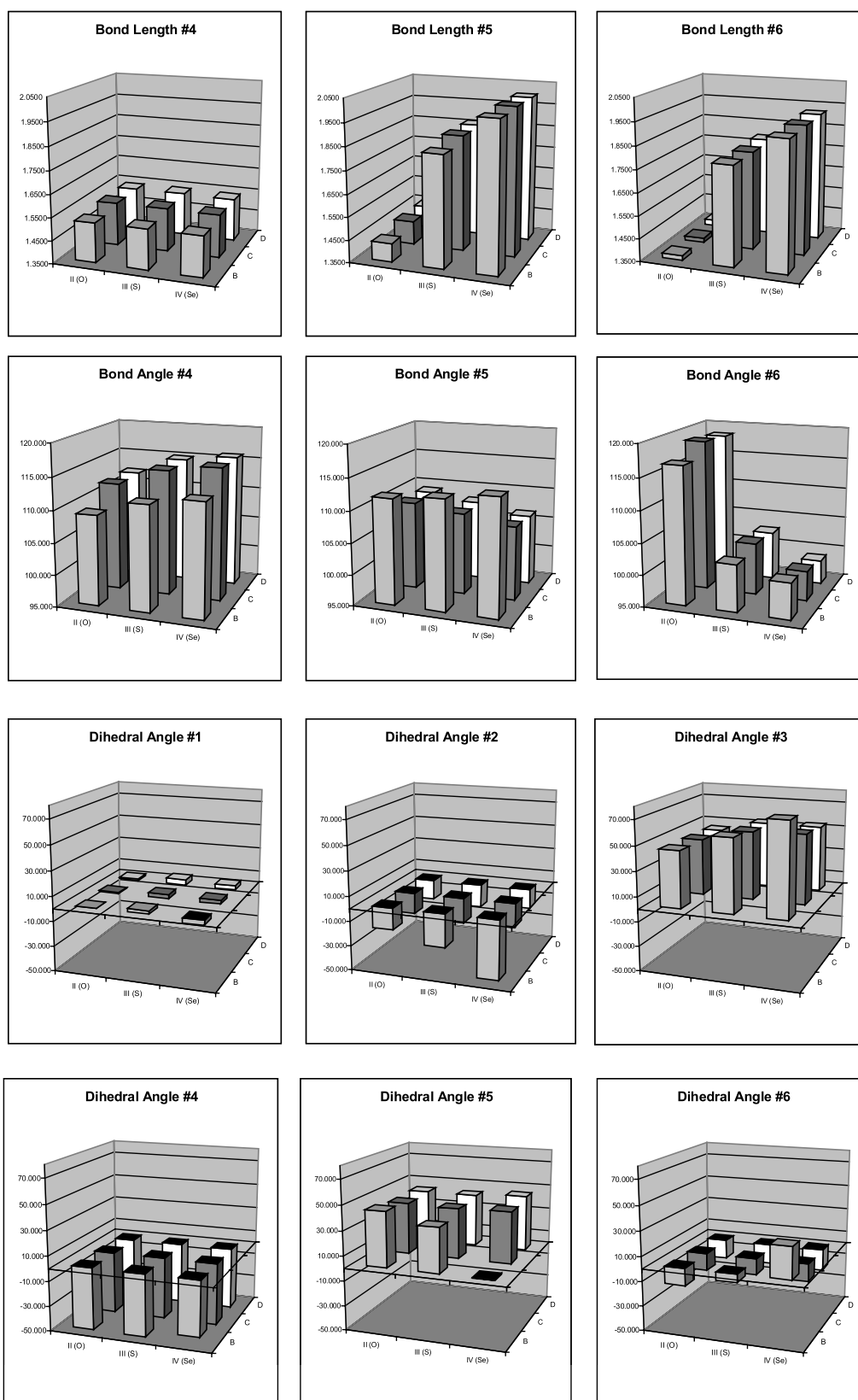


Fig. 8. Variation of selected bond lengths, bond angles and dihedral angles as a function of heteroatom type and ring substitution.

Table 1. Optimized bond lengths for the stable conformers ($\lambda = 0$) of the sixteen compounds studied at B3LYP/6-31G(d) level of theory.

Length	X		A	B	C	D
1	CH2	I	1.3370	1.4066	1.4061	1.4043
	O	II	1.3383	1.4054	1.4049	1.4015
	S	III	1.3388	1.4072	1.4065	1.4042
	Se	IV	1.3369	1.4053	1.4043	1.4022
2	CH2	I	1.5098	1.5203	1.5184	1.5181
	O	II	1.5087	1.5163	1.5128	1.5126
	S	III	1.5082	1.5182	1.5177	1.5178
	Se	IV	1.5093	1.5101	1.5205	1.5214
3	CH2	I	1.5373	1.5338	1.5351	1.5347
	O	II	1.5380	1.5338	1.5331	1.5332
	S	III	1.5363	1.5321	1.5318	1.5321
	Se	IV	1.5369	1.5421	1.5343	1.5347
4	CH2	I	1.5352	1.5327	1.5476	1.5477
	O	II	1.5277	1.5245	1.5399	1.5407
	S	III	1.5313	1.5272	1.5418	1.5423
	Se	IV	1.5282	1.5261	1.5392	1.5395
5	CH2	I	1.5373	1.5339	1.5460	1.5462
	O	II	1.4336	1.4306	1.4533	1.4509
	S	III	1.8391	1.8364	1.8635	1.8622
	Se	IV	1.9779	1.9970	2.0032	2.0017
6	CH2	I	1.5099	1.5203	1.5195	1.5191
	O	II	1.3658	1.3717	1.3702	1.3748
	S	III	1.7704	1.7884	1.7878	1.7901
	Se	IV	1.9057	1.9150	1.9205	1.9222
7	CH2	I	1.0990	1.1011	1.0995	1.0996
	O	II	1.0984	1.1002	1.0991	1.0992
	S	III	1.0987	1.1011	1.0992	1.0993
	Se	IV	1.0987	1.1009	1.0993	1.0993
8	CH2	I	1.1020	1.0977	1.0979	1.0980
	O	II	1.1008	1.0969	1.0971	1.0973
	S	III	1.1017	1.0967	1.0973	1.0975
	Se	IV	1.1020	1.0956	1.0974	1.0977
9	CH2	I	1.0970	1.0993	1.0983	1.0983
	O	II	1.0965	1.0971	1.0963	1.0963
	S	III	1.0977	1.0967	1.0994	1.0995
	Se	IV	1.0986	1.0963	1.1009	1.1009
10	CH2	I	1.0990	1.0968	1.0992	1.0991
	O	II	1.0969	1.0963	1.0972	1.0971
	S	III	1.0964	1.0977	1.0966	1.0965
	Se	IV	1.0964	1.0982	1.0965	1.0962
11	CH2	I	1.0990	1.0968	1.5389	1.5533
	O	II	1.1003	1.0932	1.5464	1.5467
	S	III	1.0954	1.0942	1.5484	1.5480
	Se	IV	1.0930	1.0921	1.5433	1.5429
12	CH2	I	1.0970	1.0993	1.5534	1.5391
	O	II	1.0933	1.1009	1.5293	1.5294
	S	III	1.0940	1.0955	1.5364	1.5365
	Se	IV	1.0928	1.0924	1.5342	1.5341
13	CH2	I	1.0897	1.4027	1.4028	1.4038
	O	II	1.0862	1.4004	1.4017	1.4017
	S	III	1.0870	1.4044	1.4056	1.4061
	Se	IV	1.0865	1.3998	1.4038	1.4045
14	CH2	I	1.0897	1.4026	1.4024	1.4020
	O	II	1.0860	1.4005	1.4007	1.4022
	S	III	1.0891	1.4024	1.4033	1.4035
	Se	IV	1.0901	1.3996	1.4041	1.4042
15	CH2	I		1.3920	1.3922	1.3891
	O	II		1.3908	1.3905	1.3882
	S	III		1.3907	1.3901	1.3872
	Se	IV		1.3935	1.3905	1.3874

Length	X		A	B	C	D
16	CH2	I		1.3920	1.3921	1.3939
	O	II		1.3930	1.3927	1.3933
	S	III		1.3920	1.3913	1.3930
	Se	IV		1.3945	1.3913	1.3929
17	CH2	I		1.3970	1.3970	1.3991
	O	II		1.3984	1.3986	1.4001
	S	III		1.3965	1.3972	1.3992
	Se	IV		1.3956	1.3967	1.3989
18	CH2	I			1.0965	1.0966
	O	II			1.0962	1.0962
	S	III			1.0954	1.0957
	Se	IV			1.0954	1.0955
19	CH2	I			1.0999	1.1000
	O	II			1.0989	1.0989
	S	III			1.1014	1.1014
	Se	IV			1.1022	1.1022
20	CH2	I			1.5347	1.5346
	O	II			1.5328	1.5327
	S	III			1.5322	1.5322
	Se	IV			1.5318	1.5318
21	CH2	I			1.0960	1.0960
	O	II			1.0956	1.0956
	S	III			1.0953	1.0953
	Se	IV			1.0954	1.0954
22	CH2	I			1.0953	1.0953
	O	II			1.0952	1.0953
	S	III			1.0950	1.0950
	Se	IV			1.0954	1.0954
23	CH2	I			1.0961	1.0960
	O	II			1.0945	1.0945
	S	III			1.0957	1.0957
	Se	IV			1.0951	1.0950
24	CH2	I			1.0957	1.0957
	O	II			1.0933	1.0933
	S	III			1.0945	1.0945
	Se	IV			1.0947	1.0948
25	CH2	I			1.0975	1.0975
	O	II			1.0957	1.0958
	S	III			1.0976	1.0976
	Se	IV			1.0985	1.0984
26	CH2	I			1.0970	1.0970
	O	II			1.0947	1.0947
	S	III			1.0944	1.0945
	Se	IV			1.0946	1.0948
27	CH2	I				1.3704
	O	II				1.3736
	S	III				1.3701
	Se	IV				1.3697
28	CH2	I				0.9698
	O	II				0.9694
	S	III				0.9697
	Se	IV				0.9697
29	CH2	I	1.1020	1.1010	1.0961	1.0974
	O	II	-	-	-	-
	S	III	-	-	-	-
	Se	IV	-	-	-	-
30	CH2	I	1.0990	1.0977	1.1012	1.1014
	O	II	-	-	-	-
	S	III	-	-	-	-
	Se	IV	-	-	-	-

than that for the oxygen and selenium-containing compound.

Take for example bond angle 9 in Model D.

$$112.1^\circ \rightarrow 111.6^\circ \rightarrow 112.4^\circ$$

$$\text{O} \rightarrow \text{S} \rightarrow \text{Se}. \quad (8)$$

Of the geometrical parameters, noting the dihedral angles, D_1 is close to 0° and D_4 is close to 60° ; which would not commonly be expected. D_2 , D_3 , D_5 and D_6 values were

plotted against the covalent radii of the heteroatoms O, S and Se in Figure 9.

On going from the single heterocyclic ring (A) to the next larger system where a benzene ring is fused to the heterocycle (B) a large amplification in dihedral angles were noticed. This amplification was followed by two consecutive attenuations on going from B to C and subsequently from C to D. Thus, the final system (D) did not differ much from the original (A) ring structure.

Table 2. Optimized bond angles for the stable conformers ($\lambda = 0$) of the sixteen compounds studied at B3LYP/6-31G(d) level of theory.

Angle	X		A	B	C	D
1	CH2	I	123.551	121.478	121.403	121.656
	O	II	125.660	123.140	123.513	123.685
	S	III	126.839	124.430	124.472	124.568
	Se	IV	126.352	121.524	123.923	123.950
2	CH2	I	123.549	121.474	121.208	121.146
	O	II	121.987	120.367	120.085	120.099
	S	III	125.694	123.008	123.250	123.290
	Se	IV	126.717	120.500	124.359	124.497
3	CH2	I	112.032	113.377	113.683	113.516
	O	II	109.598	110.734	110.770	110.799
	S	III	113.681	114.512	115.197	115.362
	Se	IV	114.923	111.714	117.150	117.394
4	CH2	I	110.975	110.288	113.362	113.422
	O	II	109.817	109.179	112.098	112.208
	S	III	112.563	111.518	114.838	114.991
	Se	IV	113.271	112.709	115.859	115.864
5	CH2	I	110.968	110.291	106.822	106.868
	O	II	112.052	111.805	109.102	109.018
	S	III	112.355	112.445	108.124	107.948
	Se	IV	111.242	113.499	106.813	106.393
6	CH2	I	112.024	113.385	114.651	114.549
	O	II	114.478	116.747	118.922	118.457
	S	III	99.425	102.512	103.294	102.744
	Se	IV	96.134	100.694	99.749	98.873
7	CH2	I	105.362	105.707	105.339	105.408
	O	II	105.785	106.132	105.771	105.798
	S	III	105.316	105.813	105.294	105.325
	Se	IV	105.189	106.843	105.075	105.107
8	CH2	I	106.709	106.735	106.446	106.473
	O	II	107.415	107.498	107.101	107.121
	S	III	107.040	107.232	106.776	106.779
	Se	IV	107.117	107.001	106.719	106.747
9	CH2	I	106.710	106.735	110.462	110.424
	O	II	108.513	108.246	112.169	112.128
	S	III	108.019	107.869	111.628	111.632
	Se	IV	108.847	108.920	112.294	112.364
10	CH2	I			109.748	109.730
	O	II			111.681	111.662
	S	III			111.107	111.171
	Se	IV			112.215	112.277
11	CH2	I			108.711	108.644
	O	II			110.37	110.262
	S	III			109.296	109.164
	Se	IV			109.707	109.700
12	CH2	I			116.585	116.607
	O	II			115.236	115.165
	S	III			116.430	116.344
	Se	IV			115.952	115.887

Angle	X		A	B	C	D
13	CH2	I			108.968	109.023
	O	II			108.397	108.428
	S	III			108.782	108.811
	Se	IV			108.944	108.882
14	CH2	I			107.908	107.917
	O	II			108.011	108.073
	S	III			107.148	107.196
	Se	IV			107.435	107.519
15	CH2	I			112.074	112.049
	O	II			110.795	110.304
	S	III			112.170	112.143
	Se	IV			110.351	110.388
16	CH2	I			110.081	110.074
	O	II			112.234	112.230
	S	III			111.157	111.085
	Se	IV			112.237	112.266
17	CH2	I			112.212	112.248
	O	II			110.274	110.759
	S	III			110.016	110.055
	Se	IV			110.019	109.883
18	CH2	I			111.928	111.924
	O	II			110.977	110.941
	S	III			112.195	112.167
	Se	IV			112.213	112.198
19	CH2	I			111.049	111.066
	O	II			110.510	110.552
	S	III			109.607	109.662
	Se	IV			109.931	109.920
20	CH2	I			110.779	110.792
	O	II			110.246	110.246
	S	III			110.862	110.878
	Se	IV			110.856	110.906
21	CH2	I				117.565
	O	II				117.510
	S	III				117.594
	Se	IV				117.622
22	CH2	I				108.699
	O	II				108.663
	S	III				108.817
	Se	IV				108.804
23	CH2	I	105.363	105.716	106.084	105.277
	O	II	-	-	-	-
	S	III	-	-	-	-
	Se	IV	-	-	-	-

3.2 Molecular energetics

The computed total energies are summarized in Table 5. These energy values are not comparable since each of the sixteen molecular systems has a different number of electrons. In order to make an energetic comparison of the sixteen molecular structures some isodesmic reaction energy calculation should be made in order to determine the relative stabilization or destabilization exerted by the substituents on the basic structures. The calculations were carried out according to equations (3–6). Stabilization energies are summarized in Table 6.

The stabilization energies reveal that oxygen and selenium substitutions stabilize the ring system more or less to the same extent. However, sulfur destabilizes (by 6 kcal/mole) the same ring system. This is particularly clear from the last column of Table 6.

4 Conclusions

The present work shows that O and Se stabilize the fused ring system of tocopherols more or less to the same extent, while S destabilizes it slightly.

Table 3. Optimized dihedral angles for the stable conformers ($\lambda = 0$) of the sixteen compounds studied obtained at B3LYP/6-31G(d) level of theory.

Dihedral	X		A	B	C	D
1	CH2	I	-1.606	3.264	4.190	4.550
	O	II	-3.886	0.228	0.838	1.395
	S	III	-2.443	2.654	3.225	4.521
	Se	IV	-2.553	-3.888	3.088	3.371
2	CH2	I	-13.867	-18.123	-14.180	-14.817
	O	II	-12.692	-17.573	-17.223	-16.775
	S	III	-15.954	-27.094	-20.504	-19.562
	Se	IV	-17.061	-47.917	-19.002	-16.029
3	CH2	I	44.106	47.228	43.767	44.242
	O	II	42.155	45.834	45.396	44.816
	S	III	50.392	59.079	54.894	53.486
	Se	IV	54.134	75.163	56.036	53.455
4	CH2	I	-60.472	-62.512	-60.748	-60.783
	O	II	-60.193	-61.223	-57.953	-58.221
	S	III	-64.744	-64.009	-64.757	-65.148
	Se	IV	-66.598	-44.710	-66.422	-67.513
5	CH2	I	44.138	47.172	49.425	49.000
	O	II	44.287	44.939	41.987	43.101
	S	III	40.842	36.080	40.796	42.738
	Se	IV	40.154	-0.484	41.883	45.098
6	CH2	I	-13.904	-18.068	-23.282	-23.087
	O	II	-12.364	-14.149	-14.361	-15.770
	S	III	-9.428	-6.740	-13.425	-16.018
	Se	IV	-8.462	25.773	-14.412	-17.532
7	CH2	I			-178.664	-178.716
	O	II			-172.048	-172.281
	S	III			-179.108	-179.407
	Se	IV			179.959	178.890
8	CH2	I			60.422	60.469
	O	II			62.447	62.363
	S	III			57.268	57.012
	Se	IV			54.400	53.199
9	CH2	I			174.334	174.240
	O	II			-179.929	-179.936
	S	III			173.611	173.703
	Se	IV			178.813	179.196
10	CH2	I				-179.778
	O	II				179.822
	S	III				179.651
	Se	IV				179.867
11	CH2	I				-179.884
	O	II				179.794
	S	III				179.884
	Se	IV				-179.818

Table 4. Previously reported and present optimized dihedral angles of cyclohexene.

	Previously reported*	Present optimized**
D1	0.00	-1.61
D2	-15.20	-13.87
D3	44.20	44.11
D4	-60.20	-60.47
D5	44.20	44.14
D6	-15.20	-13.90

*Reference [8], ** B3LYP/6-31G(d).

The stabilization and relative stabilization are of the following order:

$$\begin{array}{ccccccc} \text{O} & \sim & \text{Se} & \gg & \text{S} & & \\ -4.82 & & -4.73 & & +1.19 & (\text{kcal mol}^{-1}) & \\ 0.00 & & +0.09 & & +6.01 & (\text{kcal mol}^{-1}). & \end{array}$$

On the basis of the present structural results it seems that the seleno congener of vitamin E is a distinct possibility.

It remains to be seen if the energies of the red-ox reaction mechanism follow the same sequence.

This work was supported by grants from Velocet Communications Inc., Toronto, Ontario, Canada and the National Science

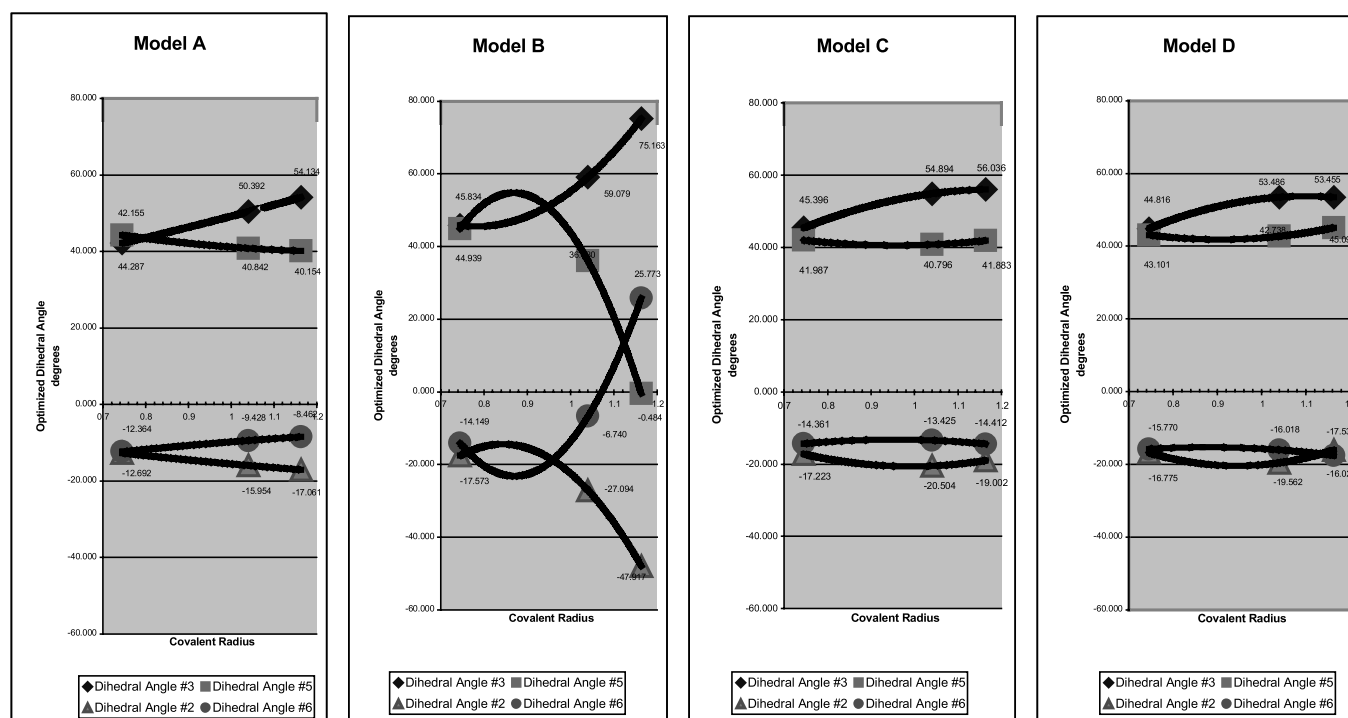


Fig. 9. Variation of selected bond lengths, bond angles and dihedral angles as a function of the heteroatom site and ring substitution.

Table 5. Optimized total energies of the sixteen compounds studied.

		Total energy (Hartree)			
X		A	B	C	D
CH ₂	I	-234.6482949	-388.3063939	-506.2415280	-581.4572576
O	II	-270.5443727	-424.2034064	-542.1505510	-617.3642250
S	III	-593.52225062	-747.1778850	-865.1177830	-940.3327840
Se	IV	-2594.7100207	-2748.3683314	-2866.3144144	-2941.5297229

Table 6. Stabilization energies exerted by oxygen, sulfur and selenium ring substitution as well as aromatic hydroxylation.

		Stabilization energy (kcal/mol) ^a				
X		IB→IC (Eq. (3))	IC→XC (Eq. (4))	XC→XD (Eq. (5))	Total (Eq. (6))	O→X (Eq. (7))
CH ₂	I	0.344	—	—	—	—
O	II	—	-6.412	1.592	-4.820	0.000
S	III	—	0.428	0.759	1.188	6.008
Se	IV	—	-5.293	0.566	-4.726	0.094

^a The following component energy values were used: $E(\text{Ph-H}) = -232.2486592$, $E(\text{Ph-OH}) = -307.4648704$, $E(\text{C}_6\text{H}_{10}) = -234.6482949$, $E(\text{C}_6\text{H}_8\text{EtMe}) = -352.5867031$.

Foundation (EPS-0091900). The authors thank Dr. Sándor Lovas at Creighton University (Omaha, NE, USA) for his continued support and guidance in helping sustain international cooperative research efforts between Canada and the USA. Also, Michelle A. Sahai, Jacqueline M.S. Law, Christopher N.J. Marai and Tania A. Pecora are thanked for helpful discussions and preparation of tables and figures and Graydon Hoare for database management, network support and soft-

ware and distributive processing development. A special thanks is extended to Andrew M. Chasse for his development of novel scripting and coding techniques which facilitate a reduction in the number of CPU cycles needed. The pioneering advances of Kenneth P. Chasse, in all composite computer-cluster software and hardware architectures, are also acknowledged. David C.L. Gilbert and Adam A. Heaney are also thanked for CPU time.

References

1. J.S. Wright, E.R. Johnson, G.A. DiLabio, J. Am. Chem. Soc. **123**, 1173 (2001)
2. M. Evans, K.S. Bishop, Science **55**, 650 (1922)
3. C.H. Schiesser, *From Marco Polo to chiral stannanes - radical chemistry for the new millennium* (Arkivoc, 2001)
4. J.B. Bauernfeind, in: *Vitamin E: a comprehensive treatise* (Marcel Dekker, New York, 1980)
5. B. Weimann, H. Weiser, Am. Clin. Nutr. **53**, 10565 (1991)
6. N. Al-Maharik, L. Engman, J. Malmstrom, C.J. Schiesser, Org Chem. **66**, 6286 (2001)
7. F.A.L. Anet, D.J. O'Leary, Tetrahedron Lett. **30**, 1059 (1989)
8. W. Auf der Heyde, W. Luttke, Chem. Ber. **111**, 2384 (1978)
9. J.F. Chiang, S.H. Bauer, J. Am. Chem. Soc. **91**, 1898 (1969)
10. H.J. Geise, H.R. Buys, Recl. Trav. Chim. Pays-Bas **89**, 1147 (1970)
11. V.A. Naumov, V.G. Dashevskii, N.M. Zaripov, J. Struct., Chem. USSR **11**, 793 (1970)
12. T. Ogata, K. Kozima, Bull. Chem. Soc. Jpn. **42**, 1263 (1969)
13. L.H. Scharpen, J.E. Wollrab, D.P. Ames, J. Chem. Phys. **49**, 2368 (1986)
14. D.H. Setiadi, G.A. Chass, L.L. Torday, A. Varro, J.Gy. Papp, Theochem (2002) in press
15. G.W. Burton, K.U. Ingold, Acc. Chem. Res. **19** 194 (1986)
16. M.J. Frisch, G.W. Trucks, H.B. Schlegel, G.E. Scuseria, M.A. Robb, J.R. Cheeseman, V.G. Zakrzewski, J.A. Montgomery Jr, R.E. Stratmann, J.C. Burant, S. Dapprich, J.M. Millam, A.D. Daniels, K.N. Kudin, M. Strain, Ö. Farkas, J. Tomasi, V. Barone, M. Cossi, R. Cammi, B. Mennucci, C. Pomelli, C. Adamo, S. Clifford, J. Ochterski, G.A. Petersson, P.Y. Ayala, Q. Cui, K. Morokuma, D.K. Malick, A.D. Rabuck, K. Raghavachari, J.B. Foresman, J. Cioslowski, J.V. Ortiz, A.G. Baboul, B.B. Stefanov, G. Liu, A. Liashenko, P. Piskorz, I. Komaromi, R. Gomperts, R.L. Martin, D.J. Fox, T. Keith, M.A. Al-Laham, C.Y. Peng, A. Nanayakkara, M. Challacombe, P.M.W. Gill, B. Johnson, W. Chen, M.W. Wong, J.L. Andres, C. Gonzalez, M. Head-Gordon, E.S. Replogle, J.A. Pople, *Gaussian*, Gaussian Inc., Pittsburgh PA, 1998
17. C. Glidwell, Inorg. Chim. Acta. **20**, 113 (1976)
18. C. Glidwell, Inorg. Chim. Acta. **36**, 135 (1979)

Vitamin E models. Shortened sidechain models of α , β , γ and δ tocopherol and tocotrienol—a density functional study

David H. Setiadi^{a,*}, Gregory A. Chass^a, Ladislaus L. Torday^b, Andras Varro^b,
Julius Gy. Papp^{b,c}

^aGlobal Institute of Computational Molecular and Materials Science, 210 Dundas Street W., Suite 810, Toronto, Ont., Canada M5G 2E8

^bDepartment of Pharmacology and Pharmacotherapy, Szeged University, Dom ter12, Szeged 6701, Hungary

^cDivision of Cardiovascular Pharmacology, Hungarian Academy of Sciences and Szeged University, Dom ter12, Szeged 6701, Hungary

Received 23 June 2002; accepted 7 August 2002

Abstract

Model compounds of α -, β -, γ -, and δ -tocopherol and Tocotrienol, as well as their sulphur and selenium congeners, were subjected to density functional analysis. The mono methyl substitution either stabilized or destabilized the ring structures to a small extent as assessed in terms of isodesmic reactions. In general, multiple methyl substitutions destabilized the ring. Dimethyl *para*-substitution results in electronic stabilization and steric repulsion being nearly additive. This was not the case for *ortho*-dimethyl derivatives, whereby steric repulsions dominate; the *meta*-substituted models reflect the same trend to a lesser degree. Structurally, the phenolic hydroxyl orientation was approximately planar, with the hydroxyl proton oriented away from the adjacent Me group whenever the structure permitted such an orientation.

© 2003 Published by Elsevier B.V.

Keywords: Tocopherol; Tocotrienol; Density functional theory; Methyl substitution; Orientation of phenolic OH

1. Preamble

The term ‘Vitamin E’ was introduced in 1922 [1]. Vitamin E includes two families of compounds: tocopherols and tocotrienols (Fig. 1). Both families consist of a chroman [benzopyrane] ring structure and an isoprenoid sidechain, which is typical of terpenes. The tocopherol family has saturated sidechains, whereas the same sidechain in the tocotrienol family has three non-conjugated double bonds. For both families, the ring carbon atom that carries the sidechain is a stereocentre of *R* configuration. The sidechain of

the tocopherols has two additional stereocentres at the branching points, both of which are of *R* configuration.

Each of these families has four homologous members (see Table 1), labelled as α , β , γ , and δ . They differ from each other in the extent of the methyl substitution in the aromatic ring. The natural abundance of the components of the Vitamin E family varies from plant to plant [2].

The most important component of the Vitamin E family is α -tocopherol. It is commercially available in its synthetic form, which comes as an enantiomeric mixture. The effectiveness of the synthetic racemic mixture has traditionally been questioned, without any explanation at the molecular level. Presently, we

* Corresponding author.

E-mail address: dsetiadi@fixy.org (D.H. Setiadi).

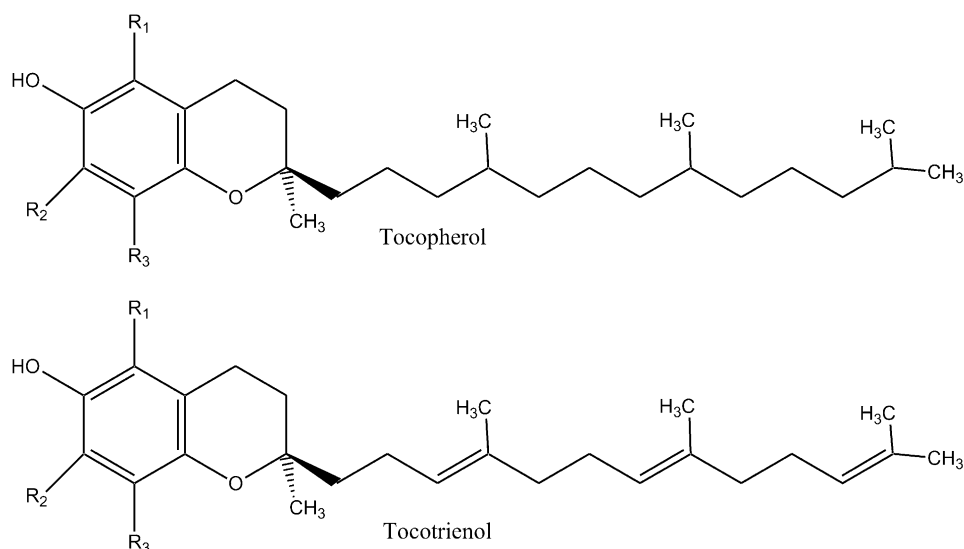


Fig. 1. General molecular structures of tocopherol and tocotrienol. aromatic substituents (R_1 , R_2 , and R_3) are specified in Table 1.

Table 1
Extent of methyl substitutions of the tocopherol and tocotrienol families

	R_1	R_2	R_3
α	Me	Me	Me
β	Me	H	Me
γ	H	Me	Me
δ	H	H	Me

have more precise data to support this traditional assumption [3].

Recently, the selenium analogue of α -tocopherol (Fig. 2) has been suggested [4] as an alternative congener which may be an effective antioxidant. For this reason we wish to study the structure of the chroman ring comparatively with its S and Se congeners.

2. Introduction

2.1. Oxidative stress and Vitamin E

Oxidative stress may be the cause of aging as well as of the origin of numerous degenerative diseases of the human body [5]. About 5% of the inhaled oxygen escapes the redox reactions associated with metabolism [6]. These by-products include the superoxide anion (O_2^-), the hydroperoxyl radical ($\cdot OOH$), hydrogen peroxide (H_2O_2) and the hydroxyl radical ($\cdot OH$). These 'reactive oxygen species' (ROS) are all very reactive and therefore short-lived in the body. Normally, there are natural mechanisms defending against free radicals [7], which may be enzymatic or non-enzymatic. If for some reason, these defense mechanisms become weakened then the free radicals can react with cellular structures such as DNA and

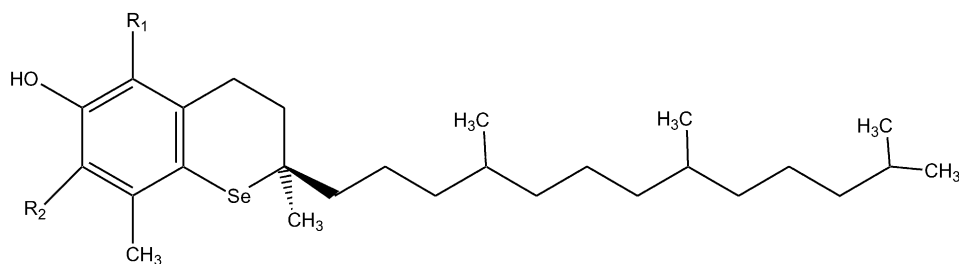


Fig. 2. A general structure of seleno-tocopherol.

proteins, or even destroy membranes through lipid peroxidation [8–10]. It is generally believed that aging and other age-related degenerative diseases such as cardiovascular disorders and cancer can be induced through these pathways [1]. Furthermore, oxidation of a methionine residue has been implicated recently [11] in Alzheimer's disease as a result of oxidative stress.

The potent antioxidant Vitamin E helps to prevent cancer by blocking lipid peroxidation and subsequently reduces the conversion of polyunsaturated fats into free radicals. Lipid peroxidation is a potential initiator not only of cardiovascular diseases but also all forms of cancers, especially of the breast and colon.

Vitamin E works synergistically with Vitamin C and with the mineral selenium, with which it has a special affinity. Selenium and Vitamin E combined constitute a double defense against cancer. As it is not possible to obtain optimally protective quantities of Vitamin E from diet alone, supplements of 400–1600 international units (IU) are recommended daily. Note that 1 mg α -tocopherol = 1.49 IU.

2.2. Structural background

Since it is generally believed that the tail end of tocopherols are only needed to enhance fat solubility [12] it is appropriate to initially concentrate on the fused ring systems (**II**, **III**, **IV**). Compound **III** and **IV** are the sulphur and selenium containing congeners respectively of chroman (**II**).

In a previous paper [13] the geometry of the chroman ring (**II**) as well as its S and Se containing congeners were studied. In the present paper, the effect of the methyl groups introduced to the aromatic ring will be reported. In a subsequent paper [14] the effect of the substituents in α -position of the heteroatom, namely methyl and ethyl, were examined using isodesmic reactions. In the same paper, the energetics of the aromatic hydroxylation were also investigated.

3. Method

Molecular orbital computations were carried out, using the GAUSSIAN98 program package [15], on

three families of compounds: chromane (**II**), thiochroman (**III**), and selenochroman (**IV**). Tetralin (**I**) is discussed in previous works [13,14] is omitted here.

Eight structures, the unsubstituted and seven methyl substituted ring structures, were considered for oxygen (**II**), sulphur (**III**), and selenium (**IV**) heteroatoms in the ring. Thus, a total of $3 \times 8 = 24$ structures are reported in the present paper. Of the seven substituted structures four are Vitamin E models (α , β , γ , δ) while the remaining three (E, E*, F), two single and one double methylated ring, respectively, have no relation to Vitamin E.

The definition of the spatial orientation, as well as the numbering of the constituent atomic nuclei, are shown in Fig. 3. The input files were numerically generated, whereby visualization tool was used for this purpose.

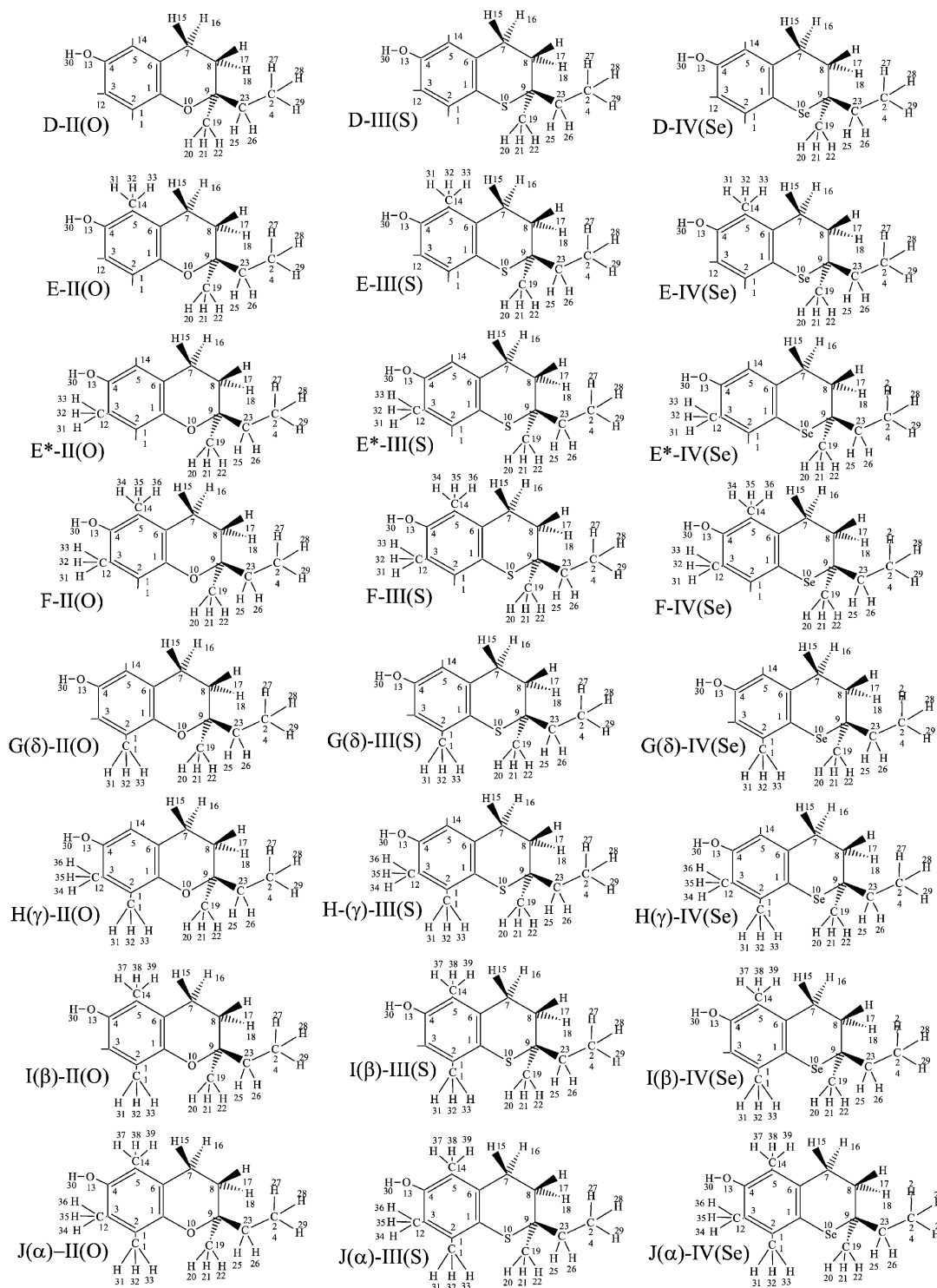
Two methods and 2 split-valence basis sets were used, mainly the RHF/3-21G, RHF/6-31G(d) and the B3LYP/6-31G(d) levels of theory. Convergence criteria of 3.0×10^{-4} , 4.5×10^{-4} , 1.2×10^{-3} , and 1.8×10^{-3} were used for the gradients of the root mean square (RMS) Force, Maximum Force, RMS Displacement and Maximum Displacement vectors, respectively. However, only the B3LYP/6-31G(d) results are reported in the present paper.

The stabilization or destabilization exerted by the methyl groups attached to the aromatic ring were studied through isodesmic reactions in which the Me group was transferred from toluene to the aromatic ring of the chroman skeleton, as well as its sulphur and selenium congeners. These isodesmic reactions are shown in Fig. 4. The following B3LYP/6-31G(d) energy values were used for toluene and benzene: (−271.56662) and (−232.248659) hartrees respectively.

4. Results and discussion

4.1. Molecular geometries

A total of twenty-four compounds were subjected to geometry optimizations. Of that total each of the oxygen, sulphur, and selenium containing rings had 8 homologues containing 0, 1, 2 and 3 methyl groups attached to the aromatic ring.

Fig. 3. Structures of the $3 \times 8 = 24$ molecules studied.

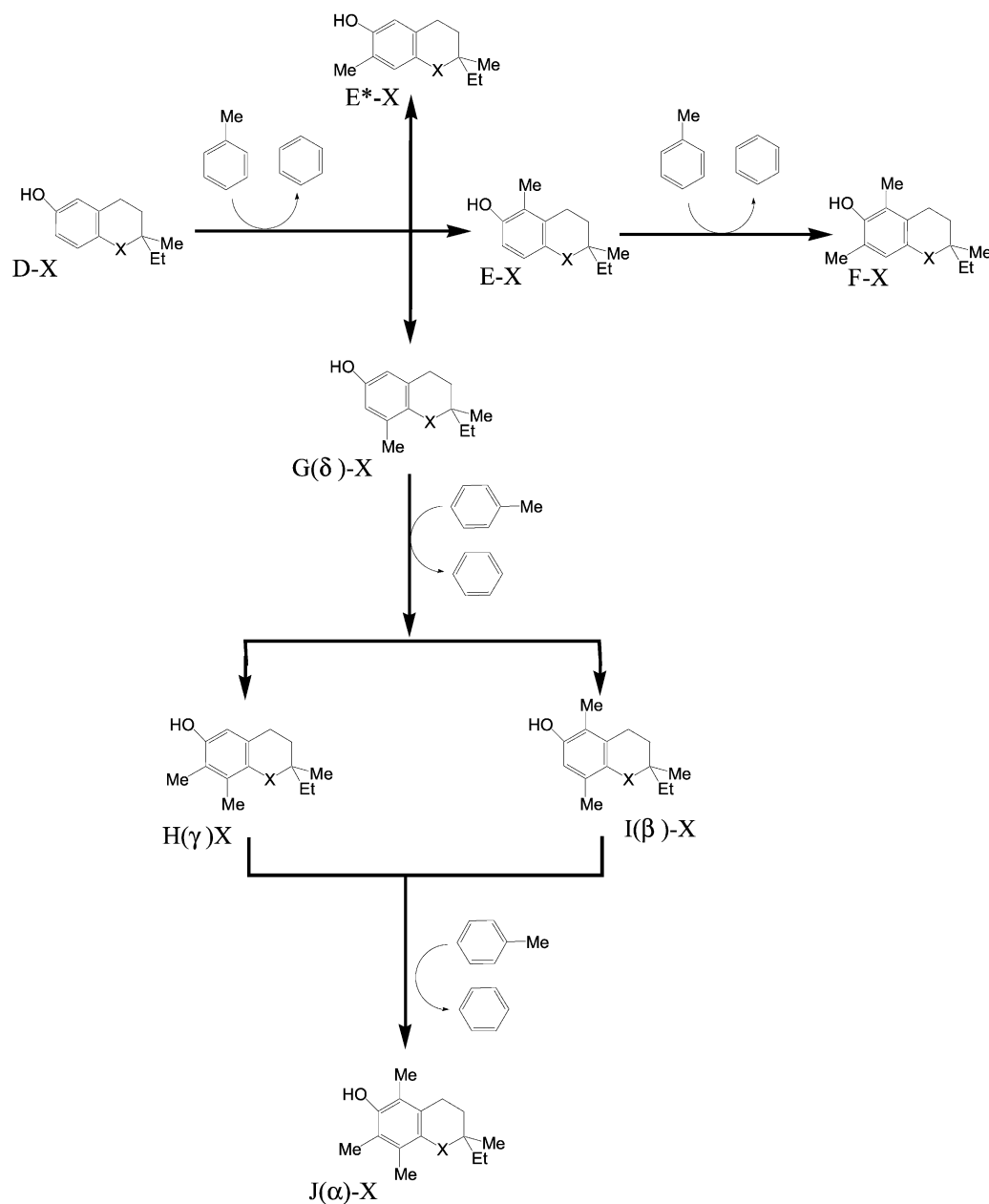


Fig. 4. Isodesmic reactions for the incorporation of aromatic methyl substituents.

These twenty-four structures are shown in Fig. 3 together with their atomic numbering system.

For the tabulation of the optimized geometrical parameters the bond lengths, bond angles, and dihedral angles, for $X = O, S$ and Se are shown in

Fig. 4. These parameters are summarized in Tables 2–4, respectively.

The structures of the triple methylated aromatic ring (α -homologues) for the O, S and Se congeners are shown in Fig. 5. The hydroxyl group (OH) was

Table 2

Optimized bond lengths of the 24 structures studied

Model	X	R2	R3	R4	R5	R6	R7	R8	R9	R(9–10)	R10
D	II(O)	1.402	1.388	1.400	1.393	1.402	1.513	1.533	1.541	1.451	1.375
D	III(S)	1.406	1.387	1.399	1.393	1.404	1.518	1.532	1.542	1.862	1.790
D	IV(Se)	1.404	1.387	1.399	1.393	1.404	1.521	1.535	1.540	2.002	1.922
E	II(O)	1.397	1.389	1.397	1.402	1.410	1.514	1.533	1.539	1.450	1.376
E	III(S)	1.401	1.387	1.396	1.403	1.413	1.519	1.533	1.540	1.859	1.791
E	IV(Se)	1.399	1.388	1.396	1.403	1.414	1.522	1.536	1.538	1.997	1.923
E*	II(O)	1.402	1.392	1.408	1.391	1.402	1.512	1.534	1.541	1.450	1.376
E*	III(S)	1.406	1.391	1.407	1.391	1.404	1.518	1.533	1.542	1.862	1.790
E*	IV(Se)	1.404	1.391	1.407	1.391	1.404	1.521	1.535	1.540	2.002	1.922
F	II(O)	1.397	1.393	1.407	1.401	1.410	1.514	1.534	1.538	1.450	1.376
F	III(S)	1.401	1.391	1.405	1.401	1.413	1.519	1.534	1.540	1.861	1.792
F	IV(Se)	1.399	1.391	1.405	1.401	1.414	1.522	1.536	1.538	2.002	1.924
G(δ)	II(O)	1.411	1.392	1.400	1.391	1.403	1.513	1.533	1.539	1.449	1.378
G(δ)	III(S)	1.418	1.393	1.397	1.391	1.403	1.519	1.531	1.540	1.859	1.795
G(δ)	IV(Se)	1.415	1.392	1.397	1.391	1.403	1.522	1.533	1.538	1.997	1.926
H(γ)	II(O)	1.411	1.404	1.406	1.391	1.398	1.513	1.532	1.540	1.449	1.380
H(γ)	III(S)	1.418	1.405	1.406	1.390	1.399	1.518	1.530	1.539	1.861	1.797
H(γ)	IV(Se)	1.415	1.404	1.406	1.390	1.399	1.521	1.533	1.537	2.001	1.928
I(β)	II(O)	1.406	1.393	1.398	1.400	1.410	1.514	1.533	1.537	1.449	1.378
I(β)	III(S)	1.413	1.393	1.394	1.400	1.413	1.520	1.531	1.538	1.858	1.796
I(β)	IV(Se)	1.409	1.392	1.394	1.401	1.414	1.523	1.534	1.536	1.997	1.927
J(α)	II(O)	1.409	1.404	1.406	1.398	1.406	1.515	1.532	1.537	1.448	1.381
J(α)	III(S)	1.414	1.404	1.407	1.398	1.411	1.523	1.533	1.535	1.857	1.932
J(α)	IV(Se)	1.414	1.404	1.407	1.398	1.411	1.523	1.533	1.535	1.997	1.932
Model	X	R11	R12	R13	R14	R15	R16	R17	R18	R19	R30
D	II(O)	1.086	1.085	1.374	1.090	1.097	1.099	1.097	1.096	1.529	0.969
D	III(S)	1.087	1.085	1.370	1.090	1.098	1.099	1.097	1.099	1.537	0.970
D	IV(Se)	1.087	1.085	1.370	1.090	1.098	1.099	1.101	1.096	1.534	0.970
E	II(O)	1.085	1.089	1.379	1.511	1.097	1.100	1.097	1.096	1.529	0.969
E	III(S)	1.087	1.089	1.375	1.512	1.097	1.100	1.096	1.100	1.536	0.969
E	IV(Se)	1.087	1.089	1.375	1.512	1.097	1.100	1.096	1.101	1.534	0.969
E*	II(O)	1.087	1.507	1.377	1.091	1.097	1.099	1.097	1.096	1.530	0.969
E*	III(S)	1.088	1.507	1.373	1.091	1.098	1.099	1.096	1.100	1.537	0.970
E*	IV(Se)	1.088	1.507	1.373	1.091	1.098	1.099	1.096	1.101	1.534	0.970
F	II(O)	1.086	1.511	1.380	1.511	1.097	1.100	1.097	1.097	1.529	0.968
F	III(S)	1.087	1.511	1.377	1.512	1.097	1.100	1.100	1.096	1.536	0.968
F	IV(Se)	1.088	1.511	1.377	1.512	1.097	1.100	1.101	1.096	1.534	0.968
G(δ)	II(O)	1.508	1.086	1.374	1.090	1.097	1.099	1.097	1.096	1.530	0.969
G(δ)	III(S)	1.510	1.086	1.371	1.090	1.097	1.099	1.097	1.100	1.537	0.970
G(δ)	IV(Se)	1.509	1.086	1.370	1.090	1.098	1.099	1.096	1.101	1.534	0.970
H(γ)	II(O)	1.511	1.510	1.378	1.090	1.097	1.099	1.097	1.096	1.530	0.969
H(γ)	III(S)	1.513	1.514	1.376	1.090	1.098	1.099	1.097	1.100	1.537	0.969
H(γ)	IV(Se)	1.511	1.513	1.375	1.090	1.098	1.099	1.096	1.101	1.534	0.969
I(β)	II(O)	1.507	1.090	1.379	1.511	1.097	1.100	1.097	1.096	1.530	0.969
I(β)	III(S)	1.510	1.090	1.376	1.512	1.097	1.100	1.096	1.100	1.537	0.969
I(β)	IV(Se)	1.509	1.090	1.375	1.512	1.097	1.100	1.096	1.101	1.534	0.969
J(α)	II(O)	1.514	1.514	1.380	1.511	1.097	1.100	1.097	1.097	1.529	0.968
J(α)	III(S)	1.513	1.515	1.378	1.512	1.097	1.100	1.096	1.101	1.534	0.968
J(α)	IV(Se)	1.513	1.515	1.378	1.512	1.097	1.100	1.096	1.101	1.534	0.968

Table 3
Optimized bond angles of the 24 structures studied

Model	X	A3	A4	A5	A6	A(5–6–1)	A(6–1–2)	A7	A(7–6–1)	A8	A9	A(10–9–8)	A(1–10–9)	A10
D	II(O)	120.81	119.65	119.53	121.40	118.57	120.02	121.32	120.10	110.79	112.20	109.02	118.45	123.68
D	III(S)	121.58	119.28	119.47	121.78	118.52	119.34	118.16	123.29	115.36	114.99	107.95	102.74	124.56
D	IV(Se)	121.71	119.11	119.49	121.87	118.37	119.44	117.11	124.50	117.39	115.86	106.39	98.87	123.95
E	II(O)	120.00	120.18	120.60	119.11	119.80	120.28	120.75	119.44	111.47	112.42	108.70	118.63	123.83
E	III(S)	120.76	119.77	120.72	119.33	119.66	119.72	117.91	122.41	116.45	115.32	107.20	102.47	124.87
E	IV(Se)	120.79	119.62	120.79	119.33	119.51	119.91	117.09	123.38	118.36	116.24	105.79	98.81	124.40
E*	II(O)	121.90	117.71	120.58	121.59	117.97	120.25	121.72	120.31	110.63	112.21	109.08	118.37	123.67
E*	III(S)	122.70	117.34	120.54	121.97	117.93	119.53	118.40	123.65	115.38	114.92	107.85	102.43	124.41
E*	IV(Se)	122.80	117.19	120.54	122.04	117.81	119.62	117.42	124.75	117.23	115.80	106.54	98.86	123.89
F	II(O)	121.07	118.30	121.52	119.35	118.79	121.09	121.15	120.15	111.45	112.33	108.95	118.75	123.77
F	III(S)	121.83	117.90	121.62	119.57	118.95	120.11	118.23	123.68	116.37	115.24	108.13	103.36	124.78
F	IV(Se)	122.00	117.75	121.65	119.59	118.68	120.30	117.34	124.73	118.23	116.25	106.76	99.14	124.34
G(6)	II(O)	118.72	120.91	119.67	120.80	119.22	120.51	121.05	119.63	110.91	112.00	108.56	118.28	123.37
G(6)	III(S)	119.39	120.81	119.49	121.24	119.10	119.94	117.35	122.65	115.63	114.58	107.15	102.27	123.70
G(6)	IV(Se)	119.62	120.48	119.55	121.35	119.02	119.97	116.57	123.63	117.51	115.57	105.78	98.65	123.50
H(γ)	II(O)	119.83	118.86	120.63	121.22	118.36	121.08	121.00	120.63	111.02	111.81	108.88	119.03	122.51
H(γ)	III(S)	120.51	118.27	120.85	121.65	118.18	120.54	117.61	124.20	115.50	114.38	108.21	103.51	123.17
H(γ)	IV(Se)	120.70	118.01	120.88	121.73	117.91	120.75	116.95	125.12	117.26	115.45	107.07	99.80	123.04
I(β)	II(O)	117.93	121.41	120.74	118.54	120.00	121.34	120.50	119.49	111.65	112.12	108.47	118.77	123.48
I(β)	III(S)	118.65	121.29	120.70	118.82	120.11	120.38	117.15	122.73	116.65	114.87	107.34	103.10	124.05
I(β)	IV(Se)	118.77	121.00	120.83	118.84	119.83	120.70	116.51	123.64	118.56	115.92	106.04	99.15	123.88
J(α)	II(O)	118.70	119.44	121.92	118.68	119.65	121.56	120.30	120.04	111.89	111.94	108.34	119.03	122.45
J(α)	III(S)	119.42	118.52	122.45	118.95	119.39	121.20	116.52	123.42	118.64	115.67	107.35	103.43	123.00
J(α)	IV(Se)	119.43	118.52	122.46	118.95	119.13	121.46	116.52	124.34	118.64	115.66	106.07	99.41	122.99

(continued on next page)

Model	X	A11	A12	A13	A14	A15	A16	A17	A18	A19	A23	A24	A30
D	II(O)	118.36	121.14	117.51	119.76	110.07	110.08	109.37	110.67	110.26	111.66	115.16	108.66
D	III(S)	119.15	121.30	117.59	119.50	108.88	108.84	109.65	108.55	109.16	111.17	116.34	108.81
D	IV(Se)	119.18	121.38	117.62	119.35	108.43	108.27	109.65	107.71	109.70	112.27	115.88	108.80
E	II(O)	118.81	119.87	121.52	120.03	110.18	110.05	109.27	110.54	110.32	111.66	115.15	108.30
E	III(S)	119.59	120.09	121.38	119.42	109.09	108.76	109.61	108.23	109.36	111.17	116.38	108.44
E	IV(Se)	119.69	120.17	121.33	119.24	108.63	108.31	109.58	107.41	109.83	112.24	115.89	108.42
E*	II(O)	118.01	122.11	116.82	119.53	110.14	110.23	109.33	110.71	110.24	111.63	115.12	108.56
E*	III(S)	118.80	122.31	116.89	119.28	108.95	108.90	109.67	108.56	109.24	111.14	116.32	108.73
E*	IV(Se)	118.85	122.36	116.91	119.19	108.48	108.43	109.65	107.77	109.70	112.17	115.93	108.74
F	II(O)	118.37	121.11	121.16	120.00	110.17	110.15	109.35	110.54	110.43	111.68	115.16	108.80
F	III(S)	119.21	121.35	121.01	119.39	109.12	108.79	109.68	108.24	109.42	111.18	116.36	108.87
F	IV(Se)	119.20	121.42	120.96	119.20	108.70	108.36	109.56	107.46	109.80	112.23	115.90	108.85
G(δ)	II(O)	119.83	120.36	117.32	120.09	109.94	110.11	109.39	110.74	110.32	111.60	115.27	108.55
G(δ)	III(S)	121.18	120.39	117.49	119.84	108.64	108.86	109.71	108.64	109.31	111.20	116.30	108.70
G(δ)	IV(Se)	120.48	120.60	117.50	119.68	108.25	108.33	109.72	107.79	109.73	112.24	115.90	108.71
H(γ)	II(O)	120.08	120.92	117.77	119.73	109.95	110.10	109.49	110.77	110.25	111.61	115.31	108.26
H(γ)	III(S)	119.12	122.45	117.85	119.44	108.64	109.01	109.77	108.74	109.32	111.13	116.39	108.37
H(γ)	IV(Se)	118.54	122.45	117.82	119.31	108.23	108.57	109.69	107.87	109.70	112.18	115.90	108.39
I(β)	II(O)	120.33	119.09	121.27	120.37	110.04	110.11	109.41	110.57	110.49	111.62	115.29	108.27
I(β)	III(S)	121.73	119.16	121.23	119.56	108.83	108.84	109.72	108.35	109.48	111.22	116.38	108.37
I(β)	IV(Se)	121.16	119.36	121.16	119.39	108.43	108.32	109.68	107.47	109.87	112.27	115.84	108.36
J(α)	II(O)	119.78	122.02	121.04	120.26	110.00	109.97	109.46	110.62	110.39	111.71	115.29	108.89
J(α)	III(S)	118.09	124.06	120.79	119.43	108.38	108.32	109.73	107.56	109.91	112.32	115.84	109.15
J(α)	IV(Se)	118.10	124.06	120.79	119.43	108.37	108.32	109.73	107.55	109.92	112.32	115.84	109.14

Table 4
Optimized dihedral angles of the 24 structures studied

Model	X	D(3–2– 1–6)	D4	D5	D6	D(1–6– 5–4)	D7	D(10–1– 2–3)	D(8–7– 6–1)	D9	D(10–9– 8–7)	D(1–10– 9–8)	D(6–1– 10–9)	D8
D	II(O)	0.17	0.17	–0.37	0.20	0.14	–179.77	178.49	–16.77	44.81	–58.22	43.10	–15.77	163.13
D	III(S)	–0.91	0.94	–0.29	–0.41	0.44	178.74	176.78	–19.56	53.48	–65.15	42.74	–17.02	162.22
D	IV(Se)	–0.81	0.55	–0.03	–0.24	–0.03	178.40	178.13	–16.03	53.45	–67.51	45.10	–17.53	165.64
E	II(O)	–0.10	0.80	–0.53	–0.48	1.17	–178.87	178.47	–15.30	43.78	–57.92	43.83	–16.35	164.73
E	III(S)	–0.49	1.07	–1.00	–1.05	1.62	179.99	177.75	–15.35	50.75	–65.58	45.17	–17.71	166.32
E	IV(Se)	–1.04	1.30	–0.33	–1.00	1.15	179.94	178.43	–12.73	51.44	–67.59	46.35	–18.22	168.53
E*	II(O)	0.38	0.08	–0.39	0.25	0.20	–179.56	178.67	–16.61	44.77	–58.31	43.01	–15.49	163.15
E*	III(S)	–0.21	0.33	–0.11	–0.24	0.36	178.69	177.60	–17.97	52.32	–65.61	44.02	–16.87	163.79
E*	IV(Se)	–0.79	0.58	–0.07	–0.22	0.04	178.48	178.29	–16.09	53.53	–67.46	44.84	–17.11	165.57
F	II(O)	0.69	0.56	–0.52	–0.42	0.22	–178.68	179.09	–16.62	43.10	–58.35	42.93	–15.08	165.85
F	III(S)	0.30	0.95	–0.26	–1.03	0.35	–180.03	178.22	–19.38	50.19	–64.89	42.12	–14.49	167.12
F	IV(Se)	–0.09	0.88	–0.14	–0.90	0.04	–180.08	178.78	–16.85	51.02	–67.04	43.94	–15.94	168.99
G(δ)	II(O)	0.33	–0.08	–0.46	0.38	1.30	–179.50	179.01	–14.12	45.05	–58.50	45.09	–17.08	163.09
G(δ)	III(S)	–0.38	0.14	–0.35	0.09	1.60	178.98	178.06	–14.57	53.76	–65.86	45.82	–18.11	162.05
G(δ)	IV(Se)	–0.67	0.16	–0.14	0.03	1.05	178.67	178.77	–12.18	54.26	–67.72	46.69	–18.45	164.61
H(γ)	II(O)	0.05	0.48	–0.65	0.28	0.25	180.41	178.22	–16.57	44.67	–16.57	–58.43	–16.36	163.26
H(γ)	III(S)	0.71	0.01	–0.50	0.29	0.43	179.21	178.45	–19.39	53.90	–19.39	–65.01	–14.11	161.91
H(γ)	IV(Se)	–0.31	0.59	–0.47	0.06	0.23	178.96	178.19	–18.59	55.51	–18.59	–66.50	–14.59	162.77
I(β)	II(O)	1.16	0.02	–0.58	–0.04	1.19	–178.64	179.67	–14.51	43.76	–14.51	–58.48	–16.11	165.31
I(β)	III(S)	0.63	0.55	–0.62	–0.52	1.68	–179.42	179.22	–15.13	51.42	–15.13	–65.61	–15.66	165.98
I(β)	IV(Se)	0.06	0.64	–0.44	–0.47	1.15	–179.83	179.62	–12.71	51.81	–12.71	–67.40	–16.87	168.31
J(α)	II(O)	–0.26	1.35	–1.06	–0.40	1.46	–178.76	178.32	–14.04	42.84	–58.47	46.24	–18.20	166.18
J(α)	III(S)	–0.94	1.97	–1.59	–0.38	2.70	–179.14	177.16	–15.07	51.46	–65.31	45.20	–16.77	168.67
J(α)	IV(Se)	–0.48	1.99	–1.61	–0.36	1.89	–179.17	178.71	–12.44	51.45	–67.32	46.16	–17.08	168.67
Model	X	D(9–10– 1–2)	D10	D12	D13	D14	D15	D16	D17	D18	D19	D23	D24	D30
D	II(O)	165.98	–178.52	–179.93	–179.82	–179.44	41.49	–74.76	–74.70	167.57	–172.28	62.36	–179.94	179.79
D	III(S)	166.43	–177.28	–179.61	179.65	179.88	39.98	–74.40	–68.87	174.83	–179.41	57.01	173.70	179.88
D	IV(Se)	163.59	–178.32	–179.82	179.86	179.78	43.17	–70.37	–69.27	174.92	178.89	53.19	179.19	–179.82
E	II(O)	165.14	–179.35	–179.71	–179.60	179.83	43.30	–72.49	–75.67	166.76	–171.84	62.75	–179.11	–1.63
E	III(S)	164.16	–178.92	–179.73	179.46	179.15	44.27	–69.54	–71.63	172.37	–179.73	56.47	174.30	–0.63
E	IV(Se)	162.34	–179.63	–179.62	179.46	179.13	46.26	–66.81	–71.40	173.10	–178.90	53.19	–179.30	–0.47
E*	II(O)	166.28	–178.67	–179.99	179.86	–179.35	41.62	–74.73	–74.67	167.55	–172.35	62.34	–179.90	179.76
E*	III(S)	165.45	–177.75	–179.85	179.86	179.99	41.53	–72.83	–69.93	173.72	–179.85	56.53	173.63	–179.93
E*	IV(Se)	163.85	–178.55	–179.72	179.85	179.81	43.17	–70.48	–69.22	174.95	178.93	53.33	179.01	–179.85
F	II(O)	166.57	–179.84	–179.78	179.77	179.93	44.41	–71.50	–76.25	166.11	–172.39	62.11	–179.41	–3.06
F	III(S)	167.67	–179.20	–179.64	179.57	179.13	44.99	–68.86	–72.13	171.81	180.00	56.17	174.40	–1.40

(continued on next page)

Table 4
(Continued)

Model	X	D(9–10– 1–2)	D10	D12	D13	D14	D15	D16	D17	D18	D19	D23	D24	D30
F	IV(Se)	165.25	–179.71	–179.69	179.62	179.16	46.73	–66.40	–71.74	172.72	178.69	53.03	–179.45	–0.36
G(δ)	II(O)	164.28	–179.03	–180.06	179.84	–179.25	41.46	–74.71	–74.37	167.76	–172.40	62.19	178.27	179.74
G(δ)	III(S)	163.54	–178.30	–179.92	179.84	–179.68	39.83	–74.35	–68.50	175.09	–179.08	57.30	173.42	179.77
G(δ)	IV(Se)	162.15	–178.79	–179.91	179.96	–179.92	42.18	–71.30	–68.50	175.65	179.19	53.56	178.89	179.94
H(γ)	II(O)	165.49	–178.47	–179.61	179.61	–179.33	41.54	–74.59	–74.60	167.41	–172.34	62.38	179.68	178.99
H(γ)	III(S)	168.23	–178.49	–179.82	179.82	–179.40	39.74	–74.51	–68.25	175.20	–179.24	57.21	173.05	179.45
H(γ)	IV(Se)	166.95	–178.50	–179.40	179.77	–179.72	40.48	–73.11	–67.30	176.82	179.67	54.24	178.54	179.35
I(β)	II(O)	165.42	–180.17	–180.08	179.68	–179.75	43.82	–71.90	–75.56	166.73	–172.39	62.10	179.14	–1.60
I(β)	III(S)	165.80	–180.23	–179.84	179.49	–179.62	43.99	–69.68	–70.82	173.03	–179.73	56.41	173.96	–1.14
I(β)	IV(Se)	163.58	–180.49	–179.81	179.62	–179.53	46.04	–66.88	–71.00	173.44	178.82	53.12	–179.66	–0.89
J(α)	II(O)	163.22	–179.67	–179.00	179.51	–179.96	44.54	–71.00	–76.30	165.89	–172.23	62.30	–179.68	–6.33
J(α)	III(S)	165.17	–180.62	–177.73	179.13	–179.91	46.34	–66.60	–71.23	173.13	179.00	53.14	179.90	–6.16
J(α)	IV(Se)	163.74	–180.62	–177.74	179.10	–179.88	46.34	–66.56	–71.23	173.13	179.01	53.16	179.89	–6.30

almost always coplanar with the aromatic ring (within ± 3 degrees), deviating at most up to ± 7 degrees as a result of the steric ‘congestion’ arising from the six-fold substitution on the benzene ring. The orientation of the OH was such that it pointed away from the adjacent CH₃ group, whenever the structure would permit. Table 4 shows this in column D30, with an optimized *anti*-orientation for the OH in models D, E*, G(δ) and H(γ) and a *syn*-orientation in models E, F, I(β) and J(α), irrespective of the starting orientation.

The variables in Tables 2 and 3 also show structural trends, whereby the C–C bonds adjacent to the C carrying the Me substitution are lengthened, irrespective of heteroatom substitution. In contrast, the bond angles change with heteroatom substitution, irrespective of Me substitution; summarized in Table 3. Several other structural trends of smaller magnitude are also apparent but not elaborated upon here.

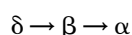
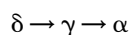
4.2. Molecular energetics

The computed total energies are summarized in Table 5. The energies of stabilization calculated according to the scheme given in Fig. 6 are tabulated in Table 6. The graphical representation of these results is shown in Fig. 7.

A comparison of the relative activity of α -tocopherols ($z = \alpha, \beta, \gamma, \delta$) as measured by $\ln\{[A_z]/[A_\alpha]\}$ may be calculated using the calculated energy of stabilization (ΔE_z).

$$\ln\{[A_z]/[A_\alpha]\} = F(\Delta E_z)$$

The numerical values are given in Table 7. Such a plot, shown in Fig. 8, suggests that there may be an exponential relationship interconnecting either one, or both, of the paths shown below:



For this reason the relationship is converted to the following form:

$$y = 1.0 - \ln\{[A_z]/[A_\alpha]\} = f(\Delta\Delta E_z) = f(x)$$

$$\text{where } x = \Delta\Delta E_z = \Delta E_\alpha - \Delta E_z$$

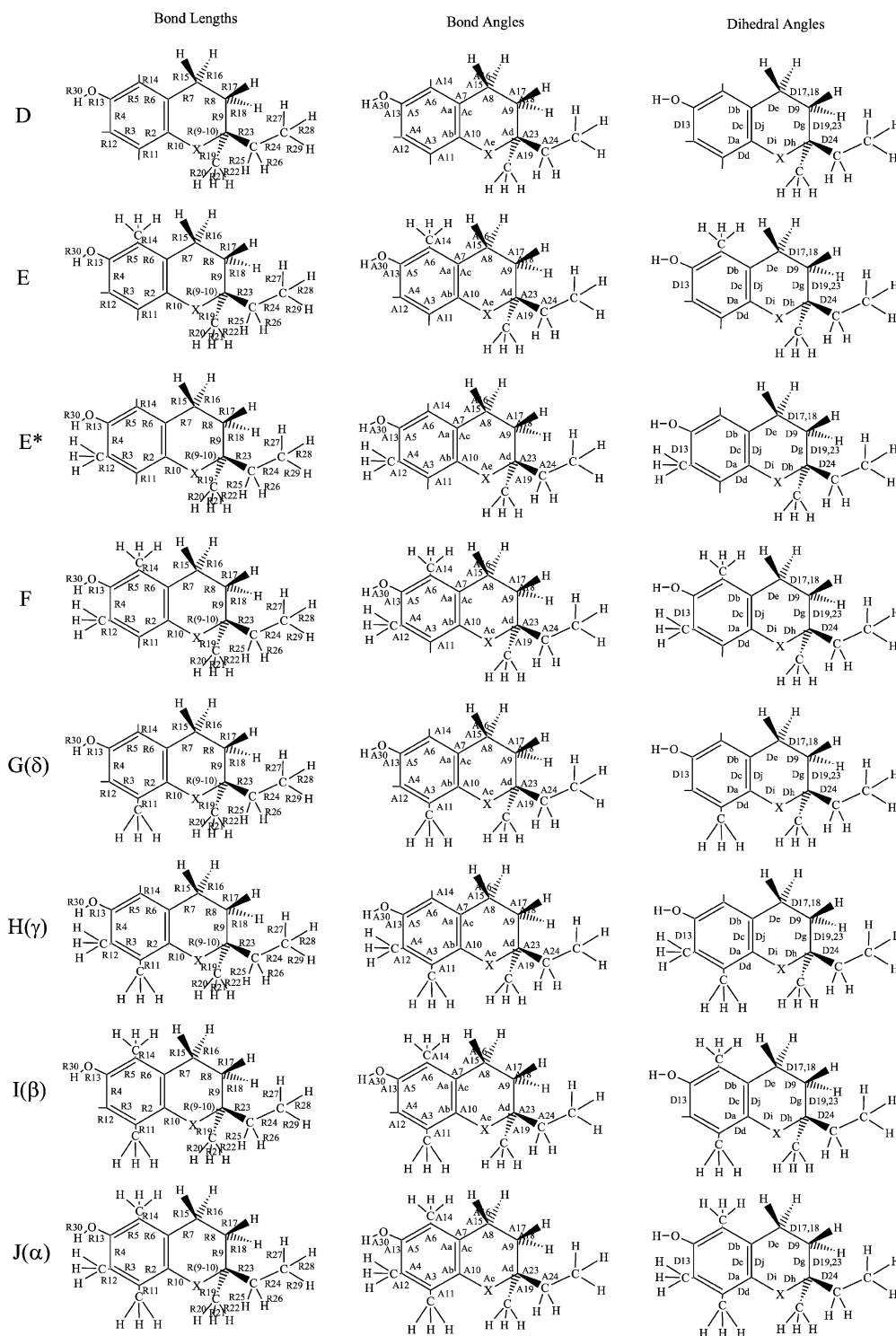


Fig. 5. Numbering of bond lengths, bond angles and dihedral angles for the eight structures investigated. X may be O, S or Se.

Table 5

Total energies (hartrees) computed for the 24 optimized structures

	II(O)	III(S)	IV(Se)
D	−617.36422	−940.33278	−2941.52972
E	−656.68052	−979.64832	−2980.84517
E*	−656.68287	−979.65164	−2980.84873
F	−695.99823	−1018.96614	−3020.16312
G(δ)	−656.68269	−979.65015	−2980.84932
H(γ)	−695.99754	−1018.96431	−3020.16386
I(β)	−695.99890	−1018.96543	−3020.16461
J(α)	−735.31221	−1058.27721	−3059.47685

The exponential function obtained for the first ($\delta \rightarrow \gamma \rightarrow \alpha$) of these two paths is shown in Fig. 9. While the fit shown in Fig. 9 was fairly good ($R^2 = 0.99$), the other path ($\delta \rightarrow \beta \rightarrow \alpha$) did not allow a fit to a reasonably good exponential function. With respect to the exponential fit obtained for the $\delta \rightarrow \gamma \rightarrow \alpha$, it seemed that β was estimated to be less stable by $1.750 \text{ kcal mol}^{-1}$.

While we have no explicit structured explanation for this derivation, it should be pointed out that the two methyl groups in the β form are in *para*-position with respect to each other. This would suggest that any electronic effects the Me-groups might exert on the aromatic ring would be cancelled, or nearly cancelled, by vectorial addition. For this reason, we collected all the computed dipole moments in Table 8, which is hoped to reveal the polarity of the various forms.

This data reveals that homologous E, F, β , and α have dipole moments less than 1 Debye due to partial cancellation of electronic effects while homologous D, E*, δ and γ have dipoles over 2 Debye. This is the case for all three congeners.

The question of arithmetical additivity in the stabilization or destabilization effects of these Me-groups on the chroman ring and its congeners has to be examined at least in passing. The results are shown in Table 9.

It appears that the stabilization energies are not additive, indicating that in addition to the electronic effects, steric ‘congestion’ occurs when the methyl groups are proximally introduced. Such an observation has been noted by Hammett [16] in studying

chemical reactivity. When the substituents were far away from the reaction site, good correlation was observed between reactivity and structure. Alternatively, when substituents were placed in an *ortho*-position, the points scattered randomly and did not correlate at all. Thus, the Hammett’s linear free-energy relationship is valid only when the substituents are far away from the reaction site.

For the I(β) isomers, where the two Me-groups are in *para*-position with respect to each other,

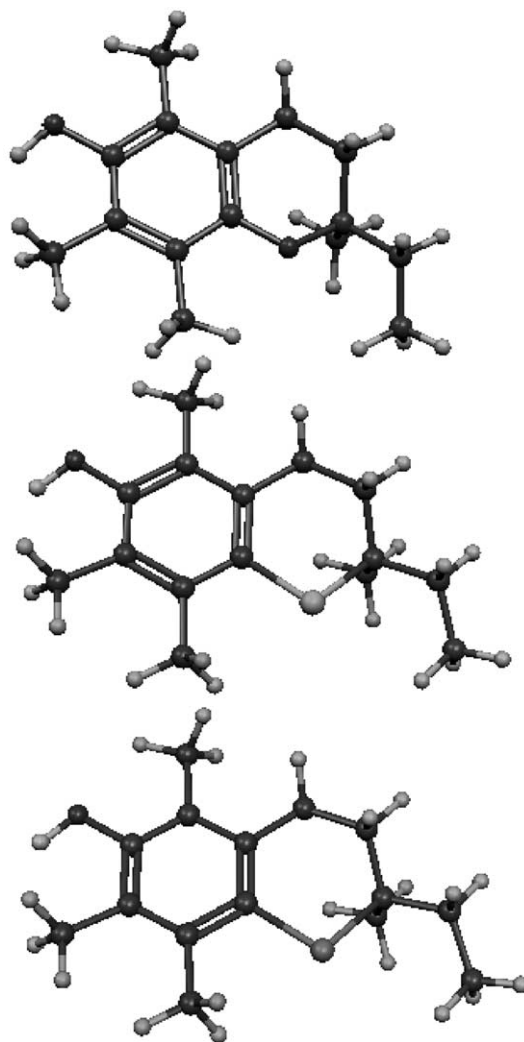


Fig. 6. Three optimized structures of the shortened sidechain model of the α -tocopherol.

Table 6

Energy of stabilization associated with single or multiple methyl group transfers

	II(X = O)		III(X = S)		IV(X = Se)	
	Single step	Accumulated steps	Single step	Accumulated steps	Single step	Accumulated steps
XD → XE	1.043	1.043	1.520	1.520	1.576	1.576
XD → XE*	−0.430	−0.430	−0.562	−0.562	−0.658	−0.658
XE → XF	0.161	1.204	0.090	1.610	0.007	1.583
XD → XG(δ)	−0.320	−0.320	0.372	0.372	−1.028	−1.028
XG(δ) → XH(γ)	1.952	1.633	2.386	2.759	2.147	1.118
XG(δ) → XI(β)	1.100	0.781	1.684	2.056	1.676	0.648
XI(β) → XJ(α)	2.918	3.699	3.879	5.934	3.587	4.235

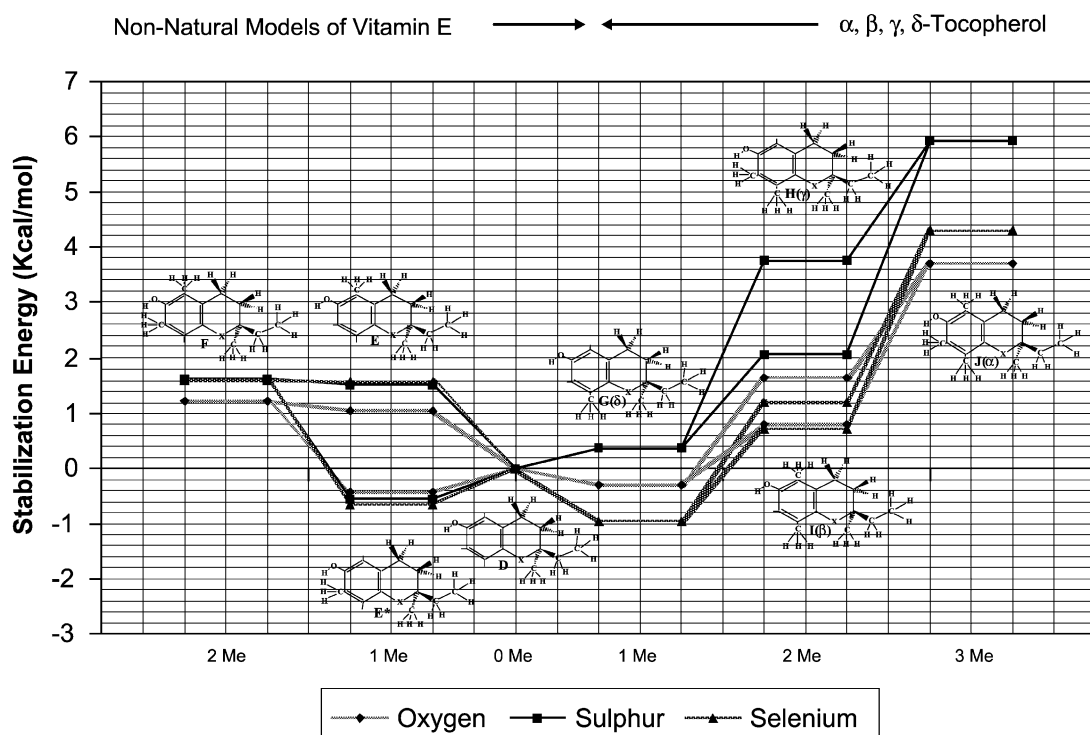


Fig. 7. Computed stabilization energies.

Table 7

Relative biological activity of tocopherols and computed stabilization energy values of model compounds

Relative activity ^a				Computed stabilization energy	
	$[A_z]/[A_\alpha]$	$\ln\{[A_z]/[A_\alpha]\}$	$1 - \ln\{[A_z]/[A_\alpha]\}$	ΔE_z	$\Delta\Delta E_z = \Delta E_\alpha - \Delta E_z$
z-tocopherol					
α	1.000	0.000	0.000	3.698	0.000
β	0.570	−0.562	1.562	0.780	2.918
γ	0.370	−0.994	1.994	1.634	2.054
δ	0.014	−4.269	5.269	−0.318	4.016

^a Activities were taken from Ref. [3], also quoted in Table 3 of Ref. [13].

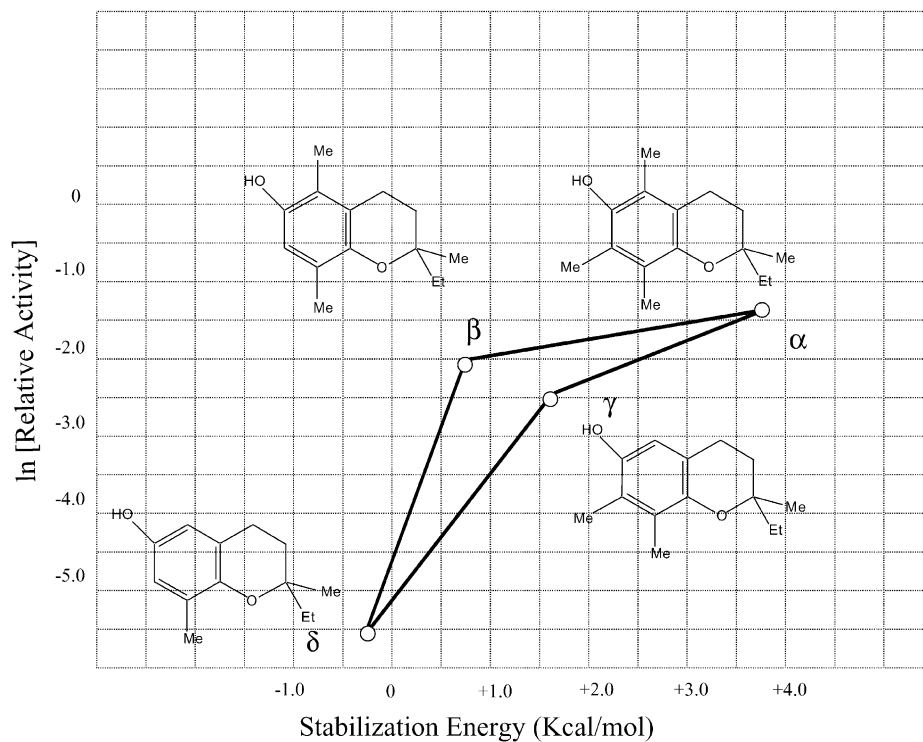


Fig. 8. Relative activity of tocopherol vs stabilization energies of tocopherol model.

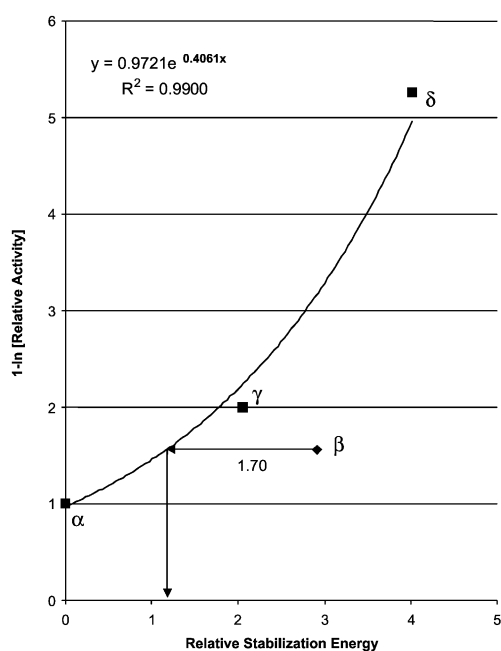


Fig. 9. Modified relative activity of tocopherol vs relative stabilization energies of tocopherol model.

the discrepancy is within $0.2 \text{ kcal mol}^{-1}$. For the F isomers, where the Me groups are in *meta*-position with respect to each other, the discrepancy is within $0.7 \text{ kcal mol}^{-1}$. In these two cases the Me groups are virtually independent of each other. However, when two Me groups are in an *ortho*-orientation, the discrepancy is $4.3 \text{ kcal mol}^{-1}$, indicating that steric destabilizing congestion dominates over electronic stabilizing effects.

Table 8
Dipole moments of optimized structures

Homologue	II(O) μ (Debye)	III(S) μ (Debye)	IV(Se) μ (Debye)
D	2.7878	3.0528	2.9677
E	0.5764	0.8893	0.8484
E*	2.4686	2.8062	2.7313
F	0.436	0.8416	0.8323
G(δ)	2.6586	2.7262	2.6327
H(γ)	2.3264	2.4493	2.3562
I(β)	0.7322	0.5561	0.5327
J(α)	0.6622	0.6971	0.6876

Table 9

Energies of stabilizations calculated as a sum of components or through direct computations

	II(X = O)		III(X = S)		IV(X = Se)	
	Sum of Components	Directly Calculated	Sum of Components	Directly Calculated	Sum of Components	Directly Calculated
XE + XE* → XF	0.613	1.205	0.958	1.613	0.918	1.581
XG(δ) + XE* → XH(γ)	−0.750	1.634	−0.190	3.758	−1.094	1.183
XG(δ) + XE → XI(β)	0.723	0.780	1.892	2.055	0.548	0.712
XI(β) + XE* → XJ(α)	0.350	3.698	1.494	5.933	−0.010	4.301

5. Conclusions

Both Me and heteroatom substitution change the molecular structure of Vitamin E, in terms of bond lengths, bond angles and dihedral angles. The effect of Me substitution was observed predominantly in the case of adjacent bond lengths, while heteroatom substitution influenced bond angles and dihedral angles.

With the exception of the model of β -tocopherol, where the 2 introduced Me groups (*para*-oreintation) nearly cancel their electronic contribution and provide little steric congestion, a general trend was observed with increasing substitution in the following sequence $\delta \rightarrow \gamma \rightarrow \alpha$. The structural contribution is measured by the relative stabilities in kcal mol^{−1} units, with δ being the most stable and α being the least stable. This trend correlated with the logarithmic relative activity of the Vitamin E homologues δ , γ and α , respectively.

This clearly indicates that there is a structural basis for the differing biological activity of the naturally occurring Tocopherol homologues.

Acknowledgements

The authors thank Michelle A. Sahai, Jacqueline M.S. Law, Christopher N.J. Marai and Tania A. Pecora for helpful discussions, and preparation of tables and figures and Graydon Hoare for database management, network support and software and distributive processing development. A special thanks is extended to Andrew M. Chasse for his development of novel scripting and coding techniques, which facilitate

a reduction in the number of CPU cycles needed. The pioneering advances of Kenneth P. Chasse, in all composite computer-cluster software and hardware architectures, are also acknowledged. David C.L. Gilbert and Adam A. Heaney are also thanked for CPU time.

References

- [1] M. Evans, K.S. Bishop, *Science* 55 (1922) 650.
- [2] J.B. Bauernfeind, *Vitamin E: a comprehensive treatise*, Marcel Dekker, New York, 1980, pp. 99–167.
- [3] B. Weimann, H. Weiser, *Am. Clin. Nutr.* 53 (1991) 1056S–1060S.
- [4] N. Al-Maharik, L. Engman, J. Malmstrom, C. Schiesser, Intramolecular homolytic substitution at selenium: synthesis of novel selenium-containing Vitamin E analogues, *J. Org. Chem.* 66 (2001) 6286–6290.
- [5] A.D.N.G. de Grey, *The Mitochondrial Free Radical Theory of Aging*, R.G. Landes Company, Austin, Teas, 1999.
- [6] B. Chance, H. Sies, A. Boveris, *Physiological Review* 59 (1979) 527.
- [7] B.N. Ames, M.K. Shigenaga, in: J.G. Scandalios (Ed.), *Molecular Biology of Free Radical Scavenging Systems*, Cold Spring Harbor Laboratory Press, New York, 1992, p. 1.
- [8] S. Steenken, *Chem. Rev.* 89 (1979) 503.
- [9] K.L. Fong, P.B. McCay, J.L. Poyer, B.H. Misra, B. Keele, *J. Biol. Chem.* 248 (1973) 7792.
- [10] T.I. Mak, W.B. Weglicki, *J. Clin. Invest.* 75 (1985) 58.
- [11] S. Varadarajan, J. Kanski, M. Aksenova, C. Lauderback, D.A. Butterfield, *J. Am. Chem. Soc.* 123 (2001) 5625.
- [12] G.W. Burton, K.U. Ingold, *Acc. Chem. Res.* 19 (1986) 194.
- [13] D.H. Setiadi, G.A. Chass, L.L. Torday, A. Varro, J.Gy. Papp, *THEOCHEM* (2002) in press.
- [14] D.H. Setiadi, G.A. Chass, L.L. Torday, A. Varro, J.Gy. Papp, I.G. Csizmadia, *Eur. Phys. J. D* (2002) in press.
- [15] M.J. Frisch, G.W. Trucks, H.B. Schlegel, G.E. Scuseria, M.A. Robb, J.R. Cheeseman, V.G. Zakrzewski, J.A. Montgomery, Jr., R.E. Stratmann, J.C. Burant, S. Dapprich, J.M. Millam,

A.D. Daniels, K.N. Kudin, M.C. Strain, Ö. Farkas, J. Tomasi, V. Barone, M. Cossi, R. Cammi, B. Mennucci, C. Pomelli, C. Adamo, S. Clifford, J. Ochterski, G.A. Petersson, P.Y. Ayala, Q. Cui, K. Morokuma, D.K. Malick, A.D. Rabuck, K. Raghavachari, J.B. Foresman, J. Cioslowski, J.V. Ortiz, A.G. Baboul, B.B. Stefanov, G. Liu, A. Liashenko, P. Piskorz,

I. Komaromi, R. Gomperts, R.L. Martin, D.J. Fox, T. Keith, M.A. Al-Laham, C.Y. Peng, A. Nanayakkara, M. Challacombe, P.M.W. Gill, B. Johnson, W. Chen, M.W. Wong, J.L. Andres, C. Gonzalez, M. Head-Gordon, E.S. Replogle, J.A. Pople, Gaussian Inc., Pittsburgh PA, 1998.
[16] L.P. Hammett, J. Am. Chem. Soc. 59 (1937) 96.

Viewpoint

Vitamin E models. Can the anti-oxidant and pro-oxidant dichotomy of α -tocopherol be related to ionic ring closing and radical ring opening redox reactions?

David H. Setiadi^{a,*}, Gregory A. Chass^a, Ladislaus L. Torday^b, Andras Varro^b,
Julius Gy. Papp^{b,c}

^aGlobal Institute of Computational Molecular and Materials Science, 210 Dundas Street W., Suite 810, Toronto, Ont.,
Canada M5G 2E8

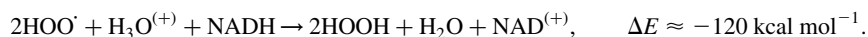
^bDepartment of Pharmacology and Pharmacotherapy, Szeged University, Dom ter12, Szeged 6701, Hungary

^cDivision of Cardiovascular Pharmacology, Hungarian Academy of Sciences and Szeged University, Dom ter12,
Szeged 6701, Hungary

Received 30 May 2002; accepted 14 August 2002

Abstract

The free radical scavenging mechanism, leading to a quinodal structure via an oxidative ring opening is exothermic. However, the ionic oxidative ring opening is endothermic. Consequently, the ionic reductive ring closing must be exothermic. This leads to the suggestion that Vitamin E may be recovered, unchanged, thus effectively acts as a catalyst for the following reaction



As Vitamin E is biologically recycled, a single α -tocopherol molecule may convert numerous $\text{HOO}\cdot$ radical to H_2O_2 which is accumulated if not removed at the same rate, enzymatically, with the participation of catalase (Fe) or glutathione peroxidase, $\text{GP}_x(\text{Se})$. This accumulation of peroxide, which may be referred to as a 'peroxide traffic jam', may well be the reason of the pro-oxidant effect of Vitamin E.

© 2002 Published by Elsevier Science B.V.

Keywords: Vitamin E; Pro-oxidant; Anti-oxidant; Free radical oxidative ring opening; Ionic reductive ring closing; Biological recycling of Vitamin E; Vitamin E as a catalyst

1. Preamble

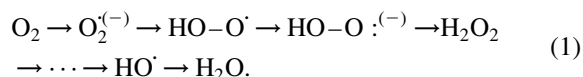
1.1. The nature of oxidative stress

Since chemical reactions are usually not quantitative, up to 5% of the oxygen we inhale may be converted to 'reactive oxygen species' (ROS) [1]. During normal metabolism, as food is oxidized in

* Corresponding author..

E-mail addresses: dsetiadi@giocomms.org (D.H. Setiadi), gchass@giocomms.org (G.A. Chass), pyro@phcol.szote.u-szeged.hu (L.L. Torday), varro@phcol.szote.u-szeged.hu (A. Varro), papp@phcol.szote.u-szeged.hu (J.G. Papp).

the living cells, oxygen is being reduced to water. The reduction (1) is a multi-step process; the intermediate stages correspond to the ROS



When any of these ROS escape from this sequence of reductive reactions, they may damage internal structures of the cell including DNA, RNA and various proteins, in addition to the cell membrane. Such damage also leads to degenerative diseases, as well as a weakened immune system [2].

As an educated guess, we might say that in every human being, ROS may strike and damage each single DNA molecule, perhaps as many as 10,000 times a day. To prevent the propagation of mutations, approximately 99% of the damaged DNA strands may be restored by DNA repair enzymes. The remaining 1% escapes the repair action of the enzymes, leaving approximately 100 damaged strands of DNA in the system. Lipid peroxidation may also cause great damage [3–5]. All of these damages can accumulate over time, eventually causing atherosclerosis, cancer and other degenerative diseases such as Parkinson's and Alzheimer's diseases.

The body has two types of mechanisms to eliminate ROS before they assert any damage. These include

- (i) Enzymatic reductions of ROS beyond the regular process,
- (ii) Scavenging of ROS by anti-oxidant compounds.

With advanced age, both of these mechanisms fight a losing battle against ROS. However, even at a younger age, the ammunition for these anti-oxidant mechanisms must come from a healthy diet, which is not always practiced or available. In such cases, the 'healthy diet' does include dietary supplement. Needless to say, it is important that young people acquire a vigilant attitude concerning their diets in order to reap the long-term benefits.

1.2. Essential nutrient components

Both of the above two mechanisms to fight ROS require special nutrients.

For mechanism (i), it may be some trace element such as magnesium, vanadium, chromium, manganese, iron, copper, zinc or selenium (Mg, V, Cr, Mn, Fe, Cu, Zn, or Se) that may be needed at the active site of some enzyme. If these trace elements are not available, mechanism (i) would not be operative. For example, the natural selenium (Se) level in the soil is highly variable. It is common knowledge that in the USA, the Eastern Coastal Plain and the Pacific Northwest have the lowest levels of Se. In these areas, the daily Se intake of the population is in the range of 60–90 µg. In contrast, in areas rich with Se, the range of daily Se intake is 60–200 µg. The average daily US intake is approximately 125 µg. Those living where the highest levels of Se exist also have the lowest levels of lung, colon, bladder, pancreas, breast and ovarian cancers. Thus, if the soil is depleted of Se, then the vegetation will not have an adequate amount of Se, and the local diet would reflect the low Se content. The recommended daily intake should be in the vicinity of 300 µg. It may well be that the diet of the whole North American continent is too low in Se. This may be responsible for North Americans having some of the highest worldwide levels of degenerative ailments such as cancer and cardiovascular diseases as well as Alzheimer's and Parkinson's diseases. Of course, an overdose of Se is dangerous, but is not expected to happen unless the daily intake reaches 1000 µg.

Selenium is at the active site of glutathione peroxidase, incorporated in the form of selenocysteine [6]. Mechanistically, selenium acts as a temporary oxygen carrier [7], consequently, by any definition, it is a catalyst as shown in Fig. 1.

Thus, while selenium is used at the active site of glutathione peroxidase (GP_x), other trace metals are also important. For example, Cu and Zn are cofactors of most superoxide dismutase (SOD). However, some SOD molecules contain manganese (Mn), iron (Fe) or even nickel (Ni). Also, while most catalase enzymes usually contain Fe in a heme, on occasion some catalase molecules will operate with the help of Mn.

For mechanism (ii), certain vitamins (like C and E) act as anti-oxidants in the battle against ROS. Vitamin C is water soluble and therefore functions in the aqueous phase, while vitamin E is fat soluble,

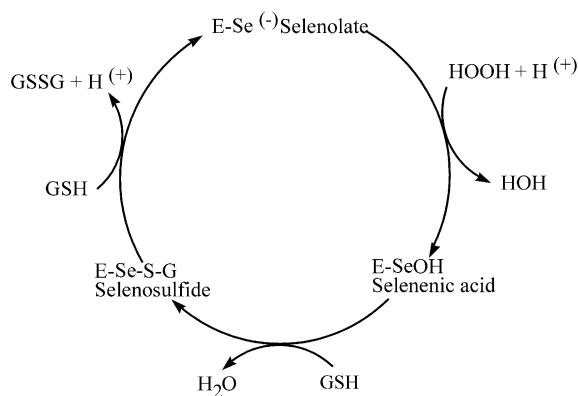


Fig. 1. A schematic mechanism of action for glutathione peroxidase (GP_x). The Se-deprotonated GP_x is denoted at the top on $E-Se^{(-)}$ selenolate. Reduced and oxidized glutathione are denoted as GSH and GSSG, respectively.

functioning in lipid bilayers and in lipoprotein micelles.

Numerous other anti-oxidants (such as lycopene, β -carotene, flavones, farnesol, allyl-methyl-disulfide, lipoic acid, coenzyme Q_{10} or ubiquinone, etc.) are also needed [8,9]. Plants produce these anti-oxidants and fruits and vegetables are expected to supply them. However, the level of these anti-oxidants in fruits and vegetables may vary not only according to the geographical location where they were produced as well as the method of production, but also vary from season to season, or with distance of transportation. Consequently, anti-oxidants may now have to be added to the food items or must be provided as a supplement in order to produce a healthy diet. If regular foodstuff was sufficiently nutritious, or if dietary supplements were included in meals, the incidence of degenerative diseases may be reduced substantially, which in turn could considerably lessen health care costs.

2. Introduction

It is generally accepted that reduction of morbidity and mortality from cardiovascular disease is associated with an increase intake of anti-oxidant vitamin E and vitamin C. This apparent cause–causality

relationship has been explained on the basis of oxidative modification of low density lipoprotein (LDL). The corollary of this assumption is that the inhibition of lipid peroxidation in LDL, by vitamin E, leads to the reduction of myocardial infarction and stroke. Numerous papers testify along this line [10–12].

In the mean time, not only does vitamin E behave as a non-anti-oxidant [13] but pro-oxidant [14] effects of vitamin E have also been demonstrated. The fact that vitamin E can act as both anti-oxidant and pro-oxidant has led to the point that vitamin E has come to know as a ‘Janus molecule’ [15].

The free radical oxidation products of α -tocopherol have been analyzed by Liebler et al. [16] in 1996 showing more other extensively oxidized products than the quinoidal structure. The ionic mechanism was suggested by Roseman et al. [17] in 1999 which has led to the quinoidal structure. These mechanisms were also reviewed recently by Brigelius-Flohe and Traber [18].

Under strong oxidative conditions vitamin E may undergo progressively more extensive oxidation that could lead to irreversible metabolization of the tocopherol molecule. Such a destructive oxidation [16], leading to a variety of epoxide, which may metabolize even further is shown in Fig. 2. Note that the steps at the left hand column in Fig. 2 are non-destructive as it corresponds to the formation of the quinone–hydroquinone analogue of vitamin E. Nevertheless, there exists an ionic oxidative mechanism of α -tocopherol leading to quinoidal or even to hydroquinone structure. Such a mechanism [17] is shown in Fig. 3. However, even here, some side reactions may occur. The left hand column of Fig. 3 shows the non-destructive process.

3. Scope

The present paper raises more questions than can be answered at this time, related to the dichotomy of the anti-oxidant as well as pro-oxidant nature of vitamin E.

Of course one may argue that the anti-oxidant and pro-oxidant natures of vitamin E depends on the redox

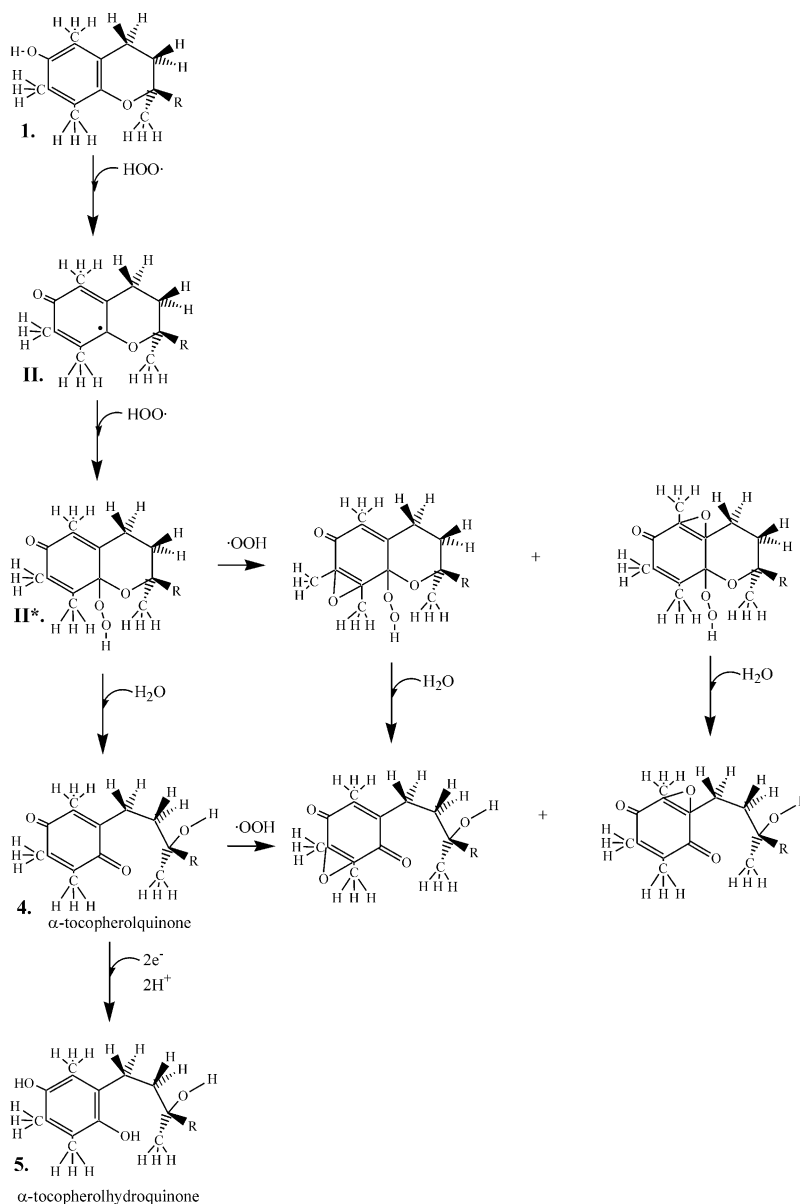


Fig. 2. A schematic mechanistic representation of non-destructive and destructive free radical oxidation of α -tocopherol by $\text{HOO}\cdot$.

potential. In turn, the redox potential varies according to the Nernst equation (2)

$$E = E^0 - RT/\nu \ln\{[\text{Red}]/[\text{Ox}]\} \quad (2)$$

where ν is the number of electrons transferred and the expression $[\text{Red}]/[\text{Ox}]$ measures the ratio of reduced and oxidized forms.

Nevertheless, it seems plausible to seek explanation at the molecular level concerning the ‘traffic’ which is passing through the overall reduction presented in Eq. (1). Sufficient computed results are presented to provide theoretical backing to the merit of the questions to be asked and some putative mechanistic answers suggested.

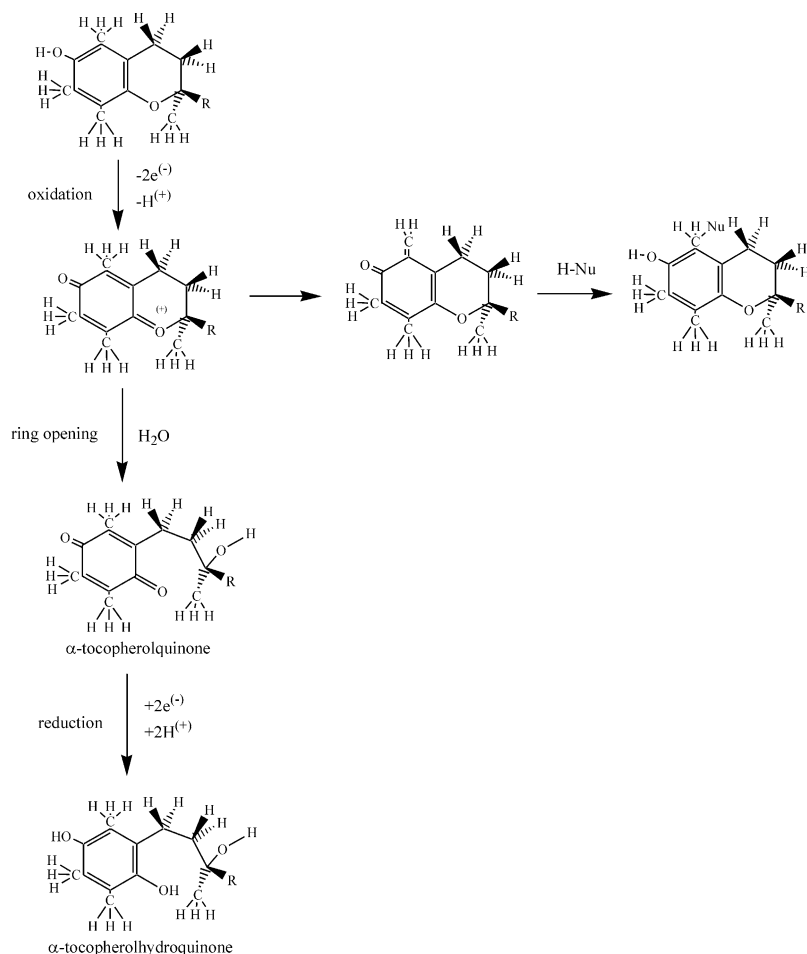


Fig. 3. A schematic mechanistic representation of non-destructive and destructive ionic oxidation of α -tocopherol.

4. Method

The definition of the relative spatial orientation as well as the numbering of the constituent atomic nuclei are shown in Fig. 3. The input files were numerically generated. No visualization tool was used for this purpose. GAUSSIAN 98 [19] calculations were carried out at the B3LYP/6-31G(d) levels of theory (Fig. 4).

For the hydride abstraction three different cations were investigated according to mild, medium and strong hydride affinity. The computed energies necessary for balanced reactions are summarized in Table 1. On the basis of the computed hydride

affinities (Table 1) it seems that the $H^{(-)}$ affinity of pyridium ion is numerically close to that of $Li^{(+)}$. For this reason instead of NADH, at least on energetic grounds, $Li-H$ may be used as a hydride donor. The computed total energies for both radical and ionic reactions are listed in Table 2.

5. Results and discussion

5.1. Molecular geometries

In the ionic mechanism, only compounds labeled 1 and 5, have unsaturated benzenoid rings.

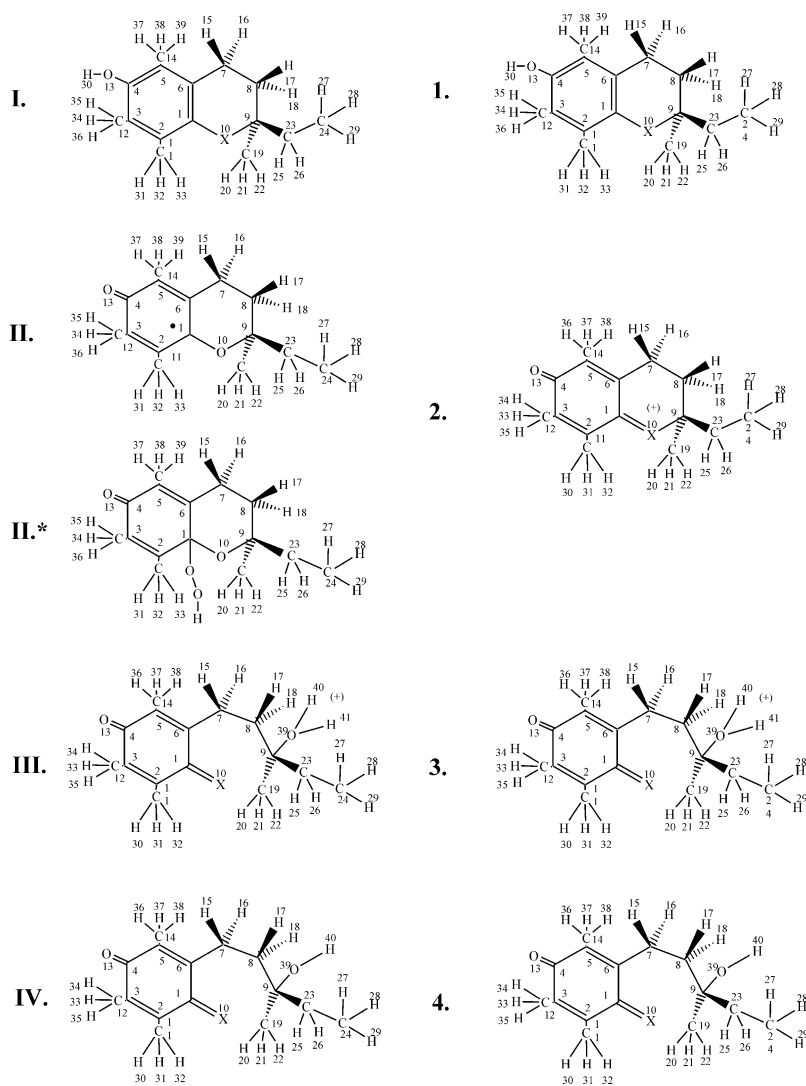


Fig. 4. Atomic numbering system of reactant, reaction intermediates and product of free radical and ionic oxidation of α -tocopherol.

Table 1

Energy components and hydride affinities for hydride abstraction as computed at the B3LYP/6-31G(d) level of theory

Cation	E (Hartree)	Neutral	E (Hartree)	Hydride affinity (kcal mol ⁻¹)
$\text{Li}^{(+)}$	-7.284544	LiH	-8.081922	210.570
$\text{C}_5\text{H}_6\text{N}^{(+)}$	-248.6569798	$\text{C}_5\text{H}_7\text{N}$	-249.455315	211.17
$\text{CH}_3^{(+)}$	-39.480388	CH_4	-40.518383	361.56

The intermediates labeled as **2** and **3** and the product molecule labeled as **4**, have quinoidal bonding. However, the quinoidal structure for **4** can clearly be seen in Fig. 5 and compared to the original vitamin E model **1**. In the free radical mechanisms reactant is labeled as **I**, intermediates as **II** and **II***, while the products are specified as **III** and **IV**. Clearly **1** = **I**, **3** = **III** and **4** = **IV**.

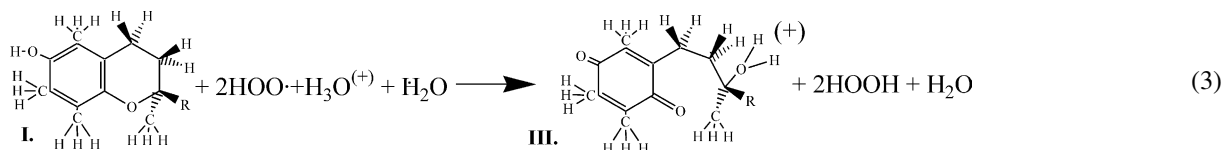
5.2. Mechanism and molecular energetics

The free radical and ionic as well as an ionic mechanism studied in the present paper are shown in Scheme 1.

5.2.1. Radical mechanism

Fig. 6 shows the energy profile for the free radical mechanism on the basis of the data presented in Table 3. The energies of water and oxonium ions necessary for the mechanism are shown in Table 2. The thermodynamic reaction profile showing only energy minima, allows a down-hill process, in the thermodynamic sense. Consequently, the radical scavenging ability of α -tocopherol is well established on energetic grounds.

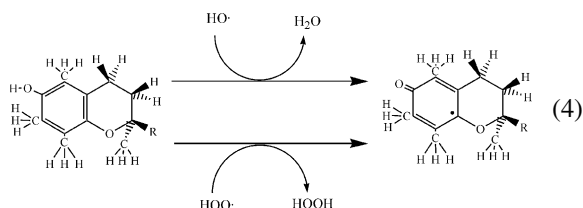
The reaction is balanced from reactant (**I**) to the first ionic product (**III**), as shown in Eq. (3)



The overall amount of energy released is -32.49 kcal-K

While the first step, the hydrogen abstraction, may occur by either $\text{HO}\cdot$ or $\text{HOO}\cdot$ attack, the energetics is expected to be considerably more exothermic, by about -32.4 kcal-K with the $\text{HO}\cdot$ radical than with the

HOO·radical



However this would only underline the validity of the conclusion reached with the use of the $\text{HOO}\cdot$ radical.

5.2.2. Ionic mechanism

The relative energies necessary to construct a thermodynamic reaction profile for the ionic reactions are summarized in Table 4. The thermodynamic reaction profile (only energy minima, without the appropriate transition states) are shown in Fig. 6 for α -tocopherol. The energies of water and oxonium ions necessary for the mechanism are shown in Table 2.

It should be emphasized that the first step involves a hydride acceptor. In biological systems it is $\text{NAD}^{(+)}$. However no full computations have been accomplished at the DFT level for the $\text{NAD}^{(+)}/\text{NADH}$ system. Protonated pyridine gives hydride

affinity close to that of $\text{Li}^{(+)}$ therefore this model appears to be fairly realistic for $\text{NAD}^{(+)}$, at least on energetic grounds.

The reaction was balanced from the reactant (**1**) to the first ionic product (**3**) as shown in Eq. (5), using $\text{Li}^{(+)}$ instead of $\text{NAD}^{(+)}$

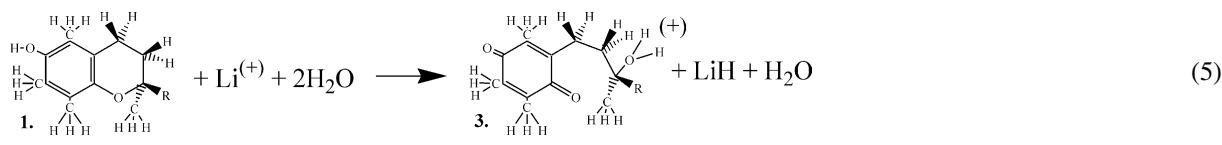


Table 2

Energy components, necessary to balance the redox reactions, computed at the B3LYP/6-31G(d) level of theory

Species	<i>E</i> (Hartree)	Species	<i>E</i> (Hartree)
E(H [−])	−0.461817	E(HOO [•])	−150.899156
E(HO [•])	−75.723455	E(HOO [−])	−151.462597
E(H ₂ O)	−76.408953	E(HOOH)	−151.532085
E(H ₃ O ⁺)	−76.685908	E(HOOLi)	−158.503570

The overall amount of energy released is +85.35 kcal·k.

It is clear from Fig. 7 that the steps are all endothermic. This indicated that the ionic mechanism is unlikely to occur. However, the reverse,

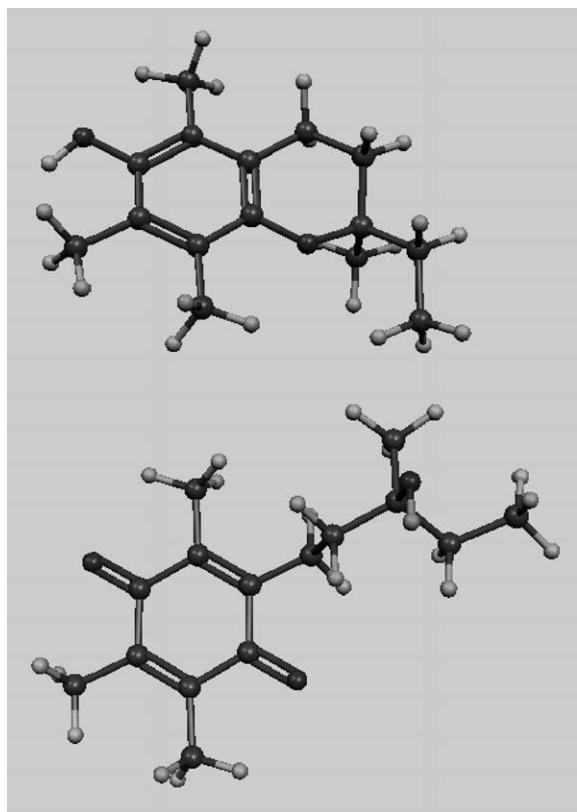
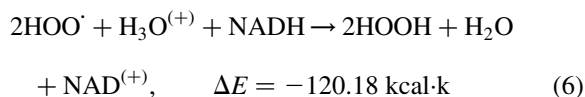


Fig. 5. Structures of α -tocopherol (top) and α -tocopherolquinone corresponding to reduced [Red] and oxidized [Ox] forms, respectively, in Eq. (2). All aromatic CC bond lengths in the top structure are in the vicinity of 1.40 Å. The single and double bond lengths in the ring of the bottom structures are in the vicinity of 1.49 and 1.35 Å, respectively.

namely the reduction back from the oxidized α -tocopherol (i.e. α -tocopherolquinone) to the original α -tocopherol would be expected to be an exothermic process (Table 5). Thus, it seems that the oxidation proceeds by the free radical mechanism while the reductive conversion, back to α -tocopherol would be expected to proceed by the ionic mechanism. This combined mechanism is shown in Fig. 8 (Table 6).

It is believed that the coupled nature of the radical and ionic oxidation is shown, for the first time, here in Fig. 8. The energy profile for the combined mechanism is shown in Fig. 9.

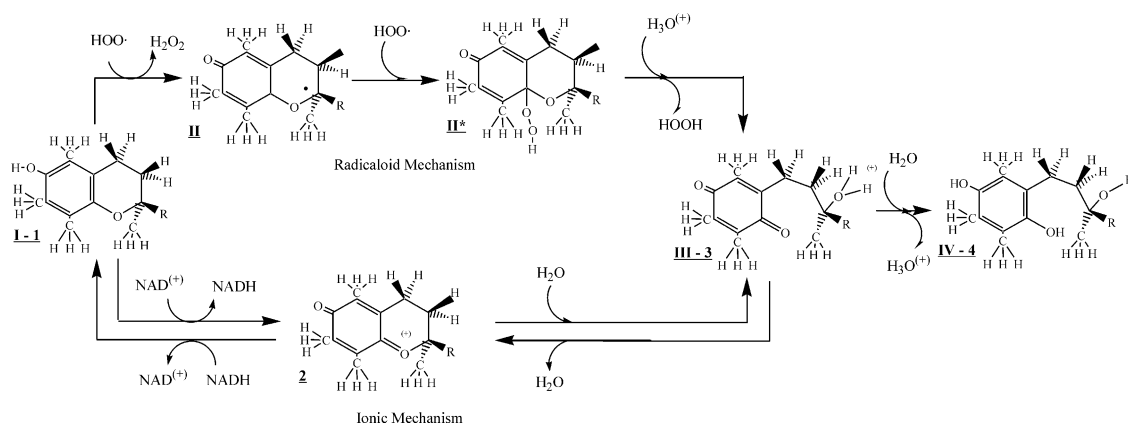
Since α -tocopherol has been used but not consumed in the coupled reaction, α -tocopherol may be regarded as a catalyst for the following overall processes



The essential point is, however, that α -tocopherol can only convert the peroxyradical only to hydrogen peroxide [H_2O_2] but not further. From that point onward, it is the job of the enzyme glutathione peroxidase $\text{GP}_x(\text{Se})$ or Catalase(Fe) to carry the process further through the full reduction to H_2O .

A schematic illustration of the overall process involving the various enzymes and non-enzymatic anti-oxidants is shown in Scheme (2).

The catalytic nature of vitamin E is shown in Fig. 10. Clearly, if vitamin E was destroyed at the end of the first step it could not produce more peroxide. Thus, under such condition its pro-oxidant nature perhaps would not ever have been ever observed. However, vitamin E is recycled, biologically, as Fig. 10 indicates and a single α -tocopherol molecule may convert numerous HOO^{\bullet} radicals to H_2O_2 which is accumulated if not removed at the same rate enzymatically with the participation of Catalase(Fe) or glutathione peroxidase, $\text{GP}_x(\text{Se})$. This accumulation of peroxide, which may be referred to as a peroxide traffic jam, may well be the reason of the pro-oxidant effect of vitamin E.



Scheme 1.

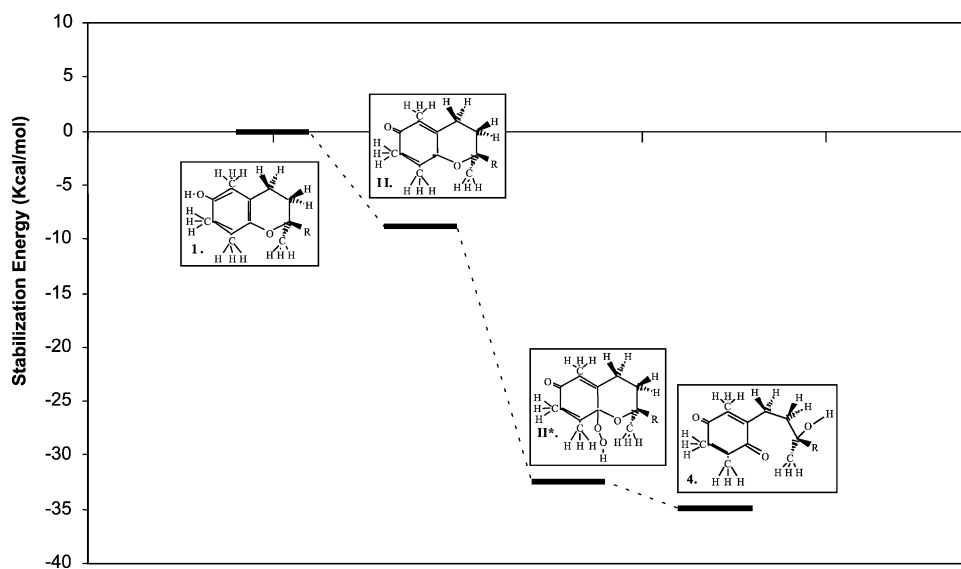
Fig. 6. Reaction profile of non-destructive free radical oxidation of α -tocopherol model by $\text{HOO}\cdot$.

Table 3

Total energy values of α -tocopherol model and its oxidized forms computed at the B3YP/6-31G(d) level of theory

Reactant, intermediates, product	<i>E</i> (Hartree)			
	Free radical route		Ionic route	
Reactant	I	− 735.31212	1	− 735.31212
Closed ring intermediate	II	− 734.69317	2	− 734.45881
Closed ring intermediate	II*	− 885.63012	—	—
Open ring intermediate	III	− 810.84221	3	− 810.84221
Product	IV	− 810.51082	4	− 810.51082

Table 4

Total and relative energies for the free radical mechanism

Route	State	<i>E</i> (Hartree)	ΔE (kcal · K)	$\Delta\Delta E$ (kcal · K)
Neutral	I + 2HOO [•] + H ₃ O ⁺ + H ₂ O	− 1190.205294	0.000	0.000
	II + HOO [•] + HOOH + H ₃ O ⁺ + H ₂ O	− 1190.219272	− 8.771	− 8.771
	II [*] + HOOH + H ₃ O ⁺ + H ₂ O	− 1190.257066	− 32.487	− 23.716
	III + 2HOOH + H ₂ O	− 1190.315332	− 69.050	− 36.563
	IV + 2HOOH + H ₃ O ⁺	− 1190.260897	− 34.892	34.159

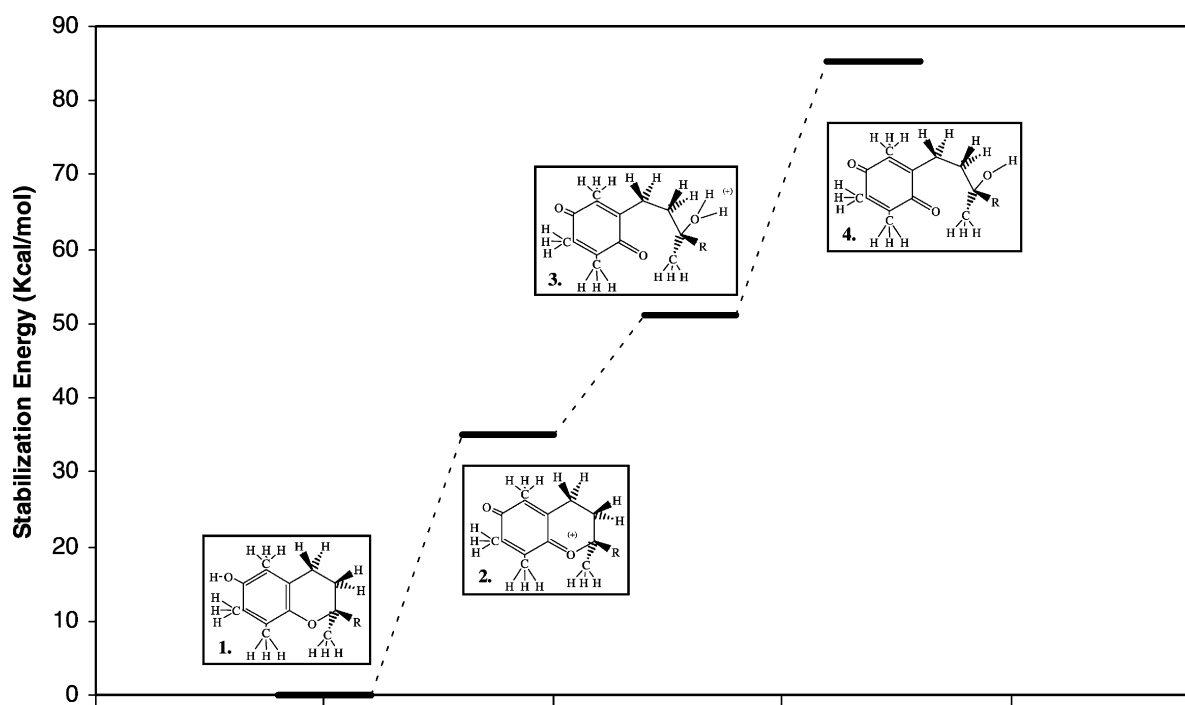
Fig. 7. Reaction profile for ionic oxidation mechanism using Li⁽⁺⁾, a hydride abstractor modeling NAD⁽⁺⁾.

Table 5

Total and relative energies for the ionic mechanism

Hydride abstraction initiator	State	<i>E</i> (Hartree)	ΔE (kcal · K)	$\Delta\Delta E$ (kcal · K)
Li ⁺	1 + Li ⁺ + 2H ₂ O	− 895.414570	0.000	0.000
	2 + LiH + 2H ₂ O	− 895.358638	35.098	35.098
	3 + LiH + H ₂ O	− 895.333085	51.133	16.035
	4 + LiH + H ₃ O ⁺	− 895.278650	85.291	34.159

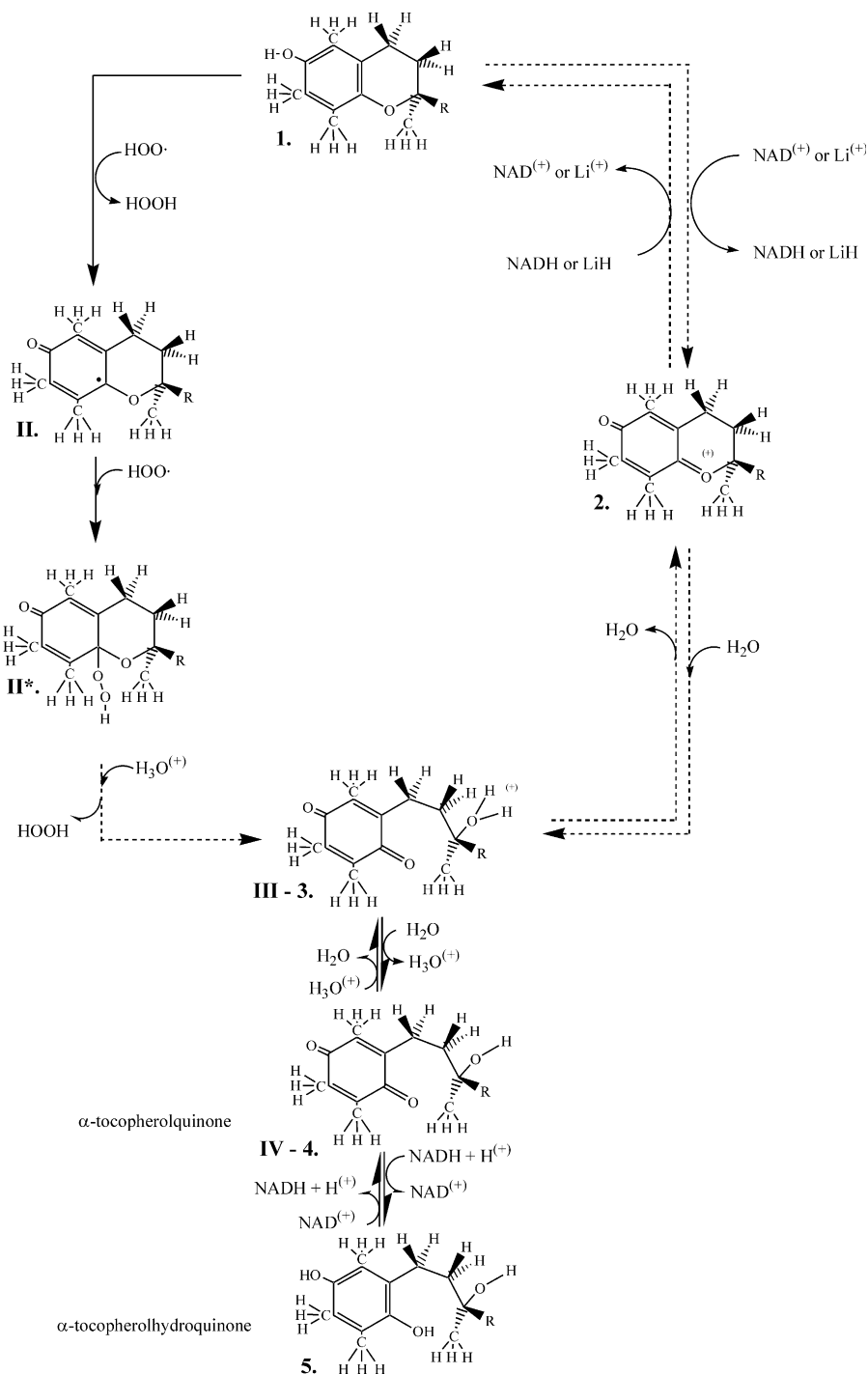


Fig. 8. The connection of a combined non-destructive free-radical and reversible ionic mechanism of oxidation of α -tocopherol quinone. Note the reversible nature of the ionic process.

Table 6

Total and relative energies for the combined mechanism of free radical oxidation and ionic reduction

Components structures	<i>E</i> (Hartree)	Sum of component energies (Hartree)	Relative energy ΔE (kcal·K)	Step height energy $\Delta\Delta E$ (kcal·K)
I = 1	–735.31212	–1121.87826	0.000	0.000
2(HOO [•])	–301.79831			
H ₃ O ⁽⁺⁾	–76.68591			
LiH	–8.08192			
Total	–1121.87826			
II	–734.69317	–1121.89224	–8.771	–8.771
HOOH	–151.53208			
HOO [•]	–150.89916			
H ₃ O ⁺	–76.68591			
LiH	–8.08192			
Total	–1121.89224			
II*	–885.63012	–1121.93003	–32.487	–23.716
HOOH	–151.53208			
H ₃ O ⁽⁺⁾	–76.68591			
LiH	–8.08192			
Total	–1121.93003			
III⁽⁺⁾ = 3⁽⁺⁾	–810.84221	–1121.98830	–69.050	–36.563
2(HOOH)	–303.06417			
LiH	–8.08192			
Total	–1121.98830			
2⁽⁺⁾	–734.45881	–1122.01385	–85.085	–16.035
2(HOOH)	–303.06417			
H ₂ O	–76.40895			
LiH	–8.08192			
Total	–1122.01385			
1	–735.31212	–1122.06979	–120.183	–35.098
2(HOOH)	–303.06417			
H ₂ O	–76.40895			
Li ⁽⁺⁾	–7.28454			
Total	–1122.06979			

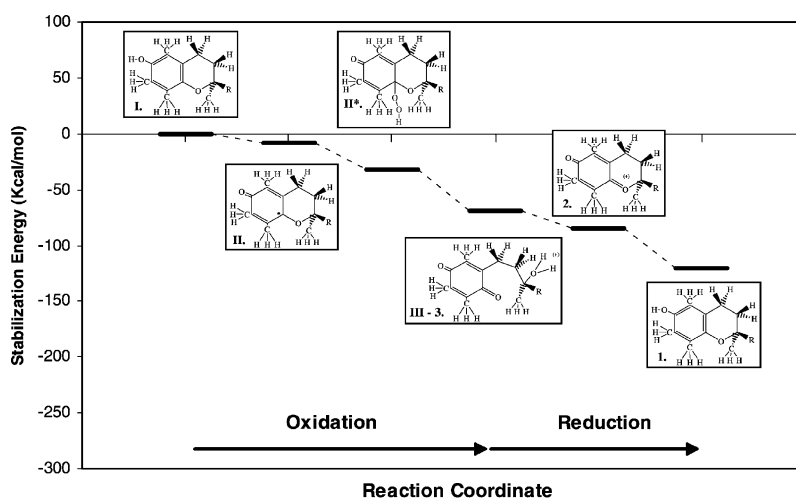
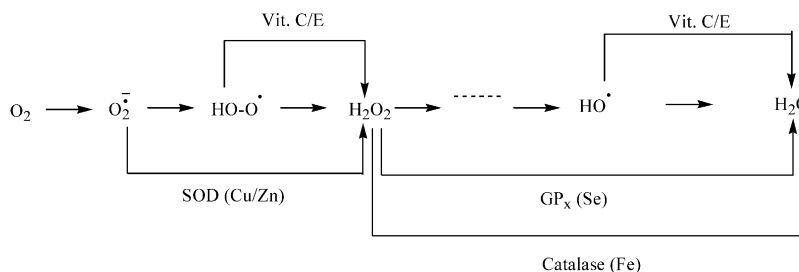
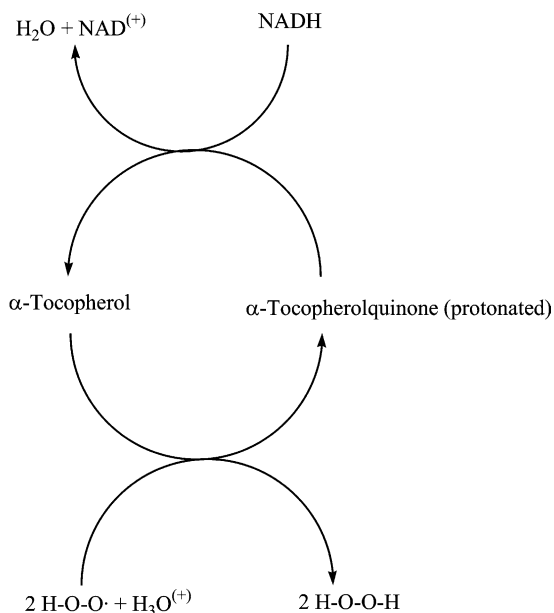


Fig. 9. Full cycle of reaction mechanism involving free radical open shell oxidation and closed shell recovery of α -tocopherol. The energy difference between initial and final states is related to the process: $2\text{HOO}^{\bullet} + \text{Li}-\text{H} \rightarrow \text{HOOH} + \text{HOOLi}$.



Scheme 2.

Fig. 10. Overall representation of the catalytic effect of α -tocopherol.

6. Conclusions

If vitamin E reacts with HO^\cdot radical then the radical is converted to H_2O which represents no further problem, as it is the last station of the overall reductive process which started at O_2 . However, when vitamin E reacts with HOO^\cdot then the peroxyradical is converted to hydrogen peroxide (H_2O_2) which could cause oxidative damage.

The present investigation has shown that a substantial fraction of the oxidized vitamin E may be reduced back to active vitamin E which could, in turn, produce more hydrogen peroxide. The responsibility of removal of the hydrogen peroxide

from the system bestowed upon two enzymes, the iron containing catalase (Fe) and the selenium containing glutathione peroxidase, $\text{GP}_x(\text{Se})$. If there is a noticeable concentration reduction of these enzymes then peroxides are accumulating, leading to a peroxide traffic-jam. This can happen for example if the Se supply is low, as discussed at the beginning of this paper. Of course, the accumulated H_2O_2 , produced by vitamin E, can make a great deal of damage and consequently vitamin E may well be misjudged to be a pro-oxidant yet the phenomenon may be due to the low level of selenium.

It now appears that future clinical studies, designed to investigate the efficacy (the anti-oxidant effect) and the toxicity of the accumulated peroxide (via the pro-oxidant effect) of vitamin E should include the monitoring of other participating components of the detoxification process of ROS. Such studies should include the monitoring of the level of catalase (Fe or Mn) as well as glutathione peroxidase (Se). Nutritionists [20] and biochemists [21] have already questioned whether the imbalance of these enzymes could be a significant contributor to the damages originated from oxidative stress.

Acknowledgements

This work was supported by grants from the Global Institute of Computational Molecular and Materials Sciences and Velocet Communications Inc., Toronto, Ontario, Canada.

The authors thank Christopher N.J. Marai, Tania A. Pecora, Jacqueline M. S. Law and Michelle A. Sahai for their helpful input and discussions, as well as for the preparation of this manuscript, tables, and figures. The work of Graydon Hoare in the areas of database

management, network support, software, and distributive processing development is also recognized. A special thanks is extended to Andrew M. Chasse for his continuing and ongoing development of novel scripting and coding techniques, indirectly bringing about a reduction in the necessary number of CPU cycles for each computation. Advanced technical support is credited to Christopher M. Andrews and Michael R. Sahai. Last but not least, the authors wish to acknowledge Kenneth P. Chasse (Jr.) of Velocet Communications Inc. for his pioneering of great advances in all composite computer-cluster software and hardware architectures. He and the other directors of Velocet Communications Inc., specifically David C.L. Gilbert and Adam A. Heaney, are also acknowledged for providing spare CPU time for the computations needed in the preparation of this article.

References

- [1] B. Chance, H. Sies, A. Boveris, *Phys. Rev.* 59 (1979) 527.
- [2] A.D.N.G. de Grey, *The Mitochondrial Free Radical Theory of Aging*, R.G. Landes Company, Austin, TX, 1999.
- [3] S. Steenken, *Chem. Rev.* 89 (1979) 503.
- [4] K.L. Fong, P.B. McCay, J.L. Poyer, H. Misra, B. Keele, *J. Biol. Chem.* 248 (1973) 7792.
- [5] T.I. Mak, W.B. Weglicki, *J. Clin. Investig.* 75 (1985) 58.
- [6] J.C. Vank, C.P. Sosa, A. Perczel, I.G. Csizmadia, *Chem. Can. J.* 78 (2000) 395–408.
- [7] M.A. Berg, G.A. Chass, E. Deretey, A.K. Fuzery, B.M. Fung, D.Y.K. Fung, H. Henry-Riyad, A.C. Lin, M.L. Mak, A. Mantas, M. Patel, I.V. Repyakh, M. Staikova, S.J. Salpietro, T.-H. Tang, J.C. Vank, A. Perczel, O. Farkas, L. Torday, Z. Szekely, I.G. Csizmadia, *J. Mol. Struct. (Millennium Volume)* 500 (2000) 5–58.
- [8] B.N. Ames, M.K. Shigenaga, in: J.G. Scandalios (Ed.), *Molecular Biology of Free Radical Scavenging Systems*, Cold Spring Harbor Laboratory Press, New York, 1992, p. 1.
- [9] G.A. Chasse, M.L. Mak, E. Deretey, I. Farkas, L.L. Torday, J.G. Papp, D.S.R. Sarma, A. Agarwal, A. Sujak, S. Agarwal, A.V. Rao, *J. Mol. Struct. (THEOCHEM)* 571 (2001) 27–37.
- [10] I. Jialal, C.F. Fuller, B.A. Huet, *Thromb. Vasc. Biol.* 15 (1995) 190.
- [11] H.M.G. Princen, W. Van Dwyvenroorde, R. Buytenhek, A. VanderLaarse, G. Van Poppel, J.A. Gevers Leuven, V.W.M. VanHinsbergh, *Thromb. Vasc. Biol.* 15 (1995) 325.
- [12] P. Weber, A. Bendich, L.J. Machlin, *Nutrition* 13 (1997).
- [13] A. Azzo, A. Stocker, *Prog. Lipid Res.* 39 (2000) 231.
- [14] J.M. Upston, A.C. Terentis, R. Stocker, *FASEB J.* 13 (1999) 977.
- [15] R. Ricciarelli, J.-M. Zingg, A. Azzi, *FASEB J.* 15 (2001) 2314.
- [16] D.C. Lieber, J.A. Burr, L. Phillips, A.J. Harm, *Anal. Biochem.* 236 (1996) 27–34.
- [17] T. Rosenau, W.B. Habicher, *Tetrahedron* 51 (1995) 7919–7926.
- [18] R. Brigelius-Flohe, G. M. F.A.S.E.B. Traber, *J.* 13 (1999) 1145–1155.
- [19] M.J. Frisch, G.W. Trucks, H.B. Schlegel, G.E. Scuseria, M.A. Robb, J.R. Cheeseman, V.G. Zakrzewski, J.A. Montgomery Jr., R.E. Stratmann, J.C. Burant, S. Dapprich, J.M. Millam, A.D. Daniels, K.N. Kudin, M.C. Strain, Ö. Farkas, J. Tomasi, V. Barone, M. Cossi, R. Cammi, B. Mennucci, C. Pomelli, C. Adamo, S. Clifford, J. Ochterski, G.A. Petersson, P.Y. Ayala, Q. Cui, K. Morokuma, D.K. Malick, A.D. Rabuck, K. Raghavachari, J.B. Foresman, J. Cioslowski, J.V. Ortiz, A.G. Baboul, B.B. Stefanov, G. Liu, A. Liashenko, P. Piskorz, I. Komaromi, R. Gomperts, R.L. Martin, D.J. Fox, T. Keith, M.A. Al-Laham, C.Y. Peng, A. Nanayakkara, M. Challacombe, P.M.W. Gill, B. Johnson, W. Chen, M.W. Wong, J.L. Andres, C. Gonzalez, M. Head-Gordon, E.S. Replogle, J.A. Pople, *GAUSSIAN 98*, Gaussian Inc., Pittsburgh, PA, 1998.
- [20] C.C. Lai, W.H. Huang, A. Askari, L.M. Klevay, T.H. Chiu, *J. Nutr. Biochem.* 6 (1995) 256.
- [21] P. Ahmsad, A. Peskin, G. Shah, M. Mirault, R. Moret, I. Zbideu, P. Cerutti, *Biochemistry* 30 (1991) 9305.

Exploratory study on the full conformation space of α -tocopherol and its selected congeners

David H. Setiadi^{a,b,*}, G.A. Chass^{a,b,c}, Joseph C.P. Koo^{a,b}, Botond Penke^{d,e},
Imre G. Csizmadia^{a,b,d}

^aGlobal Institute of Computational Molecular and Materials Science (GIOCOMMS), 1422 Edenrose Street, Mississauga, Ont., Canada, L5V 1H3

^bDepartment of Chemistry, University of Toronto, Lash Miller Chemical Laboratories, 80 St George St., Toronto, Ont., Canada, M5S 3H6

^cDepartment of Biomedical Sciences, Creighton University, 2500 California Plaza, Omaha, NE 68178, USA

^dDepartment of Medical Chemistry, University of Szeged, Dóm tér 8, 6720 Szeged, Hungary

^eProtein Chemistry Research Group, Hungarian Academy of Sciences, University of Szeged, Dóm tér 8, 6720 Szeged, Hungary

Abstract

Preliminary results for a full and comprehensive study of the tocopherol family of compounds. Previous studies have allowed for the full modelling of α -tocopherol as well as its S and Se containing congeners to be subjected to ab initio [RHF/3-21G and RHF/6-31G(d)] and DFT [B3LYP/6-31G(d)] computation. Molecular geometries with full optimized total energies were determined. Initial discussion for trends of the side-chain, which has included computation of helical tails as well as the effect on ring stabilities is also investigated.

© 2003 Elsevier B.V. All rights reserved.

Keywords: Tocopherol; Tocotrienol; Stereo isomers; Ab initio; Congeners; Molecular structure

1. Introduction

Vitamin E [1] is made up of two families of compounds: tocopherols and tocotrienols [2]. Both families consist of a chroman [benzopyran] ring structure and a side-chain. The side-chain has the characteristics of an isoprenoid skeleton, typical of terpenes with some members of the tocopherol families having saturated side-chains. There are also methyl substituted homologues of tocopherol which

can be seen in Fig. 1. There also exists eight different stereo isomers for each homologue of tocopherol with known different activities associated to them.

Past molecular computational studies have concentrated on the fused ring system and the different stabilities associated with hetero-atom substitution of the chroman molecule. It has also been suggested [3] that the selenium congener of α -tocopherol (may be a very effective antioxidant. The ring-closing and ring-opening mechanisms and transition states of ring structure was also investigated.

It has also been suggested that in a biological system where vitamin E is recycled, a single α -tocopherol molecule may convert numerous $\text{HOO}\cdot$ radicals to H_2O_2 [4]. This accumulation of peroxide

* Corresponding author. Address: Global Institute of Computational Molecular and Materials Science (GIOCOMMS), 1422 Edenrose Street, Mississauga, Ont., Canada, L5V 1H3.

E-mail addresses: dsetiadi@giocomms.org (D.H. Setiadi); gchass@giocomms.org (G.A. Chass).

molecules may be referred to as a ‘peroxide traffic jam’ that could lead to the pro-oxidant effect of Vitamin E.

Conformational analysis on vitamin E models with both the fused ring and the side-chain tail undetermined in the past by ab initio computations is now investigated with the premise of further understanding the role of vitamin E in eliminating ‘reactive oxygen species’ ROS [5].

2. Methods

As a progression from previous studies where concentration was placed on the fused ring systems, the full model of the tocopherol family of compounds is now studied. Outline of previous models studied is shown in Fig. 1.

Since the previous calculations were modelled in a modular, scalable and reusable manner, it is now possible to add the side-chain tail to the fused ring.

Molecular computations were performed using the Gaussian 98 [6] program package. Preliminary conformers were constructed from initial model A to the full tocopherol model. Energy is initially

minimized at the RHF/3-21G level of theory. These minima are brought through to the RHF/6-31G(d) and B3LYP/6-31G(d) levels of theory.

3. Results and discussions

The initial findings of the conformational study of α -tocopherol are shown in Table 1. Considering the nature of this publication, discussion will be kept to a minimum and only focus on the side-chain tail structure. A full analysis of both fused ring, and side-chain will be provided in future work.

The full α -tocopherol along with its congeners have geometry optimized stable energy conformers with all dihedrals of the side-chain in the anti position. Fig. 2a shows the fully extended alpha-tocopherol model optimized at the B3LYP/6-31g(d) level of theory with all side-chain dihedrals in the anti position. Fig. 2b shows geometry optimized energy conformer of the hetero-atom substitution of selenium computed at the RHF/6-31g(d) level of theory with all side-chain dihedrals in the anti position.

A comparison is made of the sequence of stabilization for various hetero-atoms. The geometrical

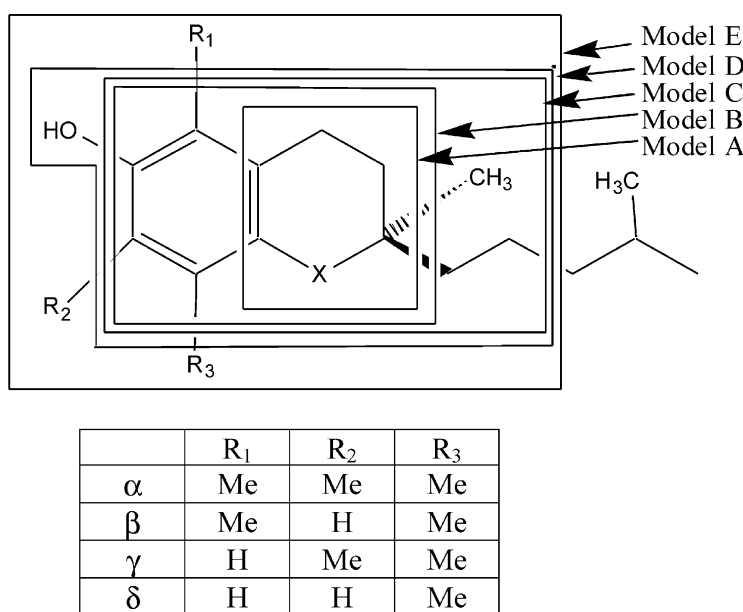
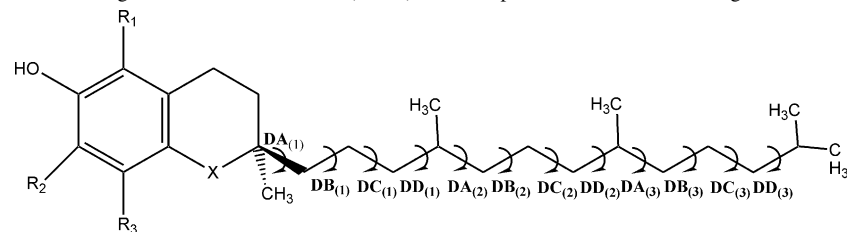


Fig. 1. Model map used for previous study of tocopherol families and selected congeners.

Table 1

Optimized total energies and side-chain dihedral angles for stable conformers ($\lambda = 0$) of α -tocopherol and its selected congeners

X	Level of theory	Dihedral trend	Selected dihedral angles												Total E (Har)	Rel. E (kcal mol ⁻¹)
			DA ₍₁₎	DB ₍₁₎	DC ₍₁₎	DD ₍₁₎	DA ₍₂₎	DB ₍₂₎	DC ₍₂₎	DD ₍₂₎	DA ₍₃₎	DB ₍₃₎	DC ₍₃₎	DD ₍₃₎		
O	RHF/3-21G	a	173.35	187.27	183.68	170.94	189.24	175.99	183.97	170.47	189.34	175.92	183.52	171.57	-1269.99688	-
O	RHF/6-31G(d)	a	178.35	187.92	186.73	172.06	189.07	174.86	185.25	171.06	188.77	174.60	184.55	172.26	-1277.04046	-
O	B3LYP/6-31G(d)	a	176.52	185.55	184.65	171.76	189.31	175.40	184.25	170.88	188.58	175.11	183.21	171.70	-1285.69823	-
S	RHF/3-21G	a	175.63	183.03	184.33	171.00	189.35	176.01	183.99	170.54	189.46	175.98	183.56	171.57	-1591.10457	-
S	RHF/6-31G(d)	a	177.44	183.10	186.75	172.00	189.12	174.86	185.24	171.04	188.74	174.59	184.53	172.25	-1599.68471	-
S	B3LYP/6-31G(d)	a	175.53	179.99	184.03	169.90	187.99	174.81	183.40	170.40	188.46	175.63	183.66	172.02	-1608.66284	-
Se	RHF/3-21G	a	175.06	181.41	184.29	171.00	189.45	175.98	183.99	170.54	189.43	175.92	183.54	171.61	-3584.04040	-
Se	RHF/6-31G(d)	a	176.59	183.86	186.47	171.95	189.09	174.90	185.27	171.09	188.78	174.60	184.55	172.26	-3599.75844	-
Se	B3LYP/6-31G(d)	a	Under computation													
O	RHF/3-21g	a	173.35	187.27	183.68	170.94	189.24	175.99	183.97	170.47	189.34	175.92	183.52	171.57	-1269.99688	0.000
O	RHF/3-21g	g^+	48.40	66.68	168.43	56.50	59.95	66.79	173.81	58.42	56.93	60.03	60.32	62.18	-1269.99031	4.122
O	RHF/3-21g	g^+	41.71	65.21	101.24	62.52	56.07	61.30	172.01	57.64	57.32	58.56	58.65	61.42	-1269.98435	3.741
O	RHF/3-21g	g^-	-68.35	-104.44	-68.97	-60.51	-45.90	-69.95	-57.45	-56.49	-63.48	-101.40	-94.10	-67.57	-1269.97133	8.168

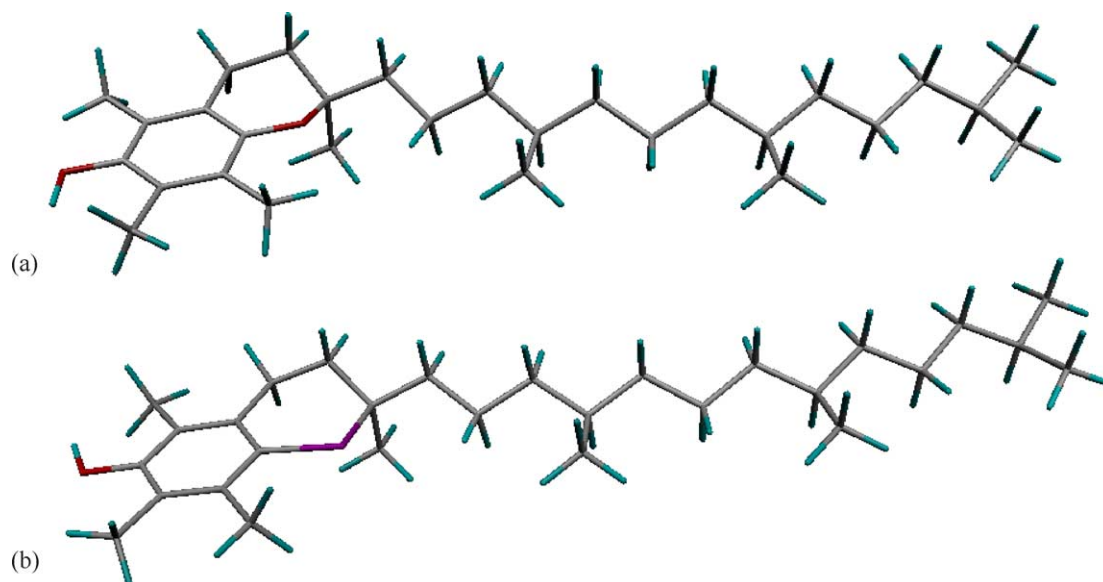


Fig. 2. (a) B3LYP/6-31G(d) optimized minimum energy structure for full extended tail structure of α -tocopherol and (b) B3LYP/6-31G(d) optimized minimum energy of its selenium congener.

parameters also show a non-monotonic change. The R–C–Me bond angles at the ring stereo center varied the following way: 112.2° (O), 111.6° (S), 112.2° (Se). This is very similar to previous reported results of the similar Et–C–Me bond angle for Model E which were also non-monotonic 112.1° (O), 111.6° (S), 112.4° (Se). It is interesting to note that when comparing the dihedral angles positioned further

away from the fused ring $D[A,B,C,D]_{(2)} - D[A,B,C,D]_{(3)}$, there is no significant difference between the dihedrals of any of the congeners while there is a monotonic change for the dihedral closest to the fused ring.

Fig. 3 shows the selenium congener of the α -tocopherol model optimized at B3LYP/6-31g(d) with a g^+ helices where the trend of the atoms in the backbone of the α -tocopherol tail is to conform to the g^+ position.

The model of α -tocopherol with all side-chain tail conformers in the anti position appears to have the least energy of stabilization at this point. While the model of α -tocopherol with all side-chain tail conformers in the g^- position appears to have the largest energy of stabilization at this point $8.168 \text{ kcal mol}^{-1}$ from the lowest energy value computer at the RHF/3-21g level of theory.

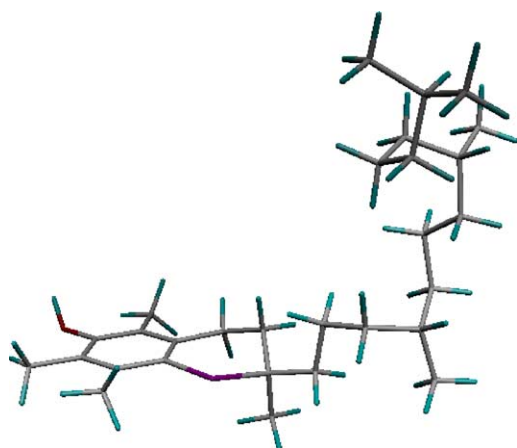


Fig. 3. B3LYP/6-31G(d) optimized minimum energy structure for g^+ trend of the side-chain tail for the selenium congener of α -tocopherol.

4. Conclusions

Taking into consideration the results shown is only a partial set of a larger, comprehensive study, further results are expected. The full study will

encompass all eight stereo isomers of all homologues and possible congeners of the tocopherol model coupled with previously reported results. This will allow a complete analysis of the full conformational states of tocopherol.

A complete study of ring stability with respect to gradual methylation as well as the trends of biological activity should also be studied. It is important to note that past studies have indicated an inverse relationship between ring stability and biological activity. A comprehensive structure activity analysis of the full model will provide a clearer answer.

With the full conformation space of the Vitamin E models defined, the doors are open for modelling the mechanisms of the antioxidant behaviour of tocopherol. Computations of the full structure of the tocopherol family with respect to exothermic free radical oxidative ring opening and endothermic ionic ring closing can be examined. Computational modelling may also be able to shed light on Vitamin E's role as an oxidative protector of LDL [7] and its relationships with enzymes such as glutathione peroxidase and catalase, and other bioactive molecules such as Vitamin C.

Acknowledgements

The authors would like to thank the Global Institute of Computational Molecular and Materials Sciences, Aristo Systems and Uniseti Inc. for their support and resources. One of the authors (I.G.C.) wishes to thank the Ministry of Education for a Szent-Györgyi Visiting Professorship. We would especially

like to thank all our many friends in many places, the work would not be possible without them. The author would also like to thank Lucha for the constant support.

References

- [1] M. Evans, K.S. Bishop, *Science* 55 (1922) 650.
- [2] J.B. Bauernfeind, *Vitamin E: a Comprehensive Treatise*, Marcel Dekker, New York, 1980, pp. 99–167.
- [3] N. Al-Maharik, L. Engman, J. Malmstrom, C. Schiesser, Intramolecular homolytic substitution at selenium: synthesis of novel selenium-containing vitamin E analogues, *J. Org. Chem.* 66 (2001) 6286–6290.
- [4] D.H. Setiadi, G.A. Chass, L.L. Torday, A. Varro, J.Gy. Papp, Vitamin E models. Can the anti-oxidant and pro-oxidant dichotomy of [alpha]-tocopherol be related to ionic ring closing and radical ring opening redox reactions?, *J. Mol. Struct.: Theochem.* 620 (2003) 93–106.
- [5] B.N. Ames, M.K. Shigenaga, in: J.G. Scandalios (Ed.), *Molecular Biology of Free Radical Scavenging Systems*, Cold Spring Harbor Laboratory Press, New York, 1992, p. 1.
- [6] M.J. Frisch, G.W. Trucks, H.B. Schlegel, G.E. Scuseria, M.A. Robb, J.R. Cheeseman, V.G. Zakrzewski, J.A. Montgomery, Jr., R.E. Stratmann, J.C. Burant, S. Dapprich, J.M. Millam, A.D. Daniels, K.N. Kudin, M.C. Strain, Ö. Farkas, J. Tomasi, V. Barone, M. Cossi, R. Cammi, B. Mennucci, C. Pomelli, C. Adamo, S. Clifford, J. Ochterski, G.A. Petersson, P.Y. Ayala, Q. Cui, K. Morokuma, D.K. Malick, A.D. Rabuck, K. Raghavachari, J.B. Foresman, J. Cioslowski, J.V. Ortiz, A.G. Baboul, B.B. Stefanov, G. Liu, A. Liashenko, P. Piskorz, I. Komaromi, R. Gomperts, R.L. Martin, D.J. Fox, T. Keith, M.A. Al-Laham, C.Y. Peng, A. Nanayakkara, M. Challacombe, P.M.W. Gill, B. Johnson, W. Chen, M.W. Wong, J.L. Andres, C. Gonzalez, M. Head-Gordon, E.S. Replogle, J.A. Pople, Gaussian Inc., Pittsburgh, PA, 1998.
- [7] M.N. Diaz, B. Frei, J.A. Vita, J.F. Keaney, Antioxidants and atherosclerotic heart disease, *New Engl. J. Med.* 337 (1997) 408–416.